USP50 IN THE DNA DAMAGE RESPONSE

and

THE ROLE OF BRCA1 AT STALLED REPLICATION FORKS

By

Kirsty Josephine Lawrence, BSc

This project is submitted in partial fulfilment of the requirements for the award of MASTER OF RESEARCH BIOMEDICAL RESEARCH to the University of Birmingham

School of Cancer Studies
College of Medical and Dental Sciences
University of Birmingham
August 2012

USP50 IN THE DNA DAMAGE RESPONSE

AND

THE ROLE OF BRCA1 AT STALLED REPLICATION FORKS

By

Kirsty Josephine Lawrence, BSc

UNIVERSITY OF BIRMINGHAM

USP50 IN THE DNA DAMAGE RESPONSE

The little-known deubiquitinating enzyme, USP50, has recently been observed to be important for G2/M cell cycle checkpoint activation and ubiquitin conjugate clearance at DNA damage repair. This project investigates the possible orthologs, predicted protein structure, protein domain active sites, conserved protein regions and cellular localisation of USP50. Also, this details the cloning strategy of creating wild-type and mutant USP50 inducible expression stable cell lines. Methodology utilised included; bioinformatics tools, protein structure modelling, immunofluorescene staining and cell culture.

USP50 is a close homologue of USP8 but has a missing catalytic residue in the active site required for ubiquitin binding. Immunofluorescent data suggests USP50 is functional as overexpression leads to cellular defects and DNA damage. Due to such damage, inducible expression stable cell lines of wild-type and mutant USP50 are required to study USP50 function further.

Evidence within the literature combined with our results suggest USP50 is active, despite the missing residue from its UCH active site. USP50 appears to be important for ubiquitin conjugate regulation at double-strand breaks.

THE ROLE OF BRCA1 AT STALLED REPLICATION FORKS

BRCA1 is a common inherited mutation in families with early onset breast and ovarian cancer. Cancers with homozygous mutations in BRCA1 are more resistant to chemotherapy due to abnormal DNA repair. Gemcitabine is a DNA replication inhibitor used to treat breast and ovarian cancer. How cancer mutations change the response of cells is poorly understood. Here, we investigate how BRCA1 mutations effect response to Gemcitabine using the cell line, HCC1937. BRCA1-proficient and –deficient cells were used to investigate the replication fork stalling, fork restart, 53BP1 and ɣH2AX foci, phospho-RPA levels, cell cycle accumulation and clonogenic survival after Gemcitabine treatment. Techniques utilised included DNA fibre analysis, immunofluorescent staining, FACS, Western blot and clonogenic survival assays.

BRCA1-deficient cells display increased fork stalling and earlier induction of phospho-RPA, 53BP1 and ɣH2AX. BRCA1 status effects the accumulation of cells in S phase after Gemcitabine treatment. BRCA1-deficient cells show decreased survival to <10μM Gemcitabine treatment.

We report that BRCA1 protects slowed and stalled forks, and prevents forks collapsing into double-strand breaks. BRCA1 status affects the sensitivity of cells to Gemcitabine treatment.

Contents

USP50 IN THE DNA DAMAGE RESPONSE

THE ROLE OF BRCA1 AT STALLED REPLICATION FORKS

FIGURES AND TABLES

USP50 IN THE DNA DAMAGE RESPONSE

THE ROLE OF BRCA1 AT STALLED REPLICATION FORKS

ACKNOWLEDGMENTS

I would like to thank Dr Eva Petermann for her support, enthusiasm and patience; Dr Rebecca Jones for her humour and company; and Islam Afzal for his technical support.

I would also like to thank the Morris lab group for their support and making the lab feel like home; to Dr Ruth Densham for her kindness, patience and knowledge; Dr Alex Garvin for all his help and humour; James Beasley for his maths; Junging Jia for being lab mum and feeding me; and last but certainly not the quietest, Wing for your candour and hilarity. I would like to thank Helen Stone for her laughter, singing and most of all her friendship. I would especially like to thank Dr Jo Morris for her support, ideas and pushing me to be a better scientist. I have started as I mean to go on; to keep improving as a scientist and keep working in the Morris lab, for 3 years at a least.

DEDICATION

I would like to dedicate this thesis to my new friends in Birmingham. Moving to a new city is difficult and scary, but with MRes group, lab friends (esp.Helen) and housemates, it has been exciting and welcoming. I am very much looking forward to spending the next three years in Birmingham and with you all.

Also I cannot and do not forget the undying support of my family, Gabrielle, Emily and the Reigate lot.

Thank you. KL

USP50 IN THE DNA DAMAGE RESPONSE

by

Kirsty Josephine Lawrence, BSc.

This project is submitted in partial fulfilment of the requirements for the award of MASTER OF RESEARCH BIOMEDICAL RESEARCH to the University of Birmingham

UNIVERSITY OF BIRMINGHAM

USP50 IN THE DNA DAMAGE RESPONSE

ABSTRACT

The little-known deubiquitinating enzyme, USP50, has recently been observed to be important for G2/M cell cycle checkpoint activation and ubiquitin conjugate clearance at DNA damage repair. This project investigates the possible orthologs, predicted protein structure, protein domain active sites, conserved protein regions and cellular localisation of USP50. Also, this details the cloning strategy of creating wild-type and mutant USP50 inducible expression stable cell lines. Methodology utilised included; bioinformatics tools, protein structure modelling, immunofluorescene staining and cell culture.

USP50 is a close homologue of USP8 but has a missing catalytic residue in the active site required for ubiquitin binding. Immunofluorescent data suggests USP50 is functional as overexpression leads to cellular defects and DNA damage. Due to such damage, inducible expression stable cell lines of wild-type and mutant USP50 are required to study USP50 function further.

Evidence within the literature combined with our results suggest USP50 is active, despite the missing residue from its UCH active site. USP50 appears to be important for ubiquitin conjugate regulation at double-strand breaks.

Word Count: 7676 words

INTRODUCTION

Ubiquitin, Ubiquitination and Deubiquitination

Ubiquitin is a highly conserved 76 amino acid protein which has 7 lysine residues (K6, 11, 27, 29, 33, 48 and 63) (Haas and Siepmann, 1997). It plays a role in the post-translational modification of proteins. Ubiquitin modifications are involved in signalling for the degradation and the re-localisation of proteins, and it is because ubiquitin is a marker for timely action, that it is important in cell regulatory processes. The addition of ubiquitin modifications has been shown to have multiple functions in the cell; in particular it is involved in degradation of proteins by the proteasome (Eytan et al., 1989) and localisation or trafficking of proteins within the cell (Hicke and Dunn, 2003). The efficient degradation of protein is heavily involved in cell cycle progression, endocytosis and various regulatory pathways of transcription (Chen and Sun, 2009) and antigen response signal transduction (Ben-Neriah, 2002). Therefore ubiquitin is involved in correct immune response (Ben-Neriah, 2002), programmed cell death and the regulation of developmental processes (Chen and Sun, 2009), and consequently aberrant ubiquitin modification is associated with diseases such as cancer (Beer-Romero et al., 1997).

Ubiquitin chains can form using the seven conserved lysines in ubiquitin. Two types of ubiquitin chain are linked by Lys48 (K48, PDB:3NS8) or Lys63 (K63, PDB:2JF5) and have specific structures. The type of chain can mark the protein for various fates. For example, K48 chains can promote degradation of the protein by the proteasome (Verma et al., 2004), whereas K63 chains can mark proteins for localization to the lysosome (Varadan et al., 2004; Yang et al., 2010).

The ligation of ubiquitin to a protein requires three types of enzymes; E1, E2 and E3. The E1 ubiquitin-activating enzyme binds and activates ubiquitin at a C-terminus glycine in an ATP-dependent manner. The ubiquitin is moved to a cysteine residue on the E1 and subsequently transferred to the cysteine residue in the active site of an E2 ubiquitin-conjugating enzyme. An E3 ubiquitin-protein ligase then transfers the ubiquitin onto a lysine residue of the protein substrate. E1's can bind to several E2 enzymes, and E2 can bind to many E3 enzymes, and it is the E3 that confers the specificity for a protein substrate (Pickart and Eddins, 2004).

The regulation of ubiquitin modifications is aided by deubiquitinating-enzymes (DUBs) which remove ubiquitin from proteins so they are no longer modified (Lam et al., 1997). This maintains the function of various proteins and maintains a constant pool of free ubiquitin in the cell. DUBs are categorised into two main classes; metalloproteases and cysteine proteases.

Metalloproteases contain JAMM domains that bind to zinc. Cysteine proteases have four superfamilies; ubiquitin-specific processing protease (USP/UBP), ubiquitin C-terminal hydrolyase (UCH), Ovarian tumour (OTU) and Machado-Josephin domain (MJD) superfamilies (Amerik and Hochstrasser, 2004). The catalytic domains of the cysteine protease superfamilies are slightly different, but all have a cysteine and a histidine residue as part of the active site. Other residues that are important include a glycine residue and an aspartate residue although they are not essential (Nijman et al., 2005).

Evolution of E1, E2, E3 ubiquitin enzymes and DUBs

Ubiquitin modifications of target proteins are important for developmental processes in *Caenorhabditis elegans* and four of the 20 nematode E2 enzymes are essential for

embryogenesis. When gene expression is altered, these essential E2 enzymes mainly cause tail malformations (Jones et al., 2002). Outside of developmental biology, genome research has suggested that E3-ligases and DUBs increased in number through eukaryote evolution. Mammals possess higher numbers of E3-ligases and DUBs than *D. melanogaster, C, elegans, S. pombe and S. cerevisiae*. When comparing the ubiquitin-related and unrelated domains in E1, E2, E3 and DUB enzymes, there was a 2.5 fold increase of non-ubiquitin associated domains in the human and mouse E3 enzymes and DUBs. This suggests that mammalian E3's and DUBs coevolved and also developed regulatory functions, other than ubiquitin binding (Semple et al., 2003). This may have aided the evolution of the substrate specificity and allowed a greater degree of regulation in mammals and not in lower eukaryote species.

Ubiquitin in the double-strand break response

Ubiquitin is heavily associated with DNA damage repair (DDR) pathways and plays a major role in the sequential accumulation of proteins at sites of damage. After a double strand DNA break (DSB) is detected, ATM phosphorylates H2AX histones (Burma et al., 2001) which is quickly bound by MDC1. The E3 ligase, RNF8 (Stucki et al., 2005), binds to MDC1 and initiates the ligation of ubiquitin onto the surrounding histones, signalling for the early response DNA damage proteins to accumulate (Huen et al., 2007). H2A and H2AX ubiquitination by RNF8 (Lok et al., 2012) allows RNF168 to accumulate at sites of damage which has E3 ligase activity that amplifies the ubiquitination of the surrounding H2A histones (Doil et al., 2009; Stewart et al., 2009). It has been shown that the E2 enzyme, Ubc13 (VanDemark et al., 2001), specifically forms K63-linked chains on the histones (Plans et al., 2006).

MDC1 and RNF8 are associated in complex with the E3 ligase HERC2 (Bekker-Jensen et al., 2010). HERC2 has been shown to promote the interaction between RNF8 and Ubc13 (Plans et al., 2006; Wang and Elledge, 2007), which allows the specific formation of K63 chains at sites of damage (Campbell et al., 2012), which are required for BRCA1 accumulation (Wang and Elledge, 2007).

BRCA1, an E3 ligase, has many roles in the DDR and associates with ubiquitinated histones via a protein complex with RAP80, Abraxas (Wang and Elledge, 2007), BRE, BRCC36 (Dong et al., 2003), Cdc98 (Liu et al., 2007) and NBA1 (Feng et al., 2009). The central protein of this complex is RAP80 (Kim et al., 2007) which has 3 Ubiquitin Interacting Motifs (UIMs), that confer specificity to K63-linked chains (Sato et al., 2009). Histone ubiquitination also promotes 53BP1 accumulation at sites of DDR (Acs et al., 2011; Mallette and Richard, 2012) although this process is not fully understood.

RNF168 deficiency in RIDDLE syndrome shows altered BRCA1 and 53BP1 accumulation, but not RAD51 recruitment (Stewart et al., 2009), which would suggest that RAD51 may be recruited independently of RNF168 (Mailand et al., 2007). Also, RIDDLE patients do not show altered replication stress, however RNF8 depletion causes replication fork collapse.

This suggests that there may be two DDR pathways that occur after RNF8 ubiquitination; firstly, RNF168-dependent pathway that is associated with K63 chains leading to BRCA1 and 53BP1 recruitment, and secondly, a VCP (Vasolin containing protein)-associated pathway that involves K48 chains and involves RAD51 recruitment (Acs et al., 2011; Ramadan, 2012).

The VCP-UFD1-NPL4 complex is recruited to DSBs by RNF8 (Meerang et al., 2011). RNF8 interacts with UbcH8, an E3 ligase, which can make K48 chains (Lok et al., 2012). The recruitment of VCP is independent of RNF168 and K63 chains and dependent on RNF8 and the formation of K48 chains (Meerang et al., 2011). It has been shown that there is an increase in the accumulation of K48-linked chains at DSBs when VCP is depleted. This suggests that VCP functions to specifically remove K48-linked ubiquitin and it is the interaction between RNF8 and VCP that regulates the turnover of K48-ubiquitin chains at the sites of DSB (Meerang et al., 2011). When looking at recruitment of proteins downstream of RNF8, it was shown that depletion of VCP partially effects BRCA1 and 53BP1, but does not reduce the accumulation of Rad51 (Meerang et al., 2011).

DUBs in the double-strand break response

DUBs have also been shown to be active in the DDR, such as USP3 which, when overexpressed, stops RAP80 and 53BP1 recruitment by deubiquitination of H2A and H2AX histones (Nicassio et al., 2007). The DUB BRCC36 is seen to localise to sites of damage and promotes DDR signalling involved in arresting the cell cycle at the G2/M checkpoint (Dong et al., 2003). BRCC36 regulates the reversal of K63-Ubiquitin chains (Shao et al., 2009) which alters the recruitment of 53BP1. The 19S proteasome DUB, POH1, has been shown to stimulate the cleavage of polyubiquitin chains from H2A histones at sites of DDR and without POH1 the cells become sensitive to DNA damaging agents such as ionising radiation (IR) (Butler et al., 2012). POH1 localises to DNA damage foci where it deubiquitinates K63-linked ubiquitin chains on H2A histones (Cooper et al., 2009). Processing of these chains regulates the accumulation of DNA repair proteins such

as BRCA1, which implicates POH1 in the regulation of homologous recombination (HR) following induction of DSBs.

It has been shown that DUBs can be specific to a particular polyubiquitinated lysine chain. K63 chains create a different structure (Varadan et al., 2004) than K48 ubiquitin chains and USP8 and USP14 cleave only K48 chains (Avvakumov et al., 2006; Borodovsky et al., 2001). Ubp2, a yeast DUB, acts conversely, cleaving only K63 chains (Kee et al., 2005). The specificity of a DUB can regulate the active function of the protein substrate, but in the case of USP8, which acts on NRDP1, it serves as an antagonist to a protein that catalyses its own degradation and regulation (Wu et al., 2004).

Introducing USP50

When DNA damage occurs the levels of polyubiquitin chains at sites of damage increases leading to the accumulation of DDR proteins for repair. These ubiquitin chains are cleaved within a number of hours following damage. In a screen of mammalian DUBs using an antibody specific for polyubiquitin chains, Ubiquitin-specific protease 50 (USP50) depletion was seen to decrease the levels of polyubiquitin chains that accumulated after DNA damage (Figure 1). This suggests USP50 may play a role in maintaining polyubiquitin chains for the effective repair of DNA. The process by which USP50 is potentially protective of ubiquitin chains is currently unknown. The depletion of USP50 also increases γH2AX staining suggesting the occurrence of spontaneous damage (Stone and Morris, unpublished data).

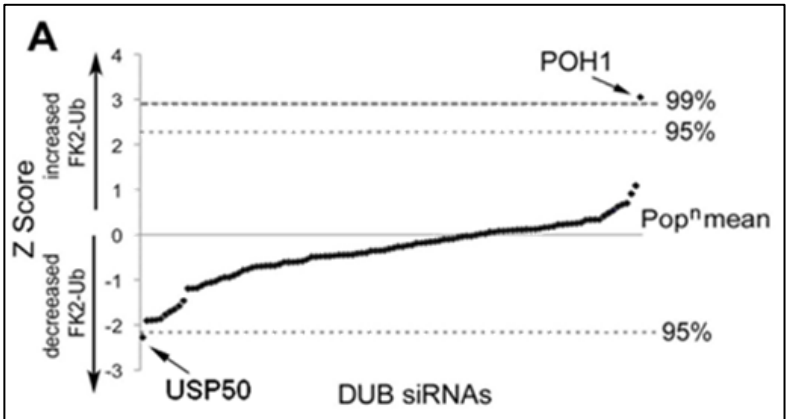

Figure 1 – *Scatter plot of averaged Z scores of FK2 luminescence readings from duplicate library screens of siRNA pools targeting 103 mammalian DUBs. Z-scores indicate the number of standard deviations from the population mean. Negative score indicates pools exhibiting decreased FK2-Ub. 95% and 99% confidence levels are shown. USP50 has a Z-score of >-2 and has a confidence level of over 95%.*

This project focuses on this little-studied DUB, USP50. *USP50* is found on chromosome 15, on the q arm at 21.1 and contains a UCH domain. The UCH domain is a conserved DUB region that contains a catalytic triad around the active site made up of three residues; a cysteine, a histidine and an aspartate residue (Johnston et al., 1999). The thiol group of the cysteine becomes deprotonated by the histidine, which itself is polarised by the aspartate residue. This allows the cysteine to form a nucleophilic bond, replacing the peptide bond between an ubiquitin and the protein substrate, with a bond between the ubiquitin and the DUB. This releases the protein substrate from ubiquitin. A water molecule then stabilises the ubiquitin, releasing it from the DUB (Johnston et al., 1999).

Bioinformatic analysis of DUBs suggests that if one of the catalytic triad is missing then the protein becomes non-functional or inactive (Nijman et al., 2005). USP50 is lacking the aspartate residue of the catalytic triad (Ye et al., 2009) due to a truncation of the protein caused by a nonsense mutation. However, other USPs that lack the aspartate residue, namely USP30 (Nakamura and Hirose, 2008) and USP16 (Kinner and Kalling, 2003), still show some enzymatic activity. This could be due to neighbouring residues stabilising the

histidine residue as in Otubain-2 protein (Nanao et al., 2004). This is not the case with the truncated USP50.

USP50 in the G2/M checkpoint response

There is very little information about the functional aspects of USP50. One paper suggested that USP50 is involved in regulation of Wee1 stability through HSP90, which affects the CDC25B-dependent G2/M checkpoint of cell cycle (Aressy et al., 2010). Wee1, a cell cycle inhibitory kinase that plays a role in ensuring the correct activation of the G2/M checkpoint (van Vugt et al., 2004). USP50 was isolated using another siRNA screen of human DUBs that showed, after DNA damage, an increase in G2/M checkpoint bypass when CDC25B was overexpressed (Aressy et al., 2010). USP50 showed approximately a 1.5-fold increase in illegitimate entry of mitosis following DNA damage. USP50 was shown to be a binding partner of HSP90, a protein that controls the stability of associated proteins by functioning as a chaperone. USP50 depletion caused a loss of Wee1 that allows the increased illegitimate entry to mitosis. Proteasome inhibitors partially rescued the levels of Wee1 (Aressy et al., 2010), suggesting that USP50 has a role in preventing Wee1 from being degraded by the proteasome. Therefore USP50 is involved in specifically stabilising Wee1. The paper looks at the localisation of USP50 in the cell as Wee1 is mainly found in the nucleus, and USP50 is predicted to be a cytoplasmic protein. After damaging cells with double strand DNA (dsDNA) damaging agents they reported that USP50 is relocated from the cytoplasm to the nucleus in response to etoposide and IR. Overall, the paper shows USP50 as a negative regulator of the G2/M checkpoint pathway (Aressy et al., 2010).

USP50 interactors

As specificity of DUBs to protein substrates is important for appropriate regulation of the targeted protein, it is important to look at the proteins that may functionally interact with USP50 as substrate for deubiquitinating activity. The Harper Lab Comparative Proteomic Analysis Software Suite (CompPASS) uses an unbiased comparative approach to identify high-confidence candidate interacting proteins (HCIPs) from Immunoprecipitation-Mass-Spectrometry/Mass-Spectrometry (IP-MS/MS) experiments. They use various statistics and scoring methods to identify possible functional interacting proteins. They performed IP-MS/MS on a screen of 102 human DUBs (Sowa et al., 2009). The Total Spectral Count (TSC) of a DUB interacting proteins from the IP-MS/MS experiment is duplicated with several runs and the protein abundance values from these duplicates feed into the scoring methods, such as the WD (Weighted-Duplicate) scoring method. WD^N (WD number) score relates to the abundance of the protein and its interactor, factoring in the background level of interaction that leads to identifying false interactors and the frequency of the interactor being identified.

The top ten USP50 interacting proteins are shown in the Table 1 with their WD^N scores and a description of their known function.

Most notable of these interactors, is VCP, which is also known as p97 and Cdc48. VCP was originally discovered due to its high abundance in the cell and has been suggested to have a broad range of functions. VCP interacting proteins can be divided into two categories; adaptors, that aid VCP in recruiting many substrates, and substrate processing factors (Ramadan, 2012).

	Interactor	WD^n Score	Full Name	Description
1	DYNC2H1	13.92	Dynein cytoplasmic 2 heavy chain 1	Transports between endoplasmic reticulum and golgi
2	USP50	13.12	Ubiquitin-specific protease 50	Substrate used for experiment
3	LUC7L	6.56	LUC7-like	Implicated in Diasporin pathway
4	IGF2R	5.68	Insulin-like growth factor 2 receptor	Localises proteins from cell surface to the lysosome and endosome
5	AMBRA1	3.81	Autophagy/beclin-1 regulator 1	Positively regulates autophagy. Binds to dynein motor complex related to cell cycle
6	AMOT	2.78	Angiomotin	Binds to USP11 and USP42 and affects BRCA2 and p53 cascades
7	KEAP1	2.44	Kelch-like ECH associated protein 1	E3 ligase. Acts to degrade NRF in anti-oxidant response. Binds USP11
8	CKAP4	2.19	Cytoskeleton-associated protein 4	Binds to APF which has antiproliferative activity. Activity in cell cycle checkpoints. ER localisation
9	VCP	1.29	Valosin containing protein	Ubiquitination control in recruitment of DNA repair proteins
10	ABCD3	1.16	ATP-binding cassette 3	Binds to USP10 and USP32 which affects p53 cascade and related to breast cancer

Table 1 - *The top ten USP50 interacting proteins with their WD^N scores and a description of their known function (Sowa et al., 2009)*

VCP binds to several DUBs such as VC1P135, Otu1, and Ataxin-3. The VCP-UFD1-NPL4 complex, as previously mentioned, has a key role in the regulation of ubiquitin during the DDR (Meerang et al., 2011). VCP accumulation requires K48 chains, which are generated by RNF8 suggesting that there is a K63-independent DNA damage response that involves VCP and possibly USP50. The interaction between USP50 and VCP has not yet been studied but the known cleavage ability of the VCP complex on K48-chains, and the evidence that USP50 depleted cells show a decreased level of polyubiquitin chains and an increase in γH2AX, is intriguing.

Aims of the project

The overall target of this project was to learn more about USP50. The specific aims were as follows:-

1. Use bioinformatic resources to analyse human USP50 to develop an understanding of its structure and function. Also to investigate the evolutionary origin and changes within the gene in reference to its molecular domains and function.
2. Using fluorescence microscopy to examine the localisation of USP50 with and without damaging agents.
3. Using the structural predictions and functions, generate mutated and wild type USP50 vector constructs to make a stable induced-expression cell lines.

METHODS

Unless otherwise stated chemicals and tissue culture supplies were obtained from Sigma (St Louis, MO, USA) and Corning (Corning, NY, USA), respectively.

Materials

DNA

GFP-USP50 plasmid was obtained from OriGene (Rockville, MD, USA)

GFP plasmid was obtained from Clontech Laboratories Inc (Mountain View, CA, USA)

Primers

Primer structure as detailed in protocol. All primers obtained from Sigma-Aldrich (St Louis, MO, USA)

Antibodies

Murine anti-phosphorylated S138 (γH2AX) was obtained from Abcam (Cambridge, UK)

Alexafluor 555 goat anti-mouse was obtained from DAKO (Glostrup, Denmark)

Hoechst was obtained from Sigma (St Louis, MO, USA)

Restriction Enzymes

Restriction enzymes (BamH1 and EcoR1) were obtained from New England Biolabs (Ipswich, MA, USA)

Solutions

Triton -
0.2% Triton in 1x PBS

Sucrose solution-
100 mM NaCl,
300 mM sucrose,
3 mM MgCl2,
10 mM Pipes [pH 6.8],

1 mM EGTA,
0.2% Triton X-100
1x Phosphatase inhibitor tablet
1x Protease inhibitor tablet

HEPES-NP40 buffer-
20mM HEPES pH 7.5
20mM NaCl
5mM MgCl2
1mM DTT
0.5% NP-40
1x Phosphatase inhibitor tablet
1x Protease inhibitor tablet
10mM iodoacetamide

Protocols

Tissue Culture

Cells were maintained in DMEM with 10% FCS and Penicillin/Streptomycin and grown at 37°C, 5% CO_2. Passages were done regularly depending on cell confluence. When cells reached 50% they were passaged following trypsinization at a 3:10 dilution but cells that reached 80% confluence were passaged at a 1:10 dilution.

Transfection protocol

Cells were plated into 24 well plates 24 hours before transfection. The FuGene 6 (Roche, Indianapolis, IN, USA) protocol was used.

SFM (OptiMem (Invitrogen, Grand Island, NY, USA)) was added to each eppendorf before FuGene 6 was added in the quantities in the following table. The eppendorf was mixed by flicking the tube a few times and left at room temperature (RT) for 5mins. The appropriate DNA was added and vortexed for one second. The mix was left at RT for 20mins and

100µl was added to each well without removing the media. Cells were stored in the incubator for 24 or 48 hours before being treated with IR then fixed and stained.

Solution	Quantity per well
OptiMem	96µL
FuGene 6	4µL
DNA (100nM/µL)	1µL

Table 2- *FuGene protocol quantities*

Irradiation of cells

Cells were irradiated in immunofluorescence protocols with 2Gy of IR. Cells that were not irradiated were removed from the incubator and subjected to the same treatment except for the irradiation.

Immunofluorescence microscopy protocol.

Cells were plated into 24 well plates with coverslips approximately 24 hours before transfection of USP50-GFP, GFP or were not transfected as a control.

Cells were fixed and permeabilised in one of the following ways; PFA/Triton, Sucrose solution, Methanol and HEPES-NP40 buffer. Each technique is as follows:-

PFA/Triton-

Cells were fixed for 10mins with PFA (4%) at RT and washed with PBS. Cells were permeabilised using 0.2% Triton/PBS solution for 10mins at RT and washed with PBS.

Sucrose solution-

Cells were placed on ice and treated with sucrose solution for 5mins to fix and permeabilise. Cells were washed with PBS.

Methanol-

Cells were fixed and permeabilised by treating with -20°C Methanol for 3mins and air dried.

HEPES-NP40 buffer-

Cells were treated with HEPES-NP40 buffer to fix and permeabilise and washed with PBS.

Cells were either stored in PBS at 4°C overnight or stained immediately as follows. All cells were fixed with PFA (4%) for 20mins at RT prior to staining. After washing with PBS, 10% FCS/PBS was added to block for 10mins and washed with PBS.

The primary antibody was added at RT for one hour. The primary antibody was phosphorylated S138 mouse anti-γH2AX at a dilution of 1:5000 in 10% FCS/PBS. After staining the cells were washed twice with PBS.

The secondary antibody was added at RT for one hour. The secondary antibody was red goat anti-mouse at a dilution of 1:2000 in 10% FCS/PBS. After staining the cells were washed twice with PBS.

Cells were stained with Hoechst/PBS solution for 2mins at RT and washed twice with PBS.

Cells were fixed again with PFA (4%) for 10mins.

The cells were then mounted onto slides with Dako Fluorescence Mounting Medium DAKO (Glostrup, Denmark) and coverslips were sealed with clear nail varnish. Slides were stored at 4°C in the dark until assessed with a microscope.

The two cell localisation experiments had different protocols. The cell localisation experiment involved all of the previously mentioned fixing and permealibisation techniques and the time course cell localisation experiment involved only the PFA/Triton protocol.

Restriction Digest

This protocol was used to digest the DNA constructs for ligation into expression vectors. The following solutions were made in the stated quantities and put in a 37°C incubator for 2 hours.

Solution	Double Digest	Single Digest 1	Single Digest 2	Uncut
Xho1	1µL	1µL	0	0
BamH1	1µL	0	1µL	0
Buffer x10	1µL	1µL	1µL	1µL
BSA (10x)	1µL	1µL	1µL	1µL
DNA	2µL	2µL	2µL	2µL
dH_2O	4µL	5µL	5µL	6µL
Total	10µL	10µL	10µL	10µL

Table 3- *Restriction digest protocol quantities*

Primers

Several constructs were made to examine the functional regions of USP50. The following primers were used the following standard PCR reaction using Phusion (Fermentas, St. Leon-Rot, Germany) polymerase.

Primers for USP50-USP8-tail construct	
Usp50_8_tail_F	GAATTCAGTCACCCAGGCCTGGTTTAAGTTTGATGATCATGAA GTTTCTGATATCTCCGTTTCTTCTGTGAAATCTTCAG
Usp50_8_tail_R	TTCTCGAGTTATGTGGCTACATCAGTTACTCGTGGTCCCAATG AAGTATAAAAGAGGATATAAGCTGCTGAAGATTTCAC
Primers at the start and end of USP50	
pET_F_BamH (Start primer for pET28a)	ATGGGTCGCGGATCCTTTACTTCTCAGCCGTCTCTCC
pc5_F_Bam_flag_50 (Start primer for pcDNA5)	GATCCGGATCCATGGATTATAAAGACCATGACGGAGATTATA AAGATCACGACATCGACTACAAGGATGACGATGACAAG
pC5_R_Xho_50 (End primer suitable for both vectors)	ATTCTCGAGCTCGAGCTAGGCCTGGGTGACTGAATTCTTGC
Primers to create deletions 1 and 2	

186_Rev_50_del1	CAGCTCTTGGCAACCTCTATCCGGCTTTTACG AAAAAGATGCAACAAG
203_Fwd_50_del1	CCCAGCTGTTTGAAGAGCAGCTCAATGTCTT CACTGTCTTCTCACTCCCC
236_Rev_50_del2	GTTGTTCCAGGTCAGTGCG
253_Fwd_50_del2	CGCACTGACCTGGAACAACGCCAGTATTTCC AAAGCACC

Table 4- *Primer names and sequences*

Cloning and PCR

Solution	Quantity per well
5x PCR buffer	10µl
4M Betaine	10µl
20µM dNTPs	0.5µl
Phusion enzyme	0.5µl
20µl Forward primer	2µl
20µl Reverse primer	2µl
100nM Template DNA	1µl
dH_2O	24µl
Total	50µl

Table 5- *PCR protocol quantities*

PCR programme

The denaturing step was 95°C for 30 seconds (s). The annealing temperature was based on the lowest of the primers which was 42°C for 30s. The elongation temperature was 72°C for 3 mins for the first step of making the constructs and 5 mins for all other steps of PCR that were needed to make the full length USP50 constructs. This cycle was repeated 30 times and kept at 72°C for 10 mins. Reactions were stored until use at 4°C.

The constructs were made for between 8-10 tubes per reaction to make bulk of each construct. The controls for each PCR were one sample with no DNA, one sample with only the forward primer and one sample with only the reverse primer.

Agarose gel (1%) and gel electrophoresis

TAEx1 Buffer	250ml
Agarose powder	2.5g
Ethidium Bromide	2.5µL

Table 6- *Agarose gel recipe quantities*

TAEx1 buffer and Agarose, as listed above, were added to a conical flask and heated until the agarose melted. Once partially cooled, Ethidium Bromide was added and poured into a prepared gel mould with combs. The gel was left to set and placed into a gel electrophoresis tank in TAE running buffer. The gel was run at 130V and run until the bands separated.

Gel purification

Gel purification experiments followed the QIAGEN® QIAquick Gel Extraction Kit protocol (September 2010).

Phenol: Chloroform clean up

200µL of Phenol Chloroform solution was added to 200µL of DNA construct solution. They were vortexed for 10s and microcentrifuged for 15mins at 13,000 rpm at RT. The top layer from the centrifuged tubes was added to a new eppendorf and 10% of 3M sodium acetate ($C_2H_3NaO_2$) was added and vortexed. The samples had 100% ethanol added to the eppendorf (2.5 x ($C_2H_3NaO_2$ + sample)µL). The samples were centrifuged for 15 mins at 13,000 rpm at RT and the supernatant was discarded. 1ml of 70% Ethanol was added to the samples before centrifuging at 13,000 rpm for 25 mins. The supernatant was removed and the eppendorf was left to dry before resuspending in 10µL of deionised water.

Bioinformatics site uses

NCBI BLAST, iTOL and CCDS were used to search the nucleotide sequences of USP50 and USP8 and the results were used for figures.

The Ensembl Project website was used to search for either USP50 or USP8 and information was used for figures.

SwissPDB website was used to predict the structural model of USP50 and USP8.

SwissPDB Viewer was used to visualise the downloaded structural models and to overlay the structures.

The Interactive Tree of Life (iTOL) was used to create phylogenetic trees of USP50 from various species.

RESULTS

The domains and active sites of USP50

As previously mentioned, USP50 has not been studied in great detail and to understand its functionality, or lack of, more analysis was needed into the gene origin, the genomic location and protein structure and domains.

The nucleotide sequence of USP50 was searched using the NCBI BLAST database (Camacho et al., 2009) which predicted the domains and active site in *USP50* (Supplementary Figure 1). The UCH domain (DUB catalytic domain) maps from aa41-334 and the active site residues are located at aa47 and 322. The nucleotide search found other genes that showed similarity or conserved regions to USP50. The gene with the highest similarity in sequence was USP8.

USP8 was also searched using the NCBI BLAST database (Supplementary Figure 2), *USP8* gene is larger than *USP50* and they share a UCH domain and the active site. *USP8* possess two active sites which are a DUF1873 superfamily domain and a RHOD superfamily domain.

The amino acid sequences for USP8 and USP50 were aligned using NCBI BLAST and CCDS (Camacho et al., 2009; Pruitt et al., 2009) and the conserved domains containing the active site and catalytic residues were mapped (Supplementary Figure 3). The third residue of the catalytic triad (aspartate residue) is missing from USP50 as the C-terminal end of USP50 is truncated. The truncated region of USP50 and its correlating region in USP8 will be referred to as the 'tail' region for simplicity. USP50 lacks one of the catalytic residues of the protein therefore is predicted not to possess deubiquitinase activity (Nijman et al.,

2005). Figure 2 shows the alignment of USP50 against USP8 from the catalytic histidine residue to the aspartate residue. It shows the single nucleotide change that caused the stop codon which truncates USP50. A single mutation would remove the stop codon and produce a protein product that contains an aspartate residue that would complete the active site.

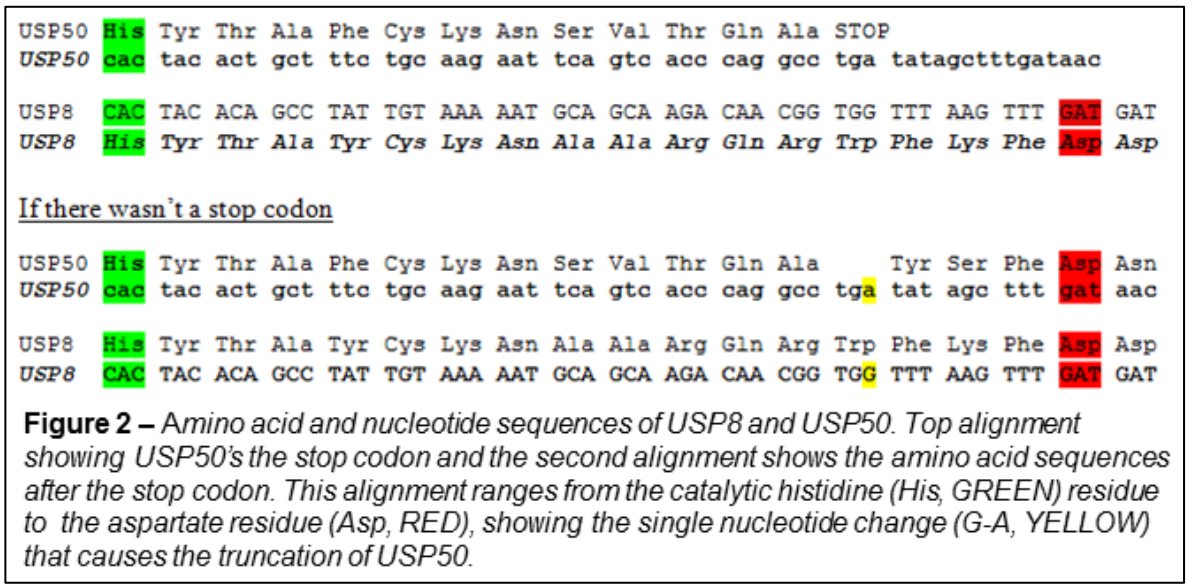

Figure 2 – *Amino acid and nucleotide sequences of USP8 and USP50. Top alignment showing USP50's the stop codon and the second alignment shows the amino acid sequences after the stop codon. This alignment ranges from the catalytic histidine (His, GREEN) residue to the aspartate residue (Asp, RED), showing the single nucleotide change (G-A, YELLOW) that causes the truncation of USP50.*

The evolutionary relationship between USP50 and USP8

The *USP50* gene was searched using The Ensembl Project website (Flicek et al., 2012). *USP50* is located on human chromosome 15 (chr15) (Supplementary Figure 4). Strikingly, *USP50* is located next to *USP8* on chr15. *USP8* is transcribed from the forward strand and *USP50* transcribes from the reverse strand, with a slight overlap of the end of the gene sequences (Figure 3). The high similarity of sequence between *USP8* and *USP50*, and the positioning on chr15, suggests that they may have originated from a single ancestral gene that has been duplicated and has diverged. This is supported by Ye *et al*, who studied the

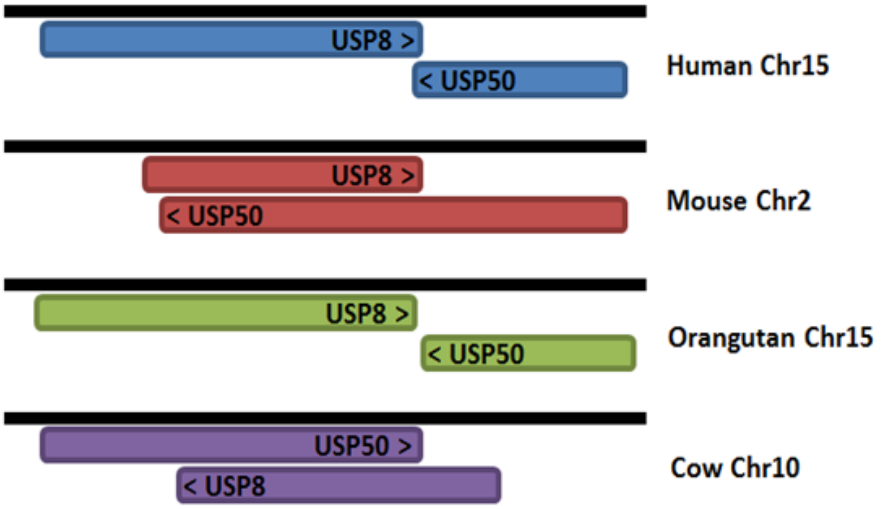

Figure 3 – *Comparative gene localisation of USP50 and USP8 on human chr15, mouse chr2, orangutan chr15 and cow chr10. Orientation of USP50 and USP8 are similar in orangutan and in mice, but there is more overlap of the two genes. In cows USP50 is on the forward strand and USP8 is on the reverse strand, unlike in humans.*

relationship between of human and yeast USP enzymes produced a phylogenetic tree showing *USP50* is closely related to *USP8* (Ye et al., 2009).

The chromosomal positioning of *USP8* and *USP50* were compared between humans and mice (Figure 3 and Supplementary Figure 5). *USP50* and *USP8* are on the same chromosome in mice and are on opposing strands, but the overlap of *USP50* and *USP8* is greater on the mouse chr2 than the human chr15. This is suggestive of a small lengthening of the DNA that caused human *USP50* and *USP8* to overlap less.

In orangutans *USP50* and *USP8* have a similar degree of overlap of *USP50* and *USP8* in humans (Figure 3). In other species such as the anole lizard, *USP50* and *USP8* do not overlap but are still on opposing strands and adjacent on the same chromosome. In cows, *USP8* and *USP50* are both on chr10 and in opposing directions, but *USP50* is on the forward strand and *USP8* is on the reverse strand (Figure 3). The comparison between species shows that this part of the genome has seen several changes in structure through evolution because of the various positions of *USP8* and *USP50*.

USP50 orthologs are not present in all chordates but are found in mammals, lizards and arthropods (Figure 4 and Supplementary Figure 6) (Camacho et al., 2009). *USP8* has homology in species which diverge as far back as yeast (Flicek et al., 2012; Pruitt et al., 2009) (TreeFam.org, TF106277, data not shown). This would suggest that *USP50* is a paralog of *USP8* that was duplicated at the level of chordate divergence.

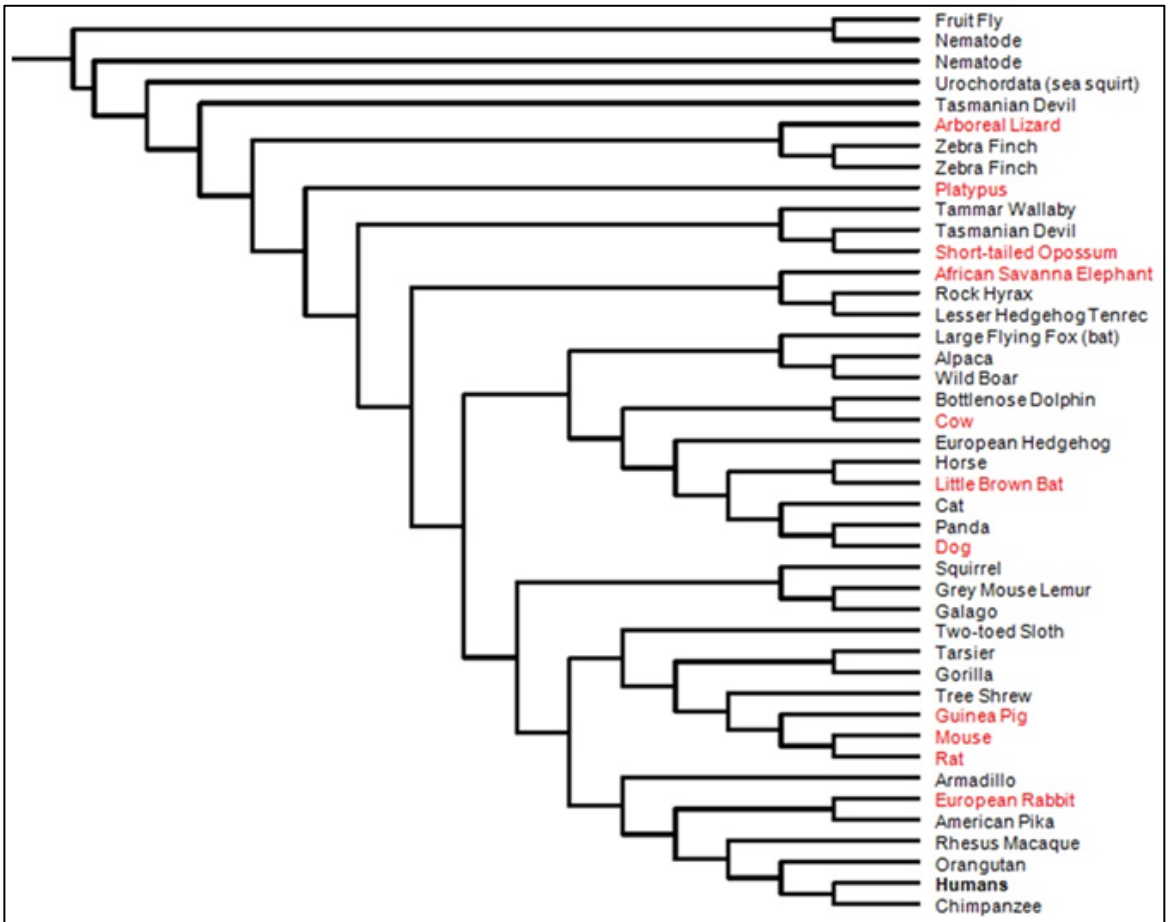

Figure 4 – *Phylogenetic tree of USP50 orthologs showing the divergence of the gene across species. Human USP50 position is highlighted in BOLD and the USP50 orthlogs that are not truncated, like human USP50, are in RED.*

The 'tail' region truncation of USP50

The 'tail' region is absent at the protein level in USP50 in many species but present in USP8 and some orthologs of USP50. The presence of the truncation in multiple species

confirms the human USP50 sequence truncation is valid and not due to a sequencing error. To locate the ancestral lineage point where the truncation occurs, the conserved regions of USP50 from all species were aligned and the catalytic trial residues were labelled to separate the orthologs into those with and without the catalytic aspartate residue (Figure 4, Supplementary Figure 6 & 7). There was no alignment on a phylogenetic tree of the 'tail' region sequence suggesting that there was not a single evolutionary event followed by divergence that truncated the 'tail' of USP50, as species known to be ancestrally close did not align closer together (Supplementary Figure 8). This data suggests the truncation event has occurred in multiple species.

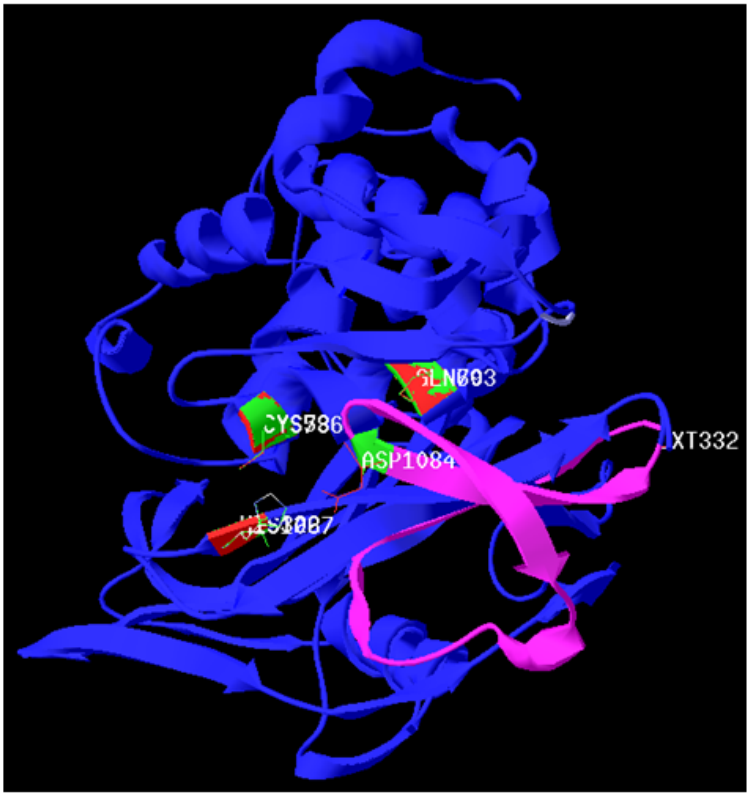

Figure 5 – *Structural alignment of USP8 and the predicted alignment of USP50, with the catalytic residues (cysteine= CYS53(USP50) /CYS786(USP8), histidine= HIS322(USP50)/HIS1067(USP8), aspartic acid= ASP1084(USP8)) and the associated glycine (GLN60/GLN703) labelled highlighted in GREEN (USP8) or RED (USP50). The blue is representative of the structures of both USP8 and the predicted USP50. The last residue (OXT332) of USP50, before the stop codon, is also labelled. The tail of USP8 is coloured PINK from where it extends beyond USP50.*

The structure of USP50 and USP8

SwissPDB was used to predict the structure of USP50 as USP50 protein has not been identified. The amino acid sequence of USP50 was threaded on to the known structure of the

catalytic domain of USP8 (PDB: P40818) (Figure 5 & Supplementary Figure 9) (Avvakumov et al., 2006).

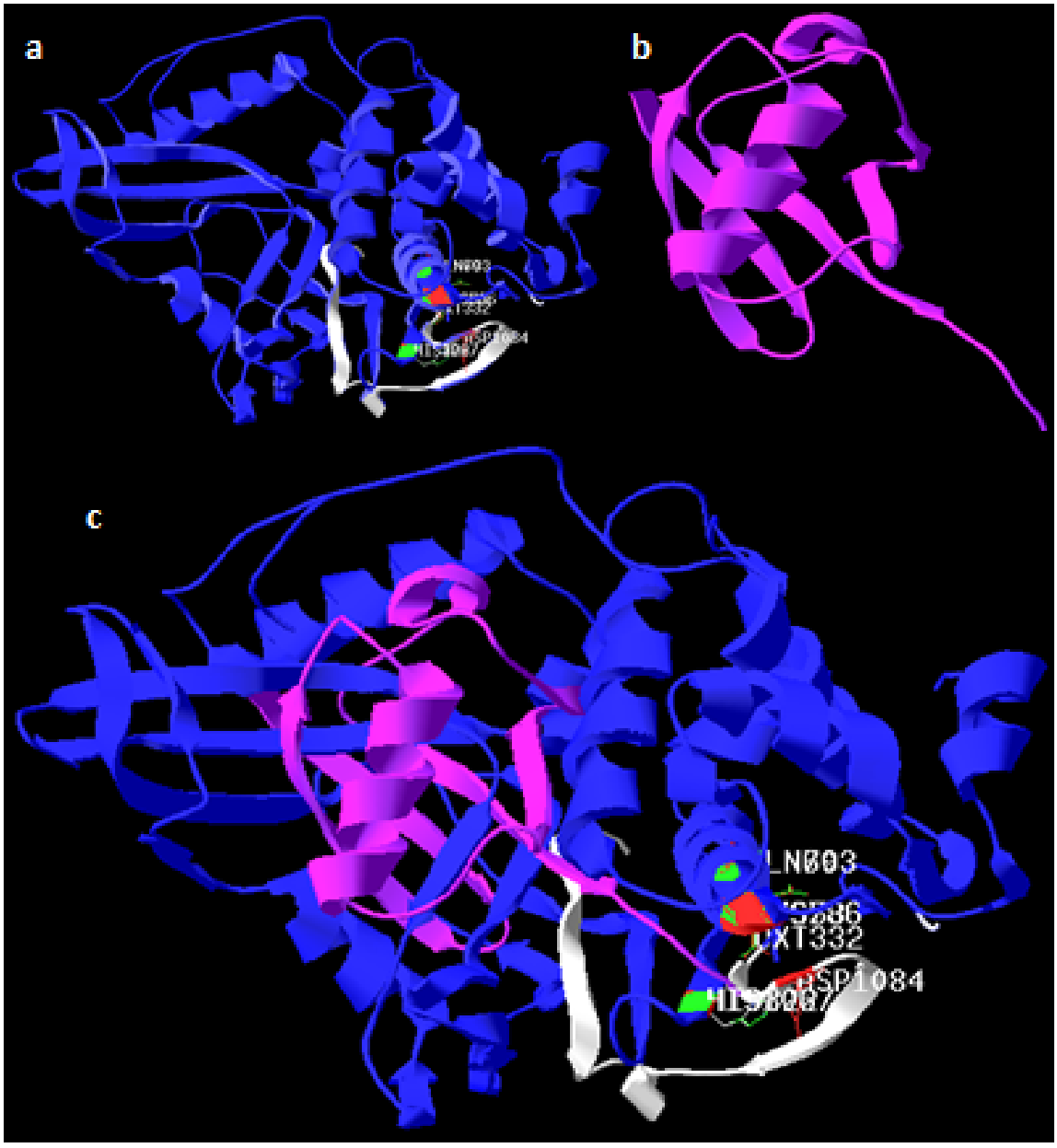

Figure 6 – *Structural models of ubiquitin with USP50 and USP8. (a) Structural prediction of the alignment of USP50 and USP8, orientated to show the site where ubiquitin binds and the fingers domain. The tail region of USP8 is labelled in WHITE. (b) Structural model of ubiquitin showing the tail region that protrudes into the UCH active site in USP DUBs. (c) Structural prediction of the alignment of USP50 and USP8, orientated to show ubiquitin (PINK) binding in the fingers/palm domains.*

The structure of USP50 was modelled and labelled with catalytic residues, associated non-essential glycine residue and the final amino acid: to highlight where the truncation occurs Figure 5 and Supplementary Figure 9). USP50 prediction and USP8 were overlaid to compare the two active sites and two tail structures (Figure 5), the combined structures shows the USP8 tail curves back to place the aspartate residue in the active site and that without the tail the active site is more open. Other DUBs have conformational changes that move the tail region which realigns the catalytic domain (Hu et al., 2002). Considering this, the missing catalytic residue and the truncation of the tail may have an additive effect on the predicted inactivity of USP50.

To examine the relationship with ubiquitin in more detail the positioning of ubiquitin in the active site was predicted using structural models of DUBs binding to ubiquitin and crystal structures of DUBs that were isolated bound with ubiquitin, such as USP14 (Borodovsky et al., 2001), HAUSP (Hu et al., 2002) and USP2 (Renatus et al., 2006). Figure 6a shows the overlaid USP50 and USP8 at an angle where the finger structural region is visible. Ubiquitin (modelled from USP14 (Borodovsky et al., 2001) and ubiquitin crystal structure, PDB: 2AYO) (Figure 6b) sits in the middle of the structure with its tail region passing between the palm and thumb into the active site (Figure 6c). USP50 is highlighted with the catalytic residues of the active site where ubiquitin is predicted to bind, which is analogous to 'holding ubiquitin in the palm of a hand' (Figure 6 & Supplementary Figure 10) (Ye et al., 2009).

The modelled structure of ubiquitin and USP50 predicts, that when ubiquitin binds, the ubiquitin tail protrudes into the catalytic triad (Figure 7a) where it lies between the cysteine

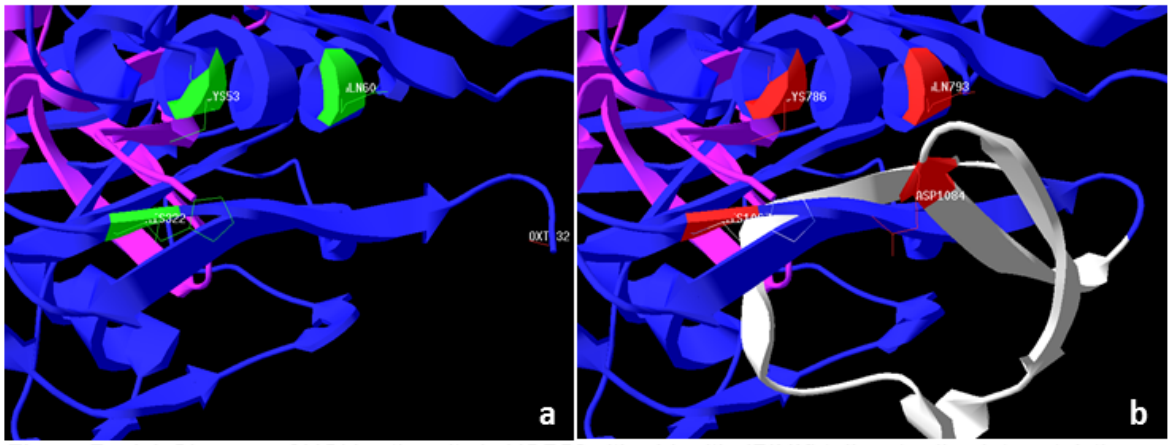

Figure 7 – (a) *Close up of UCH active site in USP50 with ubiquitin (PINK) tail protruding into catalytic triad. The two catalytic residues (cysteine= CYS53, histidine= HIS322) and the associated glycine (GLN60) labelled highlighted in GREEN. The last residue (OXT332) of the protein, before the stop codon, is also labelled.* ***(b)*** *Close up of UCH active site in USP8 with ubiquitin tail protruding into catalytic triad. The catalytic triad residues (cysteine= CYS786, histidine= HIS1067, aspartic acid= 1084) and the associated glycine (GLN793) labelled highlighted in RED. The tail of USP8 is coloured in WHITE.*

and histidine residue, but when USP8 is overlaid (Figure 7b) the difference in the tail structure directly around the active site, can be seen (This model has been rotated in Supplementary Figure 11 to show the ubiquitin tail in the centre of the catalytic triad). The tail can be seen to provide a curl of protein that covers the active site. The curl structure of β-sheet-turn-β-sheet, on which the aspartate residue is located, covers the open side of the protein. Figure 8 is a planar view of the active site in USP8 and shows the distance between the side chains of the catalytic triad and the ubiquitin tail. From this analysis into the structural positioning of the catalytic triad and the

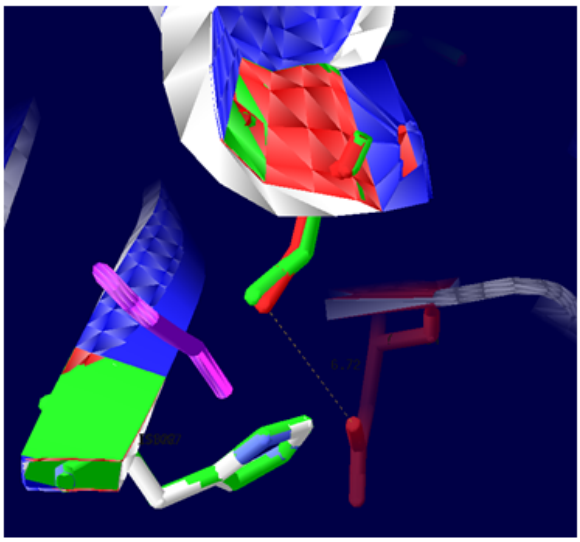

Figure 8 – *Planar view of USP8 active site showing the distance between catalytic triad residues (top protrusion in GREEN and RED= cysteine residue, left protruding ring in BLUE, GREEN and WHITE= histidine residue and right RED protrusion= aspartic acid) and ubiquitin (left protrusion in PINK).*

'tail' region of USP8 and USP50 (Camacho et al., 2009), we suggest that if the 'tail' region of the USP8 protein were to be attached to the end of USP50 protein then the function of USP50 may be altered due to the restoration of the catalytic triad and any supportive element the 'tail' structure may provide.

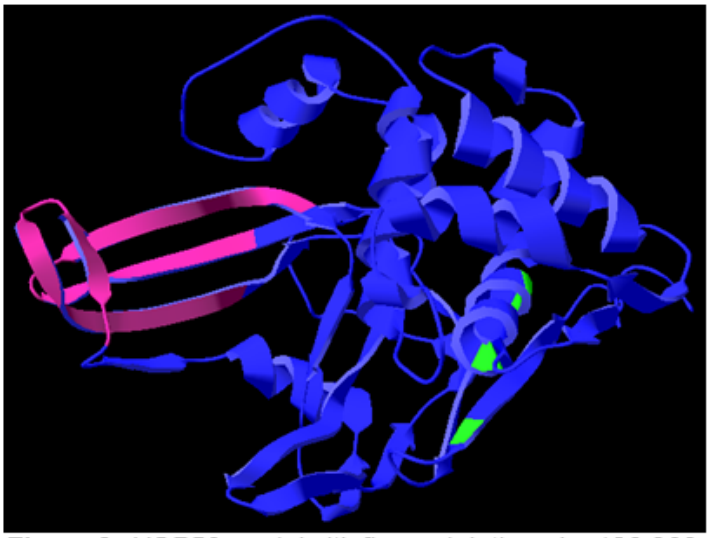

Figure 9- *USP50 model with finger deletions (aa186-203 and aa236-253) highlighted in PINK.*

The model of USP50 and ubiquitin suggests that ubiquitin interacts with the finger regions of DUBs and certain residues on the fingers are highly conserved for this reason (Hu et al., 2002). A mutation in the finger regions of USP50 could influence the binding ability of ubiquitin and the conserved finger regions in USP50 could be deleted using two deletions from aa186-203 and 236-253 (Figure 9 & Supplementary Figure 12 a&b).

Localisation of USP50 in U20S cell line

Very little is known about USP50 localisation in cells and two previous attempts to create constitutively USP50-GFP expressing cell lines failed. They showed abnormally high levels of cell defects. Aressy *et al*, suggested that USP50 translocates from the cytoplasm to the nucleus upon DNA damage (Aressy et al., 2010). To investigate this further; U20S cells were transfected either USP50-GFP or GFP vector. 16 hours after transfection cells were irradiated, or left unirradiated and were fixed and permeabilised using various buffers (HEPES-NP40 buffer, Sucrose buffer, Methanol or PFA/Triton method). First cells were

incubated with *murine* anti-phosphorylated S138 (γH2AX) antibody and Alexafluor 555 goat anti-mouse antibody, and counterstained with Hoechst to visualise DNA. Cells expressing GFP were counted (n=100) and the cellular localisations (Supplementary Figure 13), and number of GFP expressing cells showing karyorrhexis (breaking up of the nucleus, characteristic of cells undergoing apoptosis), was recorded and are shown in Supplementary Figure 14. The number of GFP positive cells showing karyorrhexis were counted due to previous cell death seen in cells overexpressing USP50.

The localisation of GFP expression was spread evenly throughout the cytoplasm and nucleus in GFP-transfected cells and there was no difference between irradiated cells and non-irradiated. The USP50-GFP was mainly expressed in the cytoplasm, but also showed pancellular localisation. The cells with USP50-GFP expression throughout the cell did increase on irradiation but not significantly. The level of karyorrhexis in irradiated GFP transfected cells was higher than in the non-irradiated, however this was converse in the USP50-GFP transfected cells.

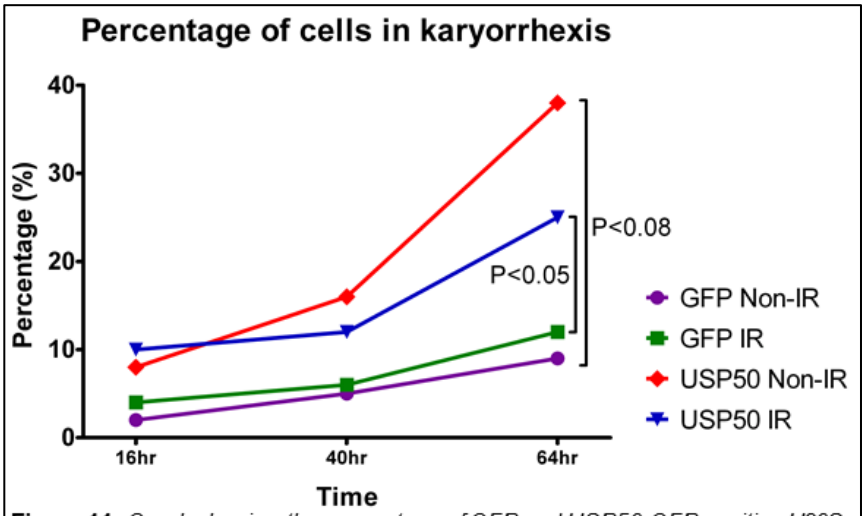

Figure 11- *Graph showing the percentage of GFP and USP50-GFP positive U20S cells that are positive for karyorrhexis. The conditions include before and after ionising radiation (IR) and fixed at three time periods after transfectionand IR; 16, 40 and 64 hours.*

A time course experiment was used to examine cell localisation of USP50-GFP and GFP in U20S cells that were transfected with GFP or USP50-GFP. Cell were

separately irradiated at 16, 40 and 64 hours after transfection, then fixed and permeablised. GFP positive cells, in comparison to background levels of fluorescence, were scored for cellular localisation and the presence of karyorrhexis (Figure 10).

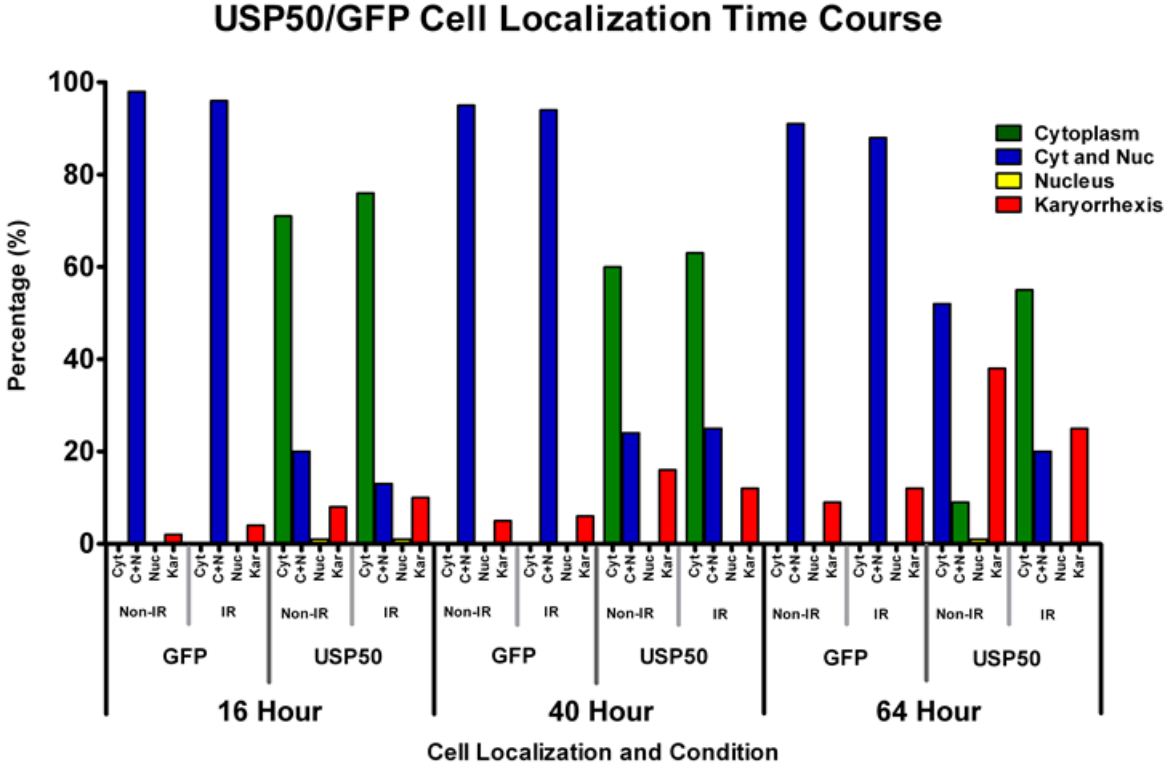

Figure 10- *Graph showing the localisation of GFP and USP50-GFP in U20S cells before and after ionising radiation (IR) given at three time periods after transfection; 16, 40 and 64 hours. The percentage of cells represents the count of 100 cells (n=100).*

Predominantly the localisation of GFP and USP50-GFP was identical to the previous experiment but the level of cells showing karyorrhexis rose with the length of time after transfection. The percentage of karyorrhexis for each time point was higher in USP50-GFP transfected cells than the GFP transfected cells. In the 40 and 64 hour experiments, there were more GFP-positive cells showing karyorrhexis that unirradiated than in irradiated cells (Figure 11). GFP transfected cells in all time course experiments showed irradiated cells to have higher levels of nuclear defects.

These experiments suggest that USP50 expression is damaging to the cells and that USP50-GFP non-irradiated cells are more defective than irradiated, which in converse to what would be expected and what is seen in the GFP transfected cells. This data shows a small amount of pancellular USP50 localisation which increase on irradiation, but not comparable to the literature (Aressy et al., 2010).

Cloning USP50 mutants

From these observations, we decided to clone several mutant versions of USP50 into inducible expression vectors to create the expression of USP50 in an induced and titratable manner, and to test the structural mutants identified in the analysis with USP8. In addition, cloning products were designed to incorporate the tail of USP8 onto USP50. Stable inducible cell lines will allow USP50 to be expressed in human cells without causing the cellular defects and death that made USP50 effects difficult to measure in the cellular localisation experiments.

Previous studies exmaining the binding of ubiquitin and USP enzymes have identified regions in the finger structures and between the thumb and palm that are conserved and hydrophobic (Hu et al., 2002). The hydrophobic nature of these areas is interesting as they are on the open side of the protein, and in most proteins this is considered to be a possible interaction site as hydrophobic residues will bind more readily to other proteins than hydrophilic residues. There are two hydrophobic regions in USP50 similar to USP enzymes, and we considered that deletion of these regions may affect USP50's ability to bind to ubiquitin. These conserved finger regions are shown in Figure 9. These regions range from amino acid (aa) 186-203 and 236-253. The second set of cloning products involved deleting the two predicted hydrophobic ubiquitin interacting regions of USP50.

Deletion 1 ranges from aa 186-203 and deletion 2 ranges from 236-253. Finally, two full length wild-type USP50 cloning products were for control purposes and to create stable cell lines. The pcDNA5/FRT/TO vector was utilised because it is an inducible expression vector.

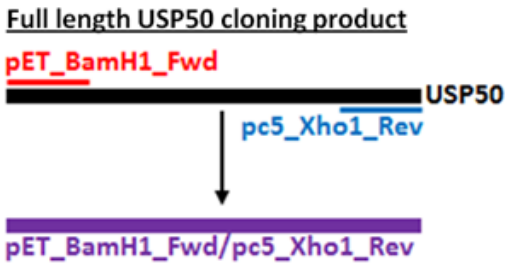

Figure 12- *Diagram of control USP50 cloning product formation. Forward primers are in RED, reverse primers are in BLUE and products are in PURPLE.USP50 DNA template is in BLACK.*

After each PCR step, products were subjected to electrophoresis with controls, to check the size. The correct sized bands were then excised and purified. The purified product was analysed by electrophoresis to confirm size, purification and presence before continuing with the next PCR cloning stage (Supplementary Figure 18 & 19).

The two full length (FL) cloning products were created using the vector specific forward primers (pET_BamH1_Fwd and pc5_Flag_Fwd) with the USP50 reverse primer (pc5_Xho1_Rev) (Figure 12 & Supplementary Figure 15).

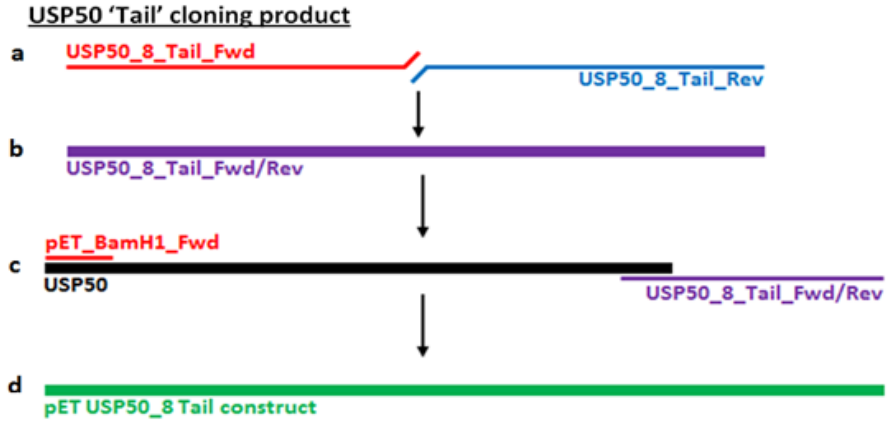

Figure 13 - *Diagram of USP50_8 Tail formation. Forward primers are in RED, reverse primers are in BLUE and tail product is in PURPLE. USP50 DNA template is in BLACK and final product is in GREEN. (a) the annealing section of the two primers, (b) the first PCR product, (c) the first PCR product used as a primer, and (d) the full USP50 product with the tail of USP8 attached, the final PCR product.*

The USP50/8 tail cloning products (Figure 13 & Supplementary Figure 16) were

made using the USP50_8_Tail_Fwd primer and USP50_8_Tail_Rev primer which creates a fragment of the end of USP50 and the USP8 tail (Supplementary Figure 18). This was termed USP50_8 Tail and used as a primer with the vector specific forward primers and USP50_8_Tail_Rev to create USP50 with the added USP8 tail region (Supplementary Figure 19).

The USP50 deletions were created in two stages using overlapping primers (Figure 14 & Supplementary 17). Firstly, the fragment before the deleted region was created, using the vector specific forward primers and either the 186_Rev or the 236_Rev primer. Secondly, the fragment after the deleted region was created using the USP50 reverse primer and the 203_Fwd or 253_Fwd primer. The primers were designed to overlap to bridge the gap over the deleted region, and used to create products of USP50 with either deletion 1 (aa186-203) or deletion 2 (aa236-253).

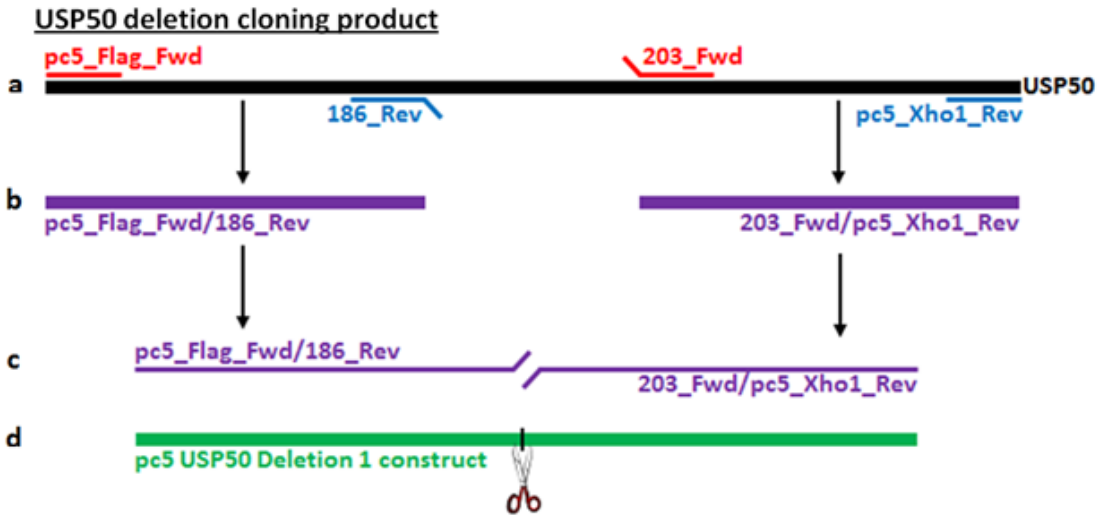

Figure 14- *Diagram of USP50 deletion 1. Forward primers are in RED, reverse primers are in BLUE and tail is in PURPLE. USP50 DNA template is in BLACK and final product is in GREEN. (a) the location of the forward and reverse primers for deletion 1, (b) the first PCR product for deletion 1, (c) the two products from the first PCR used to anneal together, and (d) the USP50 deletion 1 product.*

Both forward primer sequences include BamH1 site and the 5' coding region of USP50. The pc5_Flag_Fwd primer also includes 3x FLAG tag sequences to allow the low expression of USP50 to be better visualised in cells. The pET_BamH1_Fwd vector was used with USP50-GFP to include GFP labelled USP50 into the cloning product. pc5_Xho1_Rev primer sequence covers the 3' end of USP50 and incorporates a Xho1 restriction enzyme site. These primers were used with either USP50-GFP or Flag-USP50 cDNA in a PCR to synthesize the USP50 cloning products

The final cloning products were amplified using PCR and cleaned up with Phenol:Chloroform. The cloning products and vector DNA were digested using Xho1 and BamH1 and cleaned up by Phenol:Chloroform. The samples and vectors, including experimental controls, were electrophoresed to check for their presence (Supplementary Figure 20 & 21). The success of the cloning products at each stage are detailed in Table 7.

The PCR products successfully made were; pET control USP50, pc5 USP50_8 Tail, pET USP50 Deletion 1 and pc5 USP50 Deletion 1 (Supplementary Table 1).

DISCUSSION

The bioinformatics investigation of USP50 has shown that it is closely related to USP8, USP50 is truncated by a stop codon that causes loss of a catalytic residue in its UCH domain and has identified the finger regions of USP50 as being involved in ubiquitin binding. The cell localisation experiments have shown that USP50 mainly localises to the cytoplasm, and there was an increased rate of karyorrhexis in USP50 transfected cells compared with controls. Surprisingly, there is less karyorrhexis in cells that have been irradiated than unirradiated cells.

The early literature that identified all known DUBs suggested that USP50 is catalytically inactive due to the loss of the Asn/Asp residue of the catalytic triad. However, Aressy et al 2010 suggests USP50 associates with G2/M cell cycle checkpoint signalling proteins. USP50 stabilizes HSP90, allowing Wee1 to activate the G2/M checkpoint through CDC25B. When USP50 is depleted, illegitimate entry to mitosis increased ~1.5 fold. This could explain the high levels of nuclear karyorrhexis that is seen over time in the cellular localisation experiments. Without accurate G2/M checkpoint signalling, cells continue into mitosis with DNA damage, and this causes aberrant segregation in mitosis, DNA defects and karyorrhexis. This leads to micronuclei formation and through several cell cycles would lead to mitotic catastrophe. This DNA damage and cell death would be expected to be greater in cells treated with IR. The evidence from Aressy ((Aressy et al., 2010) and the data shown here, suggests that USP50 is functional but may not be an active deubiquitinase.

Aressy et al, shows USP50 relocating to the nucleus after damage. Although our cellular localisation experiments could not reproduce the same results at identical levels of IR, it is likely that it does relocate because of its function with HSP90 in G2/M cell cycle checkpoint which occurs in the nucleus. The association with the G2/M checkpoint signalling and the alteration of the quantity of ubiquitin chains after DSB induction suggests evidence that USP50 is either present in the nucleus, even without containing known nuclear import sequences, or regulating nuclear factors that orchestrate these effects. However, when looking at the interactors of USP50, the 11th most potent interactor is nucleoporin 214kDa (NUP214), a nucleopore complex protein that is part of a nucleoporin subcomplex. This could explain how USP50 relocates into the nucleus and further research using NUP214 overexpression may show an increase in USP50 in the nucleus.

VCP was found to be in the top ten interactors of USP50. VCP is needed for Rad51 accumulation which is crucial for replication fork restart and HR, so without VCP replication forks would collapse into DSB and HR would be faulty. The increase in γH2AX signal without damage when USP50 is depleted, may be due to not resoluting DSBs due to the alteration of ubiquitin chains, this could be indicative of spontaneous damage or of aberrant DDR signalling. The loss of Rad51 loading due to faulty VCP would lead to an increase in γH2AX signal without DNA damage in replicating cells. This could indicate that USP50's interaction with VCP may be involved in Rad51 accumulation.

The overexpression of USP50 may also affect its' activity in the DSB response. It could cause an overprotection of ubiquitin chains and this may cause persistent repair protein accumulation and delay damage repair. Interestingly, levels of karyorrhexis is lower in cells that had been irradiated compared to those that were not irradiated, which is opposed to

what was seen in the control GFP cells. This could be that the overexpression of USP50 in irradiated cells is less toxic because it is active in DNA repair or cell cycle checkpoint signalling, which is not active in unirradiated cells.

The polyubiquitin signal reduction on USP50 depletion suggests that USP50 may have a protective role with ubiquitin chains at sites of DNA damage, as it does not appear to cleave ubiquitin linkage bonds. The finger deletion constructs will identify if they are important in USP50 for binding to ubiquitin and could suggest the catalytic domain may not be essential for ubiquitin binding. The USP50 construct with USP8 tail will be able to identify if restoring the catalytic domain allows deubiquitinase activity or changes the binding activity to ubiquitin.

It would be interesting to investigate the binding region on USP50 that interacts to stabilise HSP90 as USP8, USP50's evolutionary homologue, also functions to stabilize NRDP1, an E3 ligase. It would be interesting to see if USP50 interacted and stabilised an E3 ligase like USP8, as it is involved in protecting ubiquitin chains.

The binding partners and similar functions of USP50 and USP8 could provide more evidence on the coevolution of DUBs and their specific substrates, considering that both USP50 and USP8 are known to function by stabilising a substrate to enable its function and they are very closely related genes. USP50 is smaller than USP8 and several domains are missing, it would be interesting to see which domains link to which functions in both USP8 and USP50. This could lead to a more in depth study to exactly how the changes from USP8 to USP50 adapt to serve a new function separate to USP8's activity.

It is difficult to predict, on such little evidence how USP50 directly acts in the DSB repair pathway. One idea is that the reduction in FK2 signal is indicative of less polyubiquitin

chains accumulating after damage suggesting USP50 has a protective role on the ubiquitin chains. VCP is an interactor of USP50 and is associated with a RNF8-dependent, RNF168-independent DSB repair pathway that is associated with Rad51 recruitment. It is the VCP complex that is needed for K48 chain removal, which allows K63 chain elongation and this recruits HR proteins such as BRCA1. If USP50 protects K48 chains then when USP50 is depleted, VCP would decrease K48 chains and K63 chains would accumulate, therefore still producing a FK2 signal. If USP50 protects K63 chains then the depletion would not affect the removal of K48 chains, but also would not prevent the K63 chains from being degraded. This later theory would show an overall decrease in FK2 signal, which is what we see in USP50 siRNA depletion. The interaction between USP50 and VCP could be the link between K48 chain depletion signalling K63 chain elongation.

SUPPLEMENTARY FIGURES

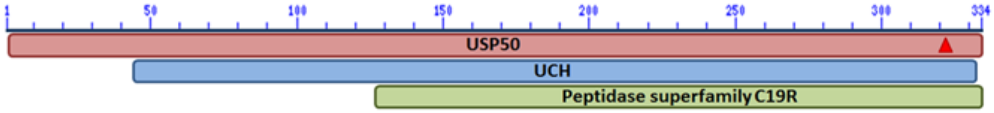

Figure 1 – *Features and domains of USP50 using NCBI BLAST nucleotide database search. USP50 (RED) contains a UCH domain (aa41-334, BLUE) which is part of the peptidase superfamily C19R(GREEN). The predicted active site of USP50 is at aa322 (RED triangle).*

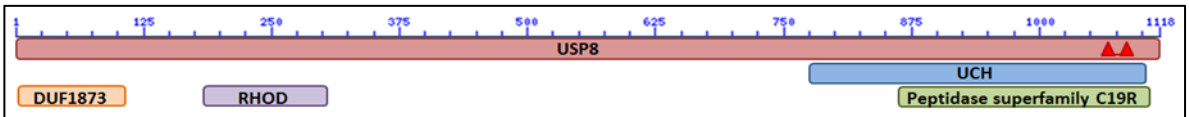

Figure 2- *Features and domains of USP8 using NCBI BLAST nucleotide database search. Like USP50, USP8 (RED) contain a UCH domain (BLUE) which is part of the peptidase superfamily C19R (GREEN). It also has DUF1873 (ORANGE) and RHOD (PURPLE) domains and two predicted active sites (RED triangles) that are linked.*

```
USP8_Human      PITGTFRYYHSPTNTVHMYPPEMAPSSAPPSTPPTHKAKPQIPAERDREPSKLKRSYSSP 720
USP50_Human     ------------------------------------MTSQPSLPAD-------------DF 12
                                                   .::*.:**:              .

USP8_Human      DITQAIQEEEKRKPTVTPTVNRENKPTCYPKAEISRLSASQIRNLNPVFGGSGPALTGLR 780
USP50_Human     DIYHVLAECTDYYDTLPVKEADGNQ--------------------PHFQG----VTGLW 47
                ** :.: *  .   *:. .    *:                      * * *    :***

USP8_Human      NLGNTCYMNSILQCLCNAPHLADYFNRNCYQDDINRSNLLGHKGEVAEEFGIIMKALWTG 840
USP50_Human     NLGNTGCVNAISQCLCSILPLVEYFLTGKYITALQN-----DCSEVATAFAYLMTDMWLG 102
                ****** :*:* ****.   *.:**  . *   ::.     . .***  *. :*. :* *

USP8_Human      QYRYISPKDFKITIGKINDQFAGYSQQDSQELLLFLMDGLHEDLNKADNRKRYKEENNDH 900
USP50_Human     DSDCVSPEIFWSALGNLYPAFTKKMQQDAQEFLICVLNELHEALKKYHYSRRRSYEKG-- 160
                :   :**: *  ::*::   *:   ***:**:*: ::: *** *:* .  :* . *:.

USP8_Human      LDDFKAAEHAWQKHKQLNESIIVALFQGQFKSTVQCLTCHKKSRTFEAFMYLSLPLASTS 960
USP50_Human     -----STQRCCRKWITTETSIITQLFEEQLNYSIVCLKCEKCTYKNEVFTVFSLPIPSKY 215
                     ::::. :*    : ***. **: *:: :: **.*.* : . *.*  :***:.*.

USP8_Human      KCTLQDCLRLFSKEEKLTDNNRFYCSHCRARRDSLKKIEIWKLPPVLLVHLKRFSYDGRW 1020
USP50_Human     ECSLRDCLQCFFQQDALTWNNEIHCSFCETKQETAVRASISKAPKIIIFHLKRFDIQGTT 275
                :*:*:***: * ::: ** **.::**.*.:::::  : .* * * :::.*****. :*

USP8_Human      KQKLQTSVDFPLENLDLSQYVIGPKNNLKKYNLFSVSNHYGGLDGGHYTAYCKNAARQRW 1080
USP50_Human     KRKLRTDIHYPLTNLDLTPYICSIFRKYPKYNLCAVVNHFGDLDGGHYTAFCKNSVTQA- 334
                *:**:*.:.:** ****: *: .  .:  **** :* **:*.********:***:. *

USP8_Human      FKFDDHEVSDISVSSVKSSAAYILFYTSLGPRVTDVAT 1118
USP50_Human     ---------------------------------------
```

Figure 3 – *Alignment of catalytic triad region of USP50 and USP8. The catalytic residues are highlighted; cysteine (C) in PURPLE, histidine (H) GREEN and aspartate (D) is RED. Human USP50 is truncated after Ala334, before the aspartate residue. This was created using the protein sequence from GenBank and NCBI Reference Sequence (USP8:*AAH26954.1, USP50:NP_987090.2). The punctuation beneath the sequences show the predicted conserved regions and the strength at which they are conserved in USP50 (.=partially conserved, *=always conserved).

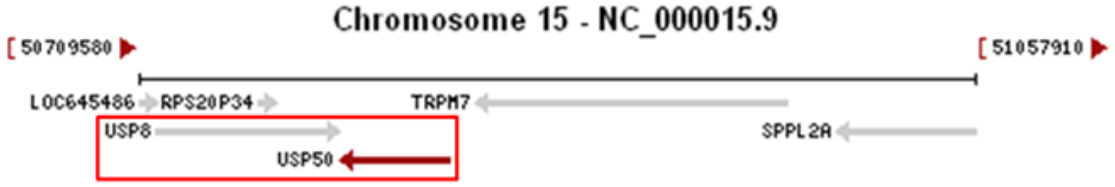

Figure 4 –*Localisation of USP50 and USP8 on human chromosome 15. USP8 is transcribed from the forward strand adjacent to USP50 which is transcribed from the reverse strand (RED box).*

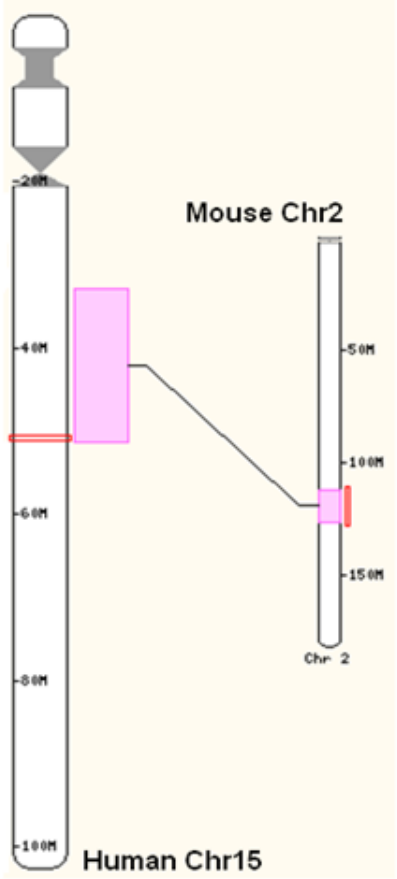

Figure 5 – *Mouse chr2 and human chr15 sequence homology. The PINK boxes show the region in which USP50 and USP8 are found on both chromosomes.*

Figure 6- *Alignment of the full USP50 from 8 species including humans (BOLD), labelled with the catalytic residues (Cysteine, C= RED, histidine, H= GREEN, aspartic acid, D=YELLOW). The underlined amino acids are those that are conserved and the RED amino acids are those that are considered highly conserved. The highly conserved regions are shown in humans only, except the final highly conserved region is shown in mouse USP50 as it is not present in human USP50. The aa sequences were obtained from GenBank and aligned using ClustalW. Conserved regions were taken from GenBank information.*

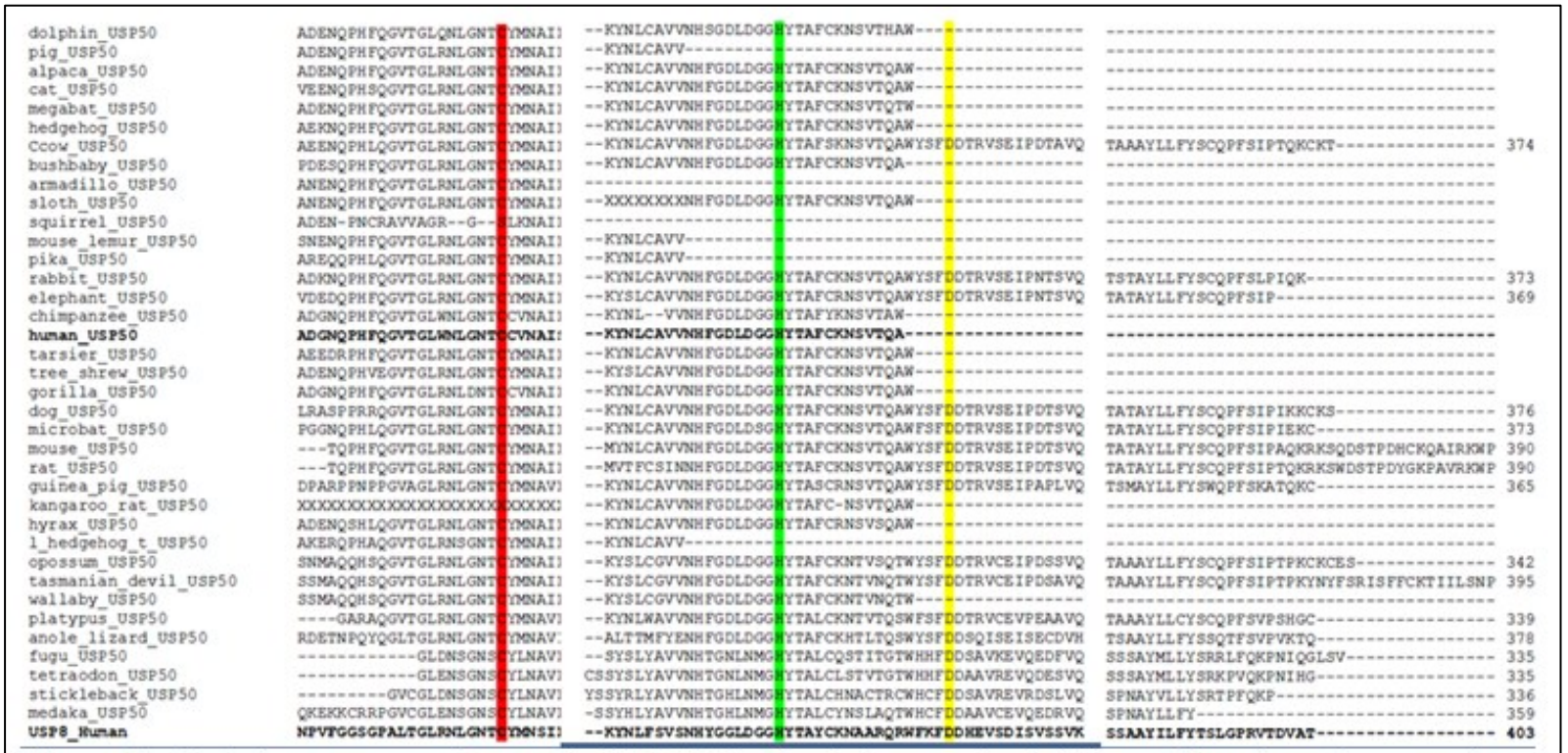

Figure 7- *Protein sequence alignment of USP50 'tail' variations and catalytic residues in various species and of human USP8. The three catalytic residues are highlighted; cysteine= RED, histidine= GREEN, aspartic acid= YELLOW.*

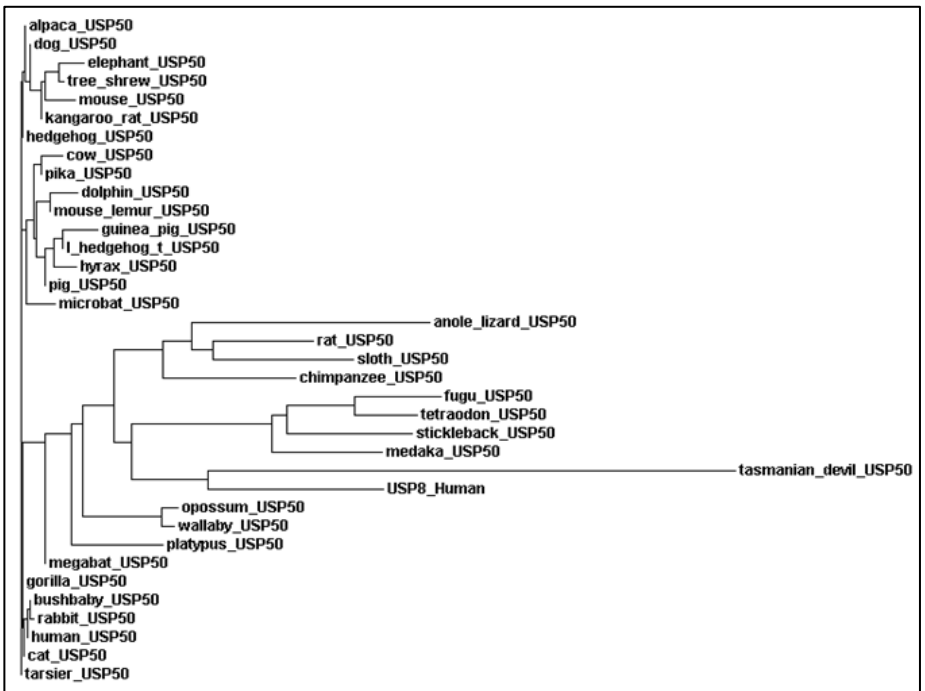

Figure 8 – *Phylogenetic tree of the 'tail' regions of USP50 from orthologs showing no alignment to closely related species.*

Figure 9 – *Structural prediction of USP50 with two catalytic residues (cysteine= CYS53, histidine= HIS322) and the associated glycine (GLN60) labelled highlighted in GREEN. The last residue (OXT332) of the protein, before the stop codon, is also labelled.*

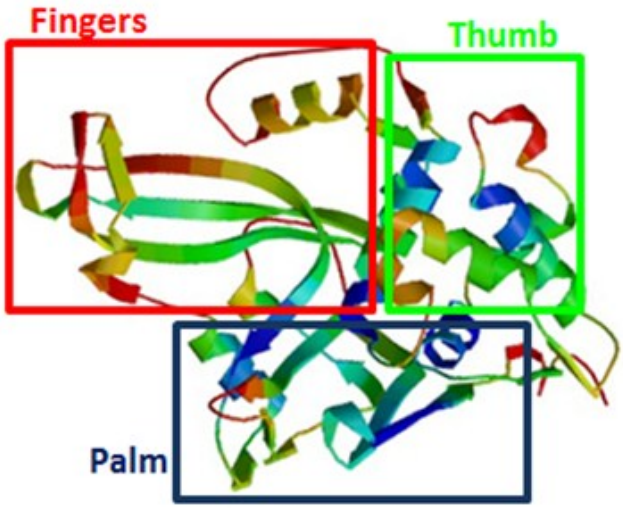

Figure 10- *SwissPDB predicted structural model of USP50 labelled with structural features. The structure is analogous to a hand-like structure as it has a domain with β-sheets that are like fingers (RED box), a region that is concave where ubiquitin sits like a palm (BLUE box) and a protruding region like a thumb (GREEN box).*

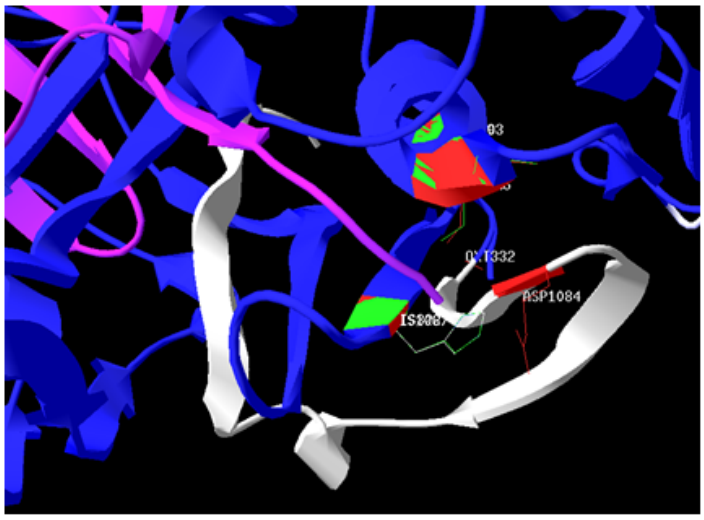

Figure 11 – *Close up of UCH active site in USP8 and USP50 overlaid, with ubiquitin (PINK) tail protruding into catalytic triad. The catalytic triad residues (cysteine= CYS786/ CYS53, histidine= HIS1067/ HIS322, aspartic acid= 1084) and the associated glycine (GLN793/GLN60) labelled highlighted in RED (USP8) or GREEN (USP50). The tail of USP8 is coloured in WHITE.*

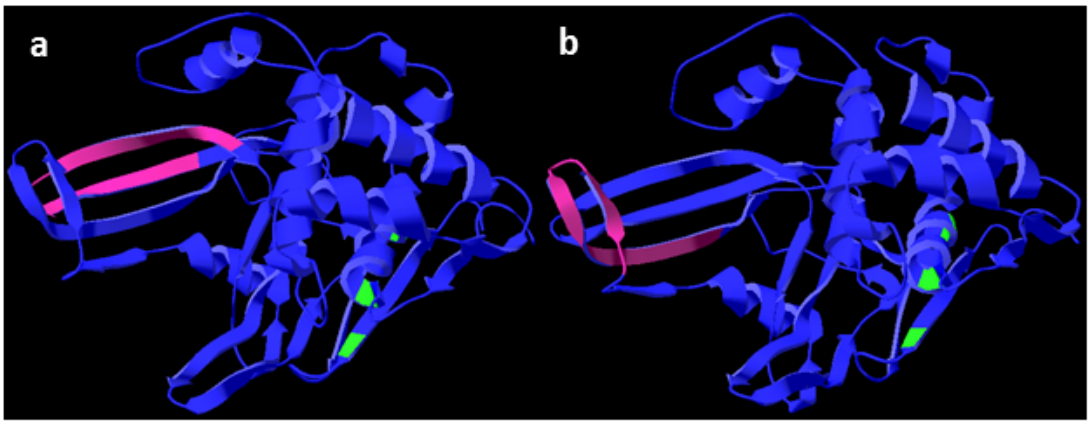

Figure 12– USP50 with (a) d*eletion 1, and (b) deletion 2, highlighted (PINK). Catalytic residues are highlighted in GREEN.*

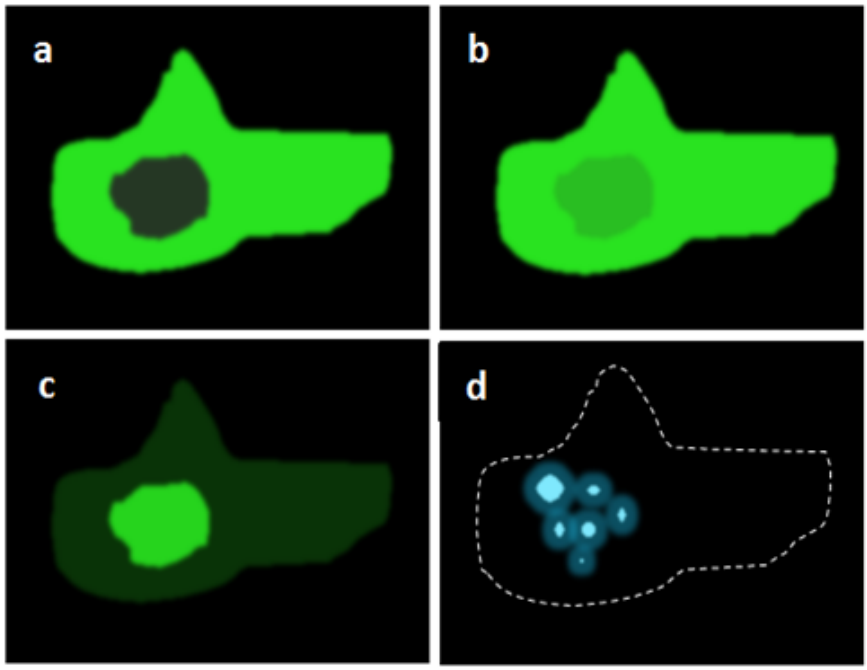

Figure 13- *Simplified representation of the types of cell characteristics used to classify cells in the USP50/GFP and GFP cellular localisation experiment. (a) cytoplasmic localisation only, (b) cytoplasmic and nuclear localisation, (c) nuclear localisation only, and (d) karyorrhexis (breaking up of nucleus).*

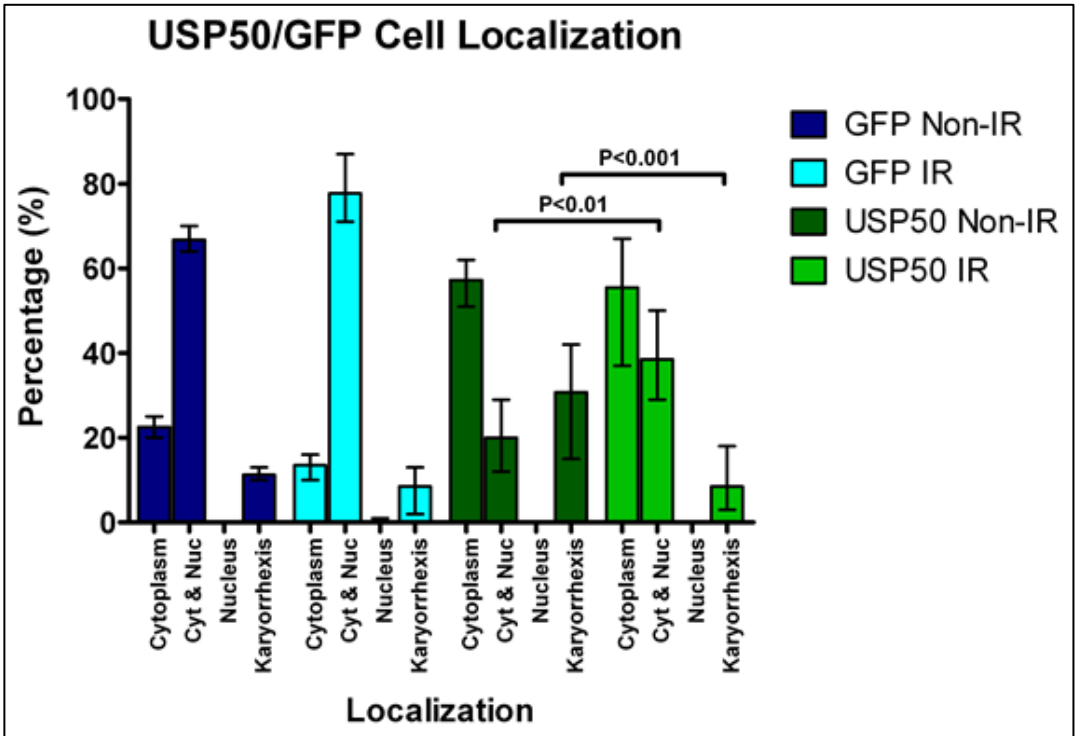

Figure 14 - *Graph showing the localisation of GFP and USP50-GFP in U20S cells before and after ionising radiation (IR).*

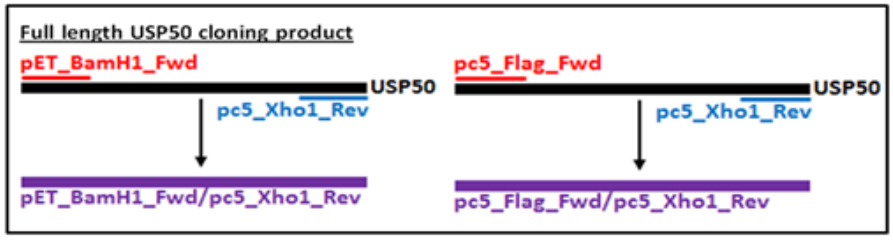

Figure 15 – *Diagram of control USP50 cloning product formation. Forward primers are in RED, reverse primers are in BLUE and products are in PURPLE. USP50 DNA template is in BLACK.*

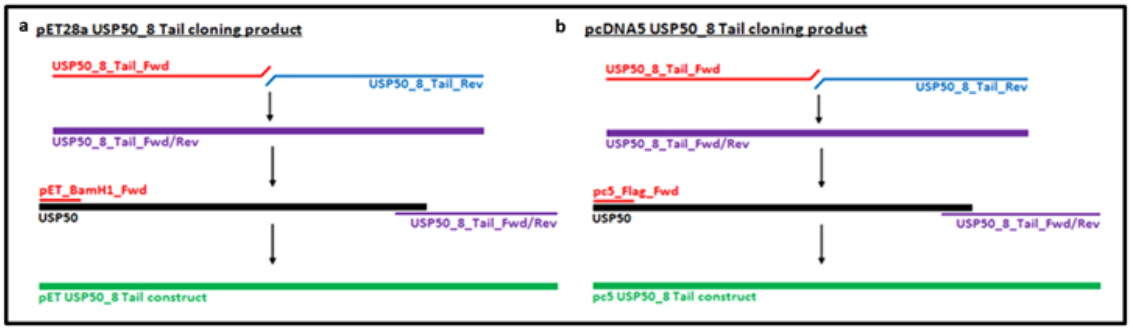

Figure 16 – *Diagram of USP50_8 Tail formation. Forward primers are in RED, reverse primers are in BLUE and tail product is in PURPLE. USP50 DNA template is in BLACK and final product is in GREEN. (a) construct formation is to be ligated into pET28a and (b) construct formation is to be ligated into pcDNA5/FRT/TO.*

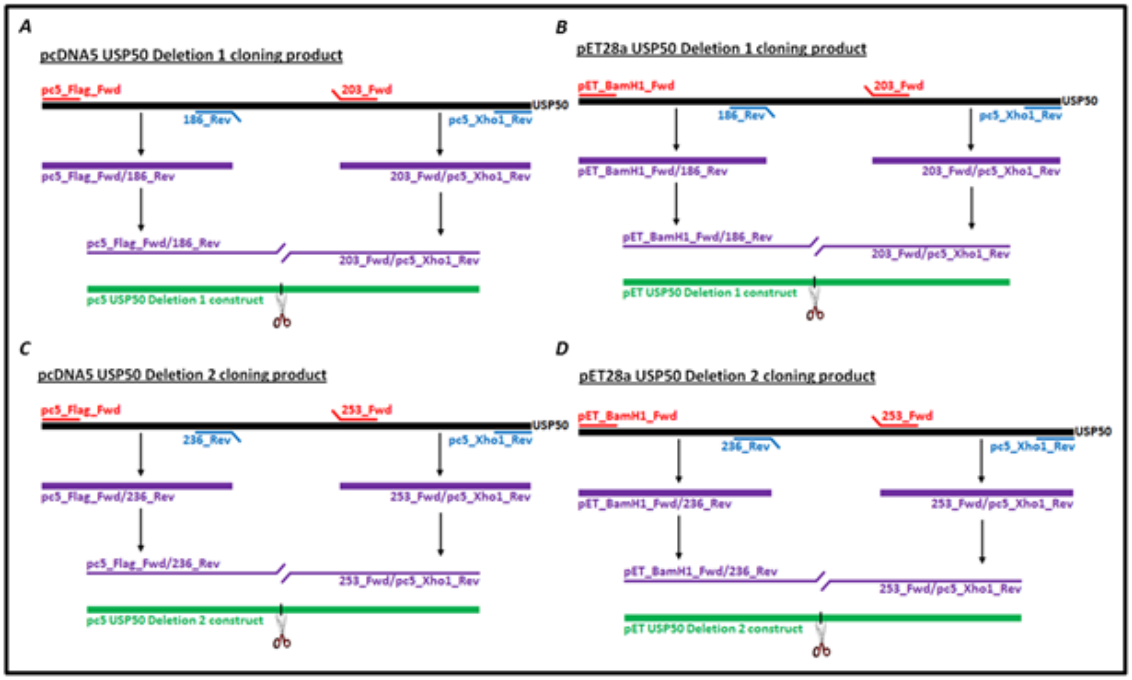

Figure 17 – *Diagram of USP50 deletion 1 (a and b) and deletion 2 (c and d) formation. Forward primers are in RED, reverse primers are in BLUE and tail is in PURPLE. USP50 DNA template is in BLACK and final product is in GREEN. (a & c) construct formation is to be ligated into pET28a and (b & d) construct formation is to be ligated into pcDNA5/FRT/TO.*

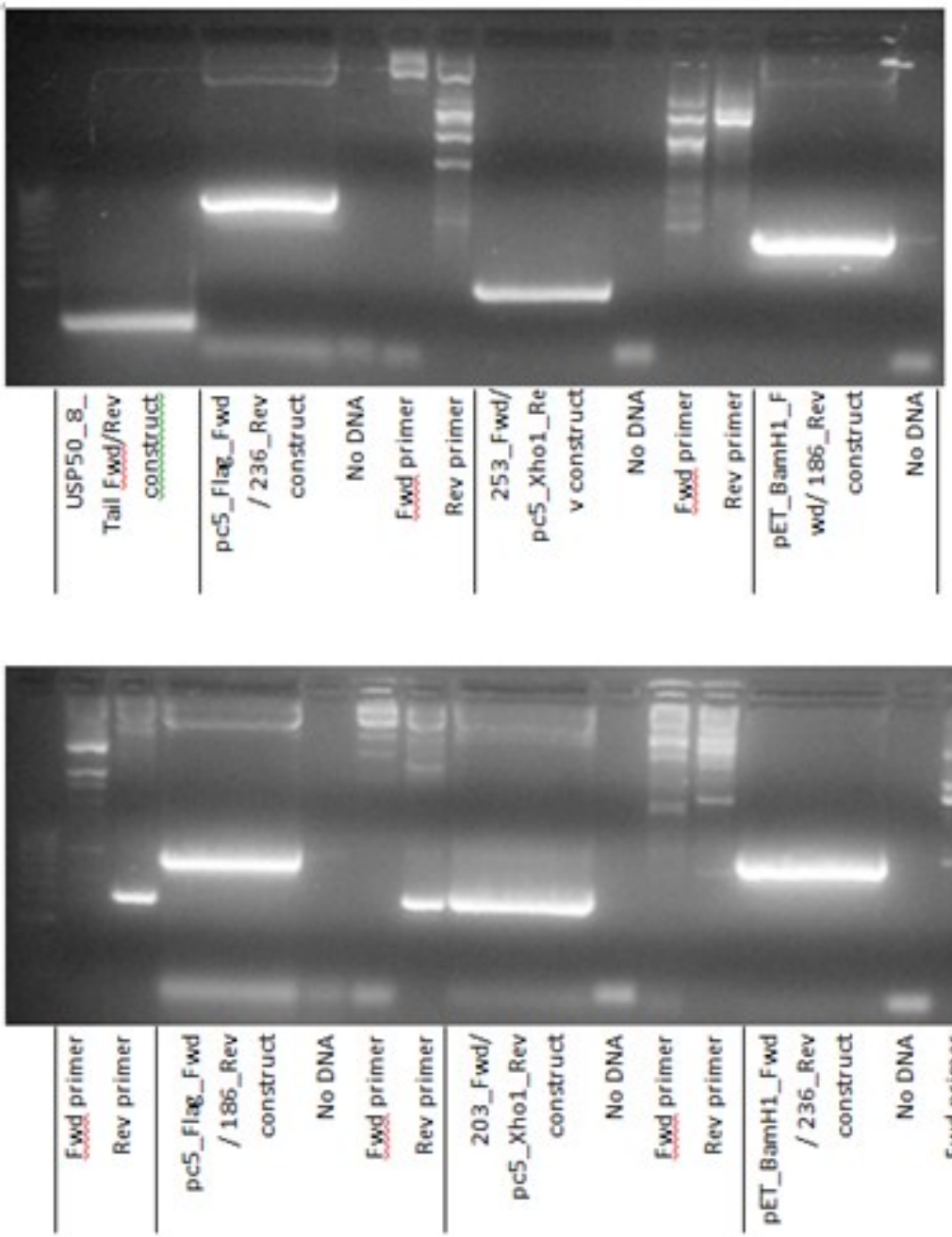

Figure 18- *Agarose (1%) Gel electrophoresis of PCR cloning products to check the size and presence of the primary constructs from the original primers of USP50_8 tail, and the two USP50 deletion primary constructs. Primary constructs for the USP50 deletion constructs have 3 controls; no DNA, forward primer and reverse primer.*

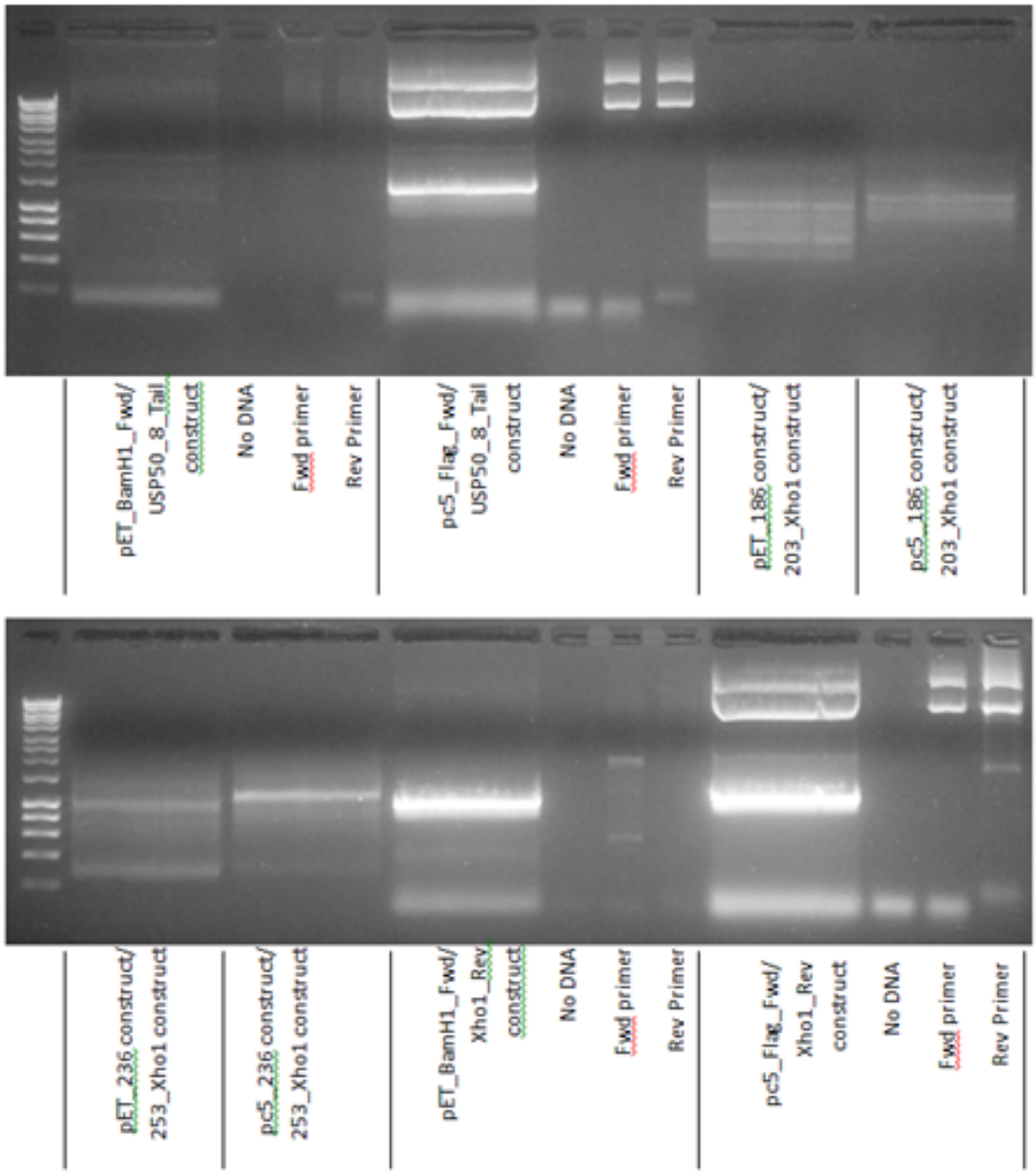

Figure 19-*Agarose (1%) Gel electrophoresis of PCR Cloning products to check the size and presence of the control constructs, the secondary constructs of USP50 deletions1 and 2, and the USP50_8 Tail final constructs. Constructs for the control USP50 constructs and the final USP50_8 Tail constructs have 3 controls; no DNA, forward primer and reverse primer.*

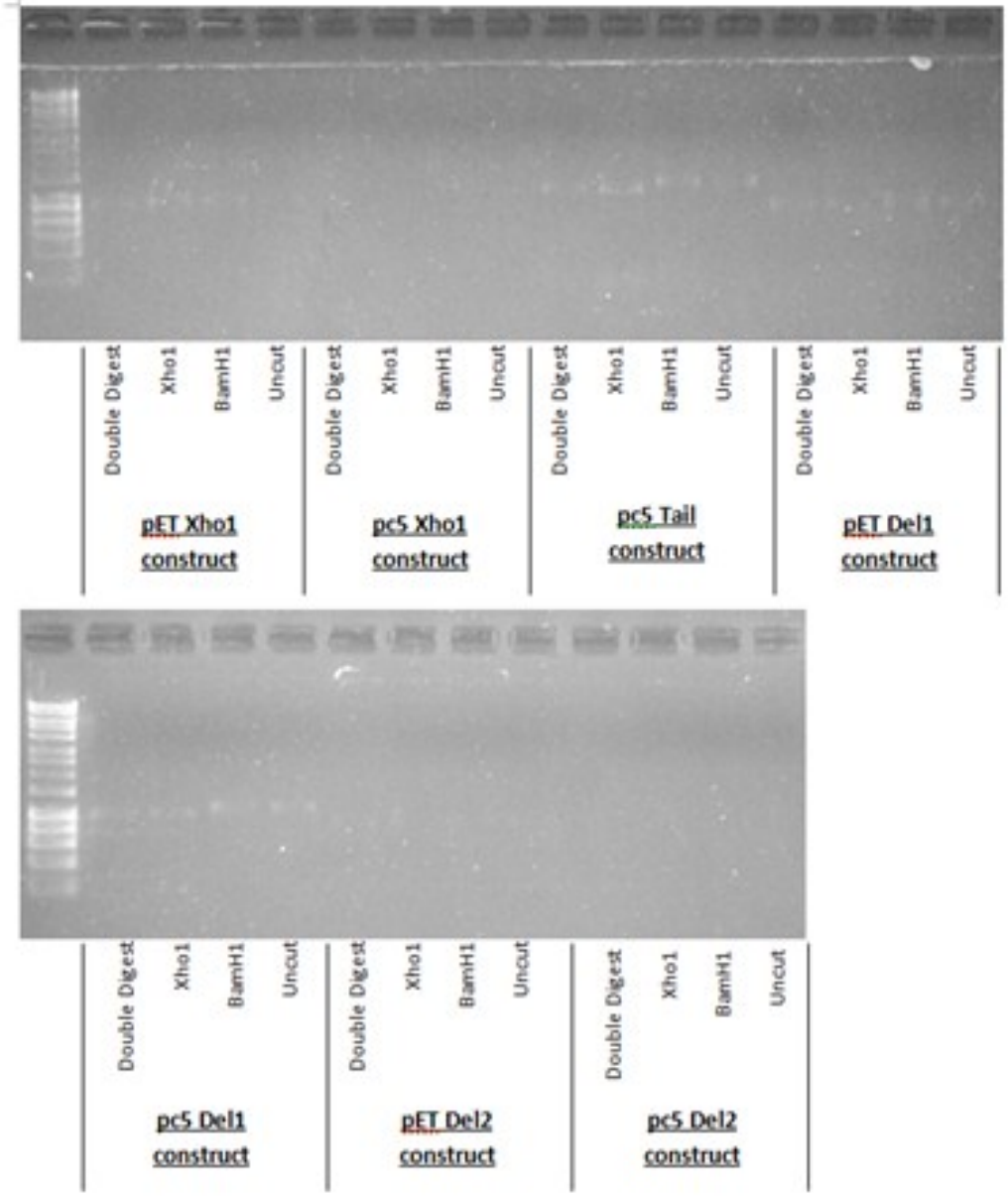

Figure 20- *Agarose (1%) Gel electrophoresis of final constructs after Phenol: chloroform clean up, restriction digest with Xho1 and BamH1, and a second Phenol: chloroform clean up. This was to check the size and presence of the products after restriction digest. Each digest has 3 controls; Xho1 only, BamH1 only and uncut.*

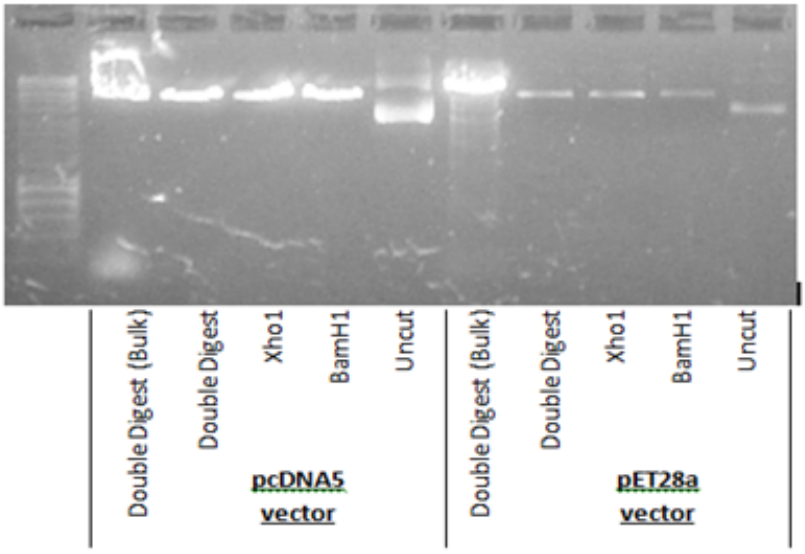

Figure 21- *Agarose (1%) Gel electrophoresis of pET28a and pcDNA5/FRT/TO vector after restriction digest with Xho1 and BamH1, and Phenol: chloroform clean up. This was to check the size and presence of the products after restriction digest. Each digest has 3 controls; Xho1 only, BamH1 only and uncut. Double Digest (Bulk) products were experimentally identical to the Double Digest, but scaled up in volume.*

Vector	Construct name	Primary construct	Full construct	Restriction Digest
pET28a	Control construct	N/A	Yes	Yes
	USP50_8 Tail construct	Yes	No	No
	USP50 Deletion 1	Yes	Yes	Yes
	USP50 Deletion 2	Yes	Yes	No
pcDNA5/FRT/TO	Control construct	N/A	Yes	No
	USP50_8 Tail construct	Yes	Yes	Yes
	USP50 Deletion 1	Yes	Yes	Yes
	USP50 Deletion 2	Yes	Yes	No

Table 1 – *USP50 control and mutant cloning constructs and to which stage they were successfully made.*

BIBLIOGRAPHY

Acs, K., Luijsterburg, M.S., Ackermann, L., et al. (2011) The AAA-ATPase VCP/p97 promotes 53BP1 recruitment by removing L3MBTL1 from DNA double-strand breaks. **Nat Struct Mol Biol,** 18 (12): 1345-1350.

Al-Hakim, A., Escribano-Diaz, C., Landry, M., et al. (2010) The ubiquitous role of ubiquitin in the DNA damage response. **DNA Repair,** 9 (12): 1229-1240.

Amerik, A.Y. and Hochstrasser, M. (2004) Mechanism and function of deubiquitinating enzymes. **Biochimica et Biophysica Acta (BBA) - Molecular Cell Research,** 1695 (1): 189-207.

Aressy, B., Jullien, D., Cazales, M., et al. (2010) A screen for deubiquitinating enzymes involved in the G/M checkpoint identifies USP50 as a regulator of HSP90-dependent Wee1 stability. **Cell cycle (Georgetown, Tex.),** 9 (18): 3815-3822.

Avvakumov, G.V., Walker, J.R., Xue, S., et al. (2006) Amino-terminal Dimerization, NRDP1-Rhodanese Interaction, and Inhibited Catalytic Domain Conformation of the Ubiquitin-specific Protease 8 (USP8). **Journal of Biological Chemistry,** 281 (49): 38061-38070.

Beer-Romero, P., Glass, S. and Rolfe, M. (1997) Antisense targeting of E6AP elevates p53 in HPV-infected cells but not in normal cells. **Oncogene,** 14 (5): 595-602.

Bekker-Jensen, S., Danielsen, J.R., Fugger, K., et al. (2010) HERC2 coordinates ubiquitin-dependent assembly of DNA repair factors on damaged chromosomes. **Nature cell biology,** 12 (1): 80-86.

Ben-Neriah, Y. (2002) Regulatory functions of ubiquitination in the immune system. **Nature immunology,** 3 (1): 20-26.

Borodovsky, A., Kessler, B.M., Casagrande, R., et al. (2001) A novel active site-directed probe specific for deubiquitylating enzymes reveals proteasome association of USP14. **The EMBO journal,** 20 (18): 5187-5196.

Burma, S., Chen, B.P., Murphy, M., et al. (2001) ATM Phosphorylates Histone H2AX in Response to DNA Double-strand Breaks. **Journal of Biological Chemistry,** 276 (45): 42462-42467.

Butler, L.R., Densham, R.M., Jia, J., Garvin, A.J., Stone, H.R., Shah, V., Weekes, D., Festy, F., Beesley, J., Morris, J.R. (2012) The proteasomal de-ubiquitinating enzyme POH1 promotes the double-strand DNA break response. **EMBO,** (10) 1038.

Camacho, C., Coulouris, G., Avagyan, V., et al. (2009) BLAST+: architecture and applications. **BMC bioinformatics,** 10 421.

Campbell, S.J., Edwards, R.A., Leung, C.C.Y., et al. (2012) Molecular Insights into the Function of RING Finger (RNF)-containing Proteins hRNF8 and hRNF168 in Ubc13/Mms2-dependent Ubiquitylation. **Journal of Biological Chemistry,** 287 (28): 23900-23910.

Chen, Z.J. and Sun, L.J. (2009) Nonproteolytic Functions of Ubiquitin in Cell Signaling. **Molecular cell,** 33 (3): 275-286.

Cooper, E.M., Cutcliffe, C., Kristiansen, T.Z., et al. (2009) K63-specific deubiquitination by two JAMM/MPN+ complexes: BRISC-associated Brcc36 and proteasomal Poh1. **The EMBO journal,** 28 (6): 621-631.

Doil, C., Mailand, N., Bekker-Jensen, S., et al. (2009) RNF168 Binds and Amplifies Ubiquitin Conjugates on Damaged Chromosomes to Allow Accumulation of Repair Proteins. **Cell,** 136 (3): 435-446.

Dong, Y., Hakimi, M., Chen, X., et al. (2003) Regulation of BRCC, a Holoenzyme Complex Containing BRCA1 and BRCA2, by a Signalosome-like Subunit and Its Role in DNA Repair. **Molecular cell,** 12 (5): 1087-1099.

Eytan, E., Ganoth, D., Armon, T., et al. (1989) ATP-dependent incorporation of 20S protease into the 26S complex that degrades proteins conjugated to ubiquitin. **Proceedings of the National Academy of Sciences,** 86 (20): 7751-7755.

Feng, L., Wang, J. and Chen, J. (2010) The Lys63-specific deubiquitinating enzyme BRCC36 is regulated by two scaffold proteins localizing in different subcellular compartments. **Journal of Biological Chemistry,** 285 (40): 30982-30988.

Feng, L., Huang, J. and Chen, J. (2009) MERIT40 facilitates BRCA1 localization and DNA damage repair. **Genes & development,** 23 (6): 719-728.

Flicek, P., Amode, M.R., Barrell, D., et al. (2012) Ensembl 2012. **Nucleic acids research,** 40 (Database issue): D84-90.

Gallery, M., Blank, J.L., Lin, Y., et al. (2007) The JAMM motif of human deubiquitinase Poh1 is essential for cell viability. **Molecular cancer therapeutics,** 6 (1): 262-268.

Haas, A.L. and Siepmann, T.J. (1997) Pathways of ubiquitin conjugation. **The FASEB Journal,** 11 (14): 1257-1268.

Hershko, A. and Ciechanover, A. (1998) The Ubiquitin System. **Annual Review of Biochemistry,** 67 (1): 425-479.

Hicke, L. and Dunn, R. (2003) Regulation of membrane protein transport by ubiquitin and ubiquitin-binding proteins. **Annual Review of Cell and Developmental Biology,** 19 (1): 141-172.

Hu, M., Li, P., Li, M., et al. (2002) Crystal Structure of a UBP-Family Deubiquitinating Enzyme in Isolation and in Complex with Ubiquitin Aldehyde. **Cell,** 111 (7): 1041-1054.

Huen, M.S.Y., Grant, R., Manke, I., et al. (2007) RNF8 Transduces the DNA-Damage Signal via Histone Ubiquitylation and Checkpoint Protein Assembly. **Cell,** 131 (5): 901-914.

Johnston, S.C., Riddle, S.M., Cohen, R.E., et al. (1999) Structural basis for the specificity of ubiquitin C-terminal hydrolases. **The EMBO journal,** 18 (14): 3877-3887.

Jones, D., Crowe, E., Stevens, T.A., et al. (2002) Functional and phylogenetic analysis of the ubiquitylation system in Caenorhabditis elegans: ubiquitin-conjugating enzymes, ubiquitin-activating enzymes, and ubiquitin-like proteins. **Genome biology,** 3 (1): RESEARCH0002.

Kee, Y., Lyon, N. and Huibregtse, J.M. (2005) The Rsp5 ubiquitin ligase is coupled to and antagonized by the Ubp2 deubiquitinating enzyme. **The EMBO journal,** 24 (13): 2414-2424.

Kim, H., Chen, J. and Yu, X. (2007) Ubiquitin-Binding Protein RAP80 Mediates BRCA1-Dependent DNA Damage Response. **Science,** 316 (5828): 1202-1205.

Kinner, A. and Kalling, R. (2003) The yeast deubiquitinating enzyme Ubp16 is anchored to the outer mitochondrial membrane. **FEBS letters,** 549 (1): 135-140.

Lam, Y.A., Xu, W., DeMartino, G.N., et al. (1997) Editing of ubiquitin conjugates by an isopeptidase in the 26S proteasome. **Nature,** 385 (6618): 737-740.

Lok, G.T., Sy, S.M.-., Dong, S., et al. (2012) Differential regulation of RNF8-mediated Lys48- and Lys63-based poly-ubiquitylation. **Nucleic acids research,** 40 (1): 196-205.

Mailand, N., Bekker-Jensen, S., Faustrup, H., et al. (2007) RNF8 Ubiquitylates Histones at DNA Double-Strand Breaks and Promotes Assembly of Repair Proteins. **Cell,** 131 (5): 887-900.

Mallette, F.A. and Richard, S. (2012) K48-linked ubiquitination and protein degradation regulate 53BP1 recruitment at DNA damage sites. **Cell research,** 22 (8): 1221-1223.

Mallette, F.A., Mattiroli, F., Cui, G., et al. (2012) RNF8- and RNF168-dependent degradation of KDM4A/JMJD2A triggers 53BP1 recruitment to DNA damage sites. **The EMBO journal,** 31 (8): 1865-1878.

Meerang, M., Ritz, D., Paliwal, S., et al. (2011) The ubiquitin-selective segregase VCP/p97 orchestrates the response to DNA double-strand breaks. **Nature cell biology,** 13 (11): 1376-1382.

Meyer, H., Bug, M. and Bremer, S. (2012) Emerging functions of the VCP/p97 AAA-ATPase in the ubiquitin system. **Nature cell biology,** 14 (2): 117-123.

Nakada, S., Tai, I., Panier, S., et al. (2010) Non-canonical inhibition of DNA damage-dependent ubiquitination by OTUB1. **Nature,** 466 (7309): 941-946.

Nakamura, N. and Hirose, S. (2008) Regulation of Mitochondrial Morphology by USP30, a Deubiquitinating Enzyme Present in the Mitochondrial Outer Membrane. **Molecular biology of the cell,** 19 (5): 1903-1911.

Nanao, M.H., Tcherniuk, S.O., Chroboczek, J., et al. (2004) Crystal structure of human otubain 2. **EMBO reports,** 5 (8): 783-788.

Nicassio, F., Corrado, N., Vissers, J.H.A., et al. (2007) Human USP3 Is a Chromatin Modifier Required for S Phase Progression and Genome Stability. **Current Biology,** 17 (22): 1972-1977.

Nijman, S.M.B., Luna-Vargas, M.P.A., Velds, A., et al. (2005) A Genomic and Functional Inventory of Deubiquitinating Enzymes. **Cell,** 123 (5): 773-786.

Panier, S. and Durocher, D. (2009) Regulatory ubiquitylation in response to DNA double-strand breaks. **DNA repair,** 8 (4): 436-443.

Passmore, L.A. and Barford, D. (2004) Getting into position: the catalytic mechanisms of protein ubiquitylation. **The Biochemical journal,** 379 (Pt 3): 513-525.

Patterson-Fortin, J., Shao, G., Bretscher, H., et al. (2010) Differential regulation of JAMM domain deubiquitinating enzyme activity within the RAP80 complex. **Journal of Biological Chemistry,** 285 (40): 30971-30981.

Pickart, C.M. and Eddins, M.J. (2004) Ubiquitin: structures, functions, mechanisms. **Biochimica et Biophysica Acta (BBA) - Molecular Cell Research,** 1695 (1): 55-72.

Plans, V., Scheper, J., Soler, M., et al. (2006) The RING finger protein RNF8 recruits UBC13 for lysine 63-based self polyubiquitylation. **Journal of cellular biochemistry,** 97 (3): 572-582.

Prince, T., Shao, J., Matts, R.L., et al. (2005) Evidence for chaperone heterocomplexes containing both Hsp90 and VCP. **Biochemical and biophysical research communications,** 331 (4): 1331-1337.

Pruitt, K.D., Harrow, J., Harte, R.A., et al. (2009) The consensus coding sequence (CCDS) project: Identifying a common protein-coding gene set for the human and mouse genomes. **Genome research,** 19 (7): 1316-1323.

Ramadan, K. (2012) p97/VCP- and Lys48-linked polyubiquitination form a new signaling pathway in DNA damage response. **Cell cycle (Georgetown, Tex.),** 11 (6): 1062-1069.

Renatus, M., Parrado, S.G., D'Arcy, A., et al. (2006) Structural Basis of Ubiquitin Recognition by the Deubiquitinating Protease USP2. **Structure,** 14 (8): 1293-1302.

Sato, Y., Yoshikawa, A., Mimura, H., et al. (2009) Structural basis for specific recognition of Lys 63-linked polyubiquitin chains by tandem UIMs of RAP80. **The EMBO journal,** 28 (16): 2461-2468.

Semple, C.A., RIKEN GER Group and GSL Members (2003) The comparative proteomics of ubiquitination in mouse. **Genome research,** 13 (6B): 1389-1394.

Shao, G., Lilli, D.R., Patterson-Fortin, J., et al. (2009) The Rap80-BRCC36 de-ubiquitinating enzyme complex antagonizes RNF8-Ubc13-dependent ubiquitination events at DNA double strand breaks. **Proceedings of the National Academy of Sciences,** 106 (9): 3166-3171.

Shi, D. and Grossman, S.R. (2010) Ubiquitin becomes ubiquitous in cancer: emerging roles of ubiquitin ligases and deubiquitinases in tumorigenesis and as therapeutic targets. **Cancer Biology & Therapy,** 10 (8): 737-747.

Smith, A., Simanski, S., Fallahi, M., et al. (2007) Redundant ubiquitin ligase activities regulate wee1 degradation and mitotic entry. **Cell cycle** 6 (22): 2795-2799.

Sobhian, B., Shao, G., Lilli, D.R., et al. (2007) RAP80 targets BRCA1 to specific ubiquitin structures at DNA damage sites. **Science.** 316 (5828): 1198-1202.

Sowa, M.E., Bennett, E.J., Gygi, S.P., et al. (2009) Defining the human deubiquitinating enzyme interaction landscape. **Cell,** 138 (2): 389-403.

Stewart, G.S., Panier, S., Townsend, K., et al. (2009) The RIDDLE Syndrome Protein Mediates a Ubiquitin-Dependent Signaling Cascade at Sites of DNA Damage. **Cell,** 136 (3): 420-434.

Stucki, M., Clapperton, J.A., Mohammad, D., et al. (2005) MDC1 Directly Binds Phosphorylated Histone H2AX to Regulate Cellular Responses to DNA Double-Strand Breaks. **Cell,** 123 (7): 1213-1226.

Sun, L. and Chen, Z.J. (2004) The novel functions of ubiquitination in signaling. **Current opinion in cell biology,** 16 (2): 119-126.

Ulrich, H.D. and Walden, H. (2010) Ubiquitin signalling in DNA replication and repair. **Nature reviews. Molecular cell biology,** 11 (7): 479-489.

van Vugt, M.A., Bras, A. and Medema, R.H. (2004) Polo-like kinase-1 controls recovery from a G2 DNA damage-induced arrest in mammalian cells. **Molecular cell,** 15 (5): 799-811.

VanDemark, A.P., Hofmann, R.M., Tsui, C., et al. (2001) Molecular insights into polyubiquitin chain assembly: crystal structure of the Mms2/Ubc13 heterodimer. **Cell,** 105 (6): 711-720.

Varadan, R., Assfalg, M., Haririnia, A., et al. (2004) Solution Conformation of Lys63-linked Di-ubiquitin Chain Provides Clues to Functional Diversity of Polyubiquitin Signaling. **Journal of Biological Chemistry,** 279 (8): 7055-7063.

Verma, R., Peters, N.R., D'Onofrio, M., et al. (2004) Ubistatins Inhibit Proteasome-Dependent Degradation by Binding the Ubiquitin Chain. **Science,** 306 (5693): 117-120.

Wang, B. and Elledge, S.J. (2007) Ubc13/Rnf8 ubiquitin ligases control foci formation of the Rap80/Abraxas/Brca1/Brcc36 complex in response to DNA damage. **Proceedings of the National Academy of Sciences,** 104 (52): 20759-20763.

Wojcik, C., Rowicka, M., Kudlicki, A., et al. (2006) Valosin-containing protein (p97) is a regulator of endoplasmic reticulum stress and of the degradation of N-end rule and ubiquitin-fusion degradation pathway substrates in mammalian cells. **Molecular biology of the cell,** 17 (11): 4606-4618.

Wu, X., Yen, L., Irwin, L., et al. (2004) Stabilization of the E3 ubiquitin ligase Nrdp1 by the deubiquitinating enzyme USP8. **Molecular and cellular biology,** 24 (17): 7748-7757.

Yang, W.L., Zhang, X. and Lin, H.K. (2010) Emerging role of Lys-63 ubiquitination in protein kinase and phosphatase activation and cancer development. **Oncogene,** 29 (32): 4493-4503.

Ye, Y., Scheel, H., Hofmann, K., et al. (2009) Dissection of USP catalytic domains reveals five common insertion points. **Molecular BioSystems,** 5 (12): 1797-1808.

THE ROLE OF BRCA1 AT STALLED REPLICATION FORKS

by

Kirsty Josephine Lawrence, BSc.

This project is submitted in partial fulfilment of the requirements for the award of MASTER OF RESEARCH BIOMEDICAL RESEARCH to the University of Birmingham

UNIVERSITY OF BIRMINGHAM

THE ROLE OF BRCA1 AT STALLED REPLICATION FORKS

ABSTRACT

BRCA1 is a common inherited mutation in families with early onset breast and ovarian cancer. Cancers with homozygous mutations in BRCA1 are more resistant to chemotherapy due to abnormal DNA repair. Gemcitabine is a DNA replication inhibitor used to treat breast and ovarian cancer. How cancer mutations change the response of cells is poorly understood. Here, we investigate how BRCA1 mutations effect response to Gemcitabine using the cell line, HCC1937. BRCA1-proficient and –deficient cells were used to investigate the replication fork stalling, fork restart, 53BP1 and ɣH2AX foci, phospho-RPA levels, cell cycle accumulation and clonogenic survival after Gemcitabine treatment. Techniques utilised included DNA fibre analysis, immunofluorescent staining, FACS, Western blot and clonogenic survival assays.

BRCA1-deficient cells display increased fork stalling and earlier induction of phospho-RPA, 53BP1 and ɣH2AX. BRCA1 status effects the accumulation of cells in S phase after Gemcitabine treatment. BRCA1-deficient cells show decreased survival to <10μM Gemcitabine treatment.

We report that BRCA1 protects slowed and stalled forks, and prevents forks collapsing into double-strand breaks. BRCA1 status affects the sensitivity of cells to Gemcitabine treatment.

Word Count: 7304 words

INTRODUCTION

DNA replication

For cells to replicate and divide, they need to create an exact copy of their genome to semi-conservatively pass on to daughter cells. However, DNA can become damaged through internal and external influences. Therefore, cells have evolved to have high fidelity DNA replication methods, complementary DNA repair mechanisms, and cell cycle checkpoints to ensure DNA damage is not inherited. If the damage is too great, cells will undergo cell death.

In carcinogenic cells, genes that control these processes are often mutated and many genetic diseases with high rates of cancer have been linked to mutations in these genes, i.e. BRCA1, BRCA2, and ATM. Many cancer therapies target the proteins that control cell cycle, DNA damage repair, and DNA replication to force cells into cell death. Therefore it is important to study the molecular basis of replication to have the potential to create effective DNA replication targeting cancer therapies.

In eukaryotes, there are approximately 20,000 origins of replication called 'initiation regions' (Mechali, 2001) which are DNA sequence independent (Vashee et al., 2003). The ORC (origin recognition complex) is a 6 subunit complex which binds to ORC binding sites at origins of replication (Bell and Stillman, 1992), which forms the pre-replication complex with CDC6 (cell division cycle 6) (Bell et al., 1995), CDT1 (chromatin licensing and DNA replication factor 1) (Nishitani et al., 2000) and the MCM (mini-chromosome maintenance) helicase complex (Tanaka and Diffley, 2002; Tanaka et al., 1997). ORC1 binding can only occur in G1 (Li et al., 2004) because of the absence of CDC6 due to

exportation out of the nucleus after phosphorylation by CDK1-cyclin A (Pelizon et al., 2000). The pre-replication complex is phosphorylated in early S-phase by cyclin E CDK2 (cyclin-dependent kinase 2) (Krude et al., 1997) and DDK (Dbf4/Drf1-dependent CDC7 kinase) (Lei et al., 1997), this allows the recruitment of CDC45 (Mimura and Takisawa, 1998) and the GINS (go-ichi-ni-san) complex (Takayama et al., 2003) to promote origin firing (Gambus et al., 2006; Ilves et al., 2010). Dbf4 which activates DDK is degraded by the proteasome in G1 phase (Sclafani, 2000). When both CDK and DDK pathways are inhibited, the DNA replication is arrested in G1 phase (Zegerman and Diffley, 2007).

MCM proteins 2-7 form a hexamer that binds CDC45 to form the MCM complex, which unwinds the DNA strands (Pacek and Walter, 2004). The helicase activity of the MCM complex is ATP-dependent (Pacek and Walter, 2004) and any single-stranded DNA (ssDNA) that is exposed is coated by RPA (replication protein A) (Brill and Stillman, 1989; Erdile et al., 1991).

The machinery that forms the replisome include the MCM complex, RFC (replication factor C) (Tsurimoto and Stillman, 1989), PCNA (proliferating cell nuclear antigen), DNA polymerases (Tsurimoto and Stillman, 1991), and GINS, which maintains the replisome structure (Gambus et al., 2006; Pacek and Walter, 2004). RFC is a clamp loader that loads PCNA, the DNA polymerase clamp which encircles DNA in a trimeric ring structure (Lee et al., 1991). It is PCNA that binds DNA and recruits polymerases α-primase, pol δ and pol ε to the replisome (Stukenberg et al., 1991; Tsurimoto and Stillman, 1991). Polymerase α-primase forms an 8-12 nucleotide (nt) RNA primer (Matsumoto et al., 1990) which is elongated by pol δ with ~40 DNA nt (Nethanel et al., 1988). This is called the RNA-DNA primer and it is created once on the leading strand and at the beginning of all Okazaki

fragments on the lagging strand (Murakami et al., 1992). The synthesis of DNA is carried out by pol δ on the lagging strand and pol ε on the leading strand (Tsurimoto and Stillman, 1991; Tsurimoto et al., 1990) and is regulated by RFC and PCNA (Tsurimoto and Stillman, 1991). RFC and PCNA allow FEN1 (flap endonuclease 1) and DNA ligase I to access Okazaki fragments. Once Okazaki fragments have been synthesized the primer needs to be removed from the strand. FEN1 and pol δ, together at the end of the Okazaki fragment, degrade the primer by causing dissociation from the parental DNA strand to become a flap of nucleotides which is then removed by FEN1 (Murante et al., 1996; Turchi et al., 1994). Pol δ extends the DNA to the next Okazaki fragment and DNA ligase I anneals between the two (Turchi and Bambara, 1993).

The mechanism of replication termination in eukaryotes is unclear but from studies in Xenopus, termination appears to occur where two replication forks meet each other and not at a specific location or sequence (Santamaría et al., 2000).

Fork stalling and replication restart

During DNA replication, there can be obstacles that the replisome needs to overcome to complete synthesis of the genome. These obstacles slow down or stop replication fork progression known as fork stalling. There are various types of obstacles that can cause stalled forks, such as ribosomal barriers (Brewer and Fangman, 1988), unusual DNA structures (Lobachev, Rattray and Narayanan, 2007), checkpoint proteins (Katou et al., 2003), DNA damage, fragile chromosomal regions (Subramanian, Nelson and Chinault, 1996), insufficient dNTPs (Odsbu et al., 2009) and transcription-replication collisions (Brewer and Fangman, 1988).

Stalled forks can remain stationary for many hours until, after inactivation, they collapse into double-strand breaks (DSBs). The DSBs created by fork collapse are generated by the endonuclease complex of MUS81 (MUS81 endonuclease) (Hanada et al., 2007) and EME1 (essential meiotic endonuclease 1 homologue 1) (Boddy et al., 2001). If the stalled fork is resolved, fork restart can occur. It has become apparent that there are various proteins that are associated with the stabilization of the stalled fork and can influence the length of time before stalled forks become DSBs.

Replication stalling, through these obstacles, has facilitated the development of chemotherapeutics that stall forks indefinitely, or until forks become DSBs. Examples of these chemotherapeutics are gemcitabine (Gemca) (Cerqueira et al., 2007), hydroxyurea (HU) (Timson, 1975) and camptothecin (CPT) (Wu et al., 1971).

New methods, such as double labelling with thymidine analogues (Manders et al., 1992) and DNA fibre analysis (Jackson and Pombo, 1998; Tuduri, Tourrière and Pasero , 2010), have allowed fork restart to be observed on a single molecule basis and this has alluded to an active restart pathway at stalled forks.

After the removal of replication inhibitors, replication forks can restart if the fork is not inactivated or a DSB has not formed, although replication can resume once the DSB is repaired. For the replisome to remain stalled it is likely that there are structural that increase stability after the unwinding of the parental DNA, and lead to replication restart (Petermann Helleday, 2010). These structures allow restart through different methods.

The first possible structure involves the annealing of ssDNA and fork regression creating a Holliday junction (HJ) in a chicken foot structure. The annealed daughter ssDNA would

need to be degraded and the HJ resolved before replication can restart. Mre11 has been suggested as the endonuclease that resects DNA at stalled forks. The second structure is displacement loop (D-loop) formation which occurs when strands invade the parental DNA and anneal to make a loop that forms two HJs as the replication resumes. This allows replication to restart without sister chromatid exchange when the two HJs are resolved. The third structure is restarted using a DSB on the replicated DNA that allows strand invasion of the replicating strand onto the other parental strand forming a D-loop and a single HJ. This can lead to sister chromatid exchange when the single Holliday junction is resolved (Petermann Helleday, 2010).

There are several proteins that have been associated with fork restart; FANCJ/BRIP1 (Wu et al., 2008), FANCM (Gari et al., 2008; Yan et al., 2010), WRN (Franchitto et al., 2008; Sidorova et al., 2008) and BLM (Davies et al., 2007) are all helicases that have the ability to aid the resolution of stalled fork structures and remove obstacles. Other homologous recombination (HR) proteins that have been associated with replication fork restart are PARP1 (Poly {ADP-ribose} polymerase 1), Mre11, BRCA2 and Rad51. PARP1 promotes fork restart by interacting and promoting Mre11 recruitment (Bryant et al., 2009; Haince et al., 2008). Mre11 has been shown to promote fork restart through its resection function and, in yeast, facilitating the cohesion of sister chromatids (Tittel-Elmer et al., 2009). BRCA2 promotes fork restart by regulating Rad51 filaments loading onto ssDNA, thus preventing excessive resection by Mre11 (Hashimoto et al., 2010; Schlacher et al., 2011). Rad51 is also needed for fork restart because it is needed for D-loop formation (Petermann et al., 2010).

Formation of HJs and D-loops requires HR proteins. It has been shown that the lack of functional HR proteins, such as Mre11 (Costanzo et al., 2001; Yamaguchi-Iwai et al., 1999), RAD51 (Sonoda et al., 1998), BRCA2 (Lomonosov et al., 2003), FANCD2 and FANCA (Sobeck et al., 2006), can cause a higher level of damage in replication inhibitor treated cells, compared with cells with functional HR proteins. This could equate to HR proteins being important in the stabilization of replication forks that have stalled and the resolution of stalled fork structures (Daboussi et al., 2008; Schlacher et al., 2011).

Double-strand break response

The Ku70/Ku80 heterodimer and the MRN complex appear to be recruited first to DNA DSB. The MRN complex causes the activation of ATM (Uziel et al., 2003) which phosphorylates H2AX histones (γH2AX) (Burma et al., 2001). γH2AX is bound by MDC1 (mediator of damage checkpoint 1) (Stucki et al., 2005) which associates with Nbs1 in the MRN complex (Chapman and Jackson, 2008). Nbs1 interacts with CtIP (Williams et al., 2009) and BRCA1-BARD1 in the BRCA1-C complex (Yu and Baer, 2000). 53BP1 is also recruited to DSBs, but by the methylation of histones (H4-K20) (Botuyan et al., 2006).

The first process of HR that occurs at DSBs is resection. This will only occur if Ku70 Ku80 heterodimer has been removed from the DSB DNA ends by VCP (Mimitou and Symington, 2010; Postow et al., 2008). Resection is performed by Mre11 (Taylor et al., 2010), from the MRN complex, and CtIP, from the BRCA1-C complex (Buis et al., 2012). Mre11 nuclease activity resects the 5' strand by a few bases (Taylor et al., 2010). CtIP alongside Mre11 fully resects the DSB by 50-100nt bases, to create a 3' overhang (Buis et al., 2012). This process is inhibited by 53BP1 which competes with BRCA1-C complex, to favour non-homologous end-joining (NHEJ) repair of the DSB (Bunting et al., 2010). The BRCA1-C

complex is cell cycle dependent and allows HR only in late S or G2 phase, where there is a sister chromatid to use as a template for repair synthesis (Chen et al., 2008).

MDC1 recruits RNF8 to sites of damage where it monoubiquitinates the surrounding H2A-type histones (Huen et al., 2007; Mailand et al., 2007). This causes chromatin rearrangement that allows DSB repair proteins to access the DNA which is essential for both NHEJ and HR (Mailand et al., 2007). Polyubiquitination (K48 chains) is essential for formation of 53BP1 foci, so the action of the VCP complex and K48 chains may play a role in 53BP1 recruitment (Acs et al., 2011). 53BP1, once recruited, acts to amplify the ATM signal (Bunting et al., 2010). This leads to the phosphorylation of Kap1, which allows chromatin rearrangements needed for both DSB repair pathways (Bencokova et al., 2009; White et al., 2012).

RNF8 can create both K63 and K48 chains, but RNF168 can only produce K63 chains. Polyubiquitination (K63 chains) recruits RAP80 in complex with Abraxas and BRCA1 (BRCA1-A complex) (Wang et al., 2007). Abraxas is a protein with a coiled coil structure that is thought to be the core protein on which the BRCA1-A complex assembles (Wang et al., 2007). Other proteins in the BRCA1-A complex are BRCC36 (Dong et al., 2003), Cdc98 (Liu et al., 2007), BRE (Dong et al., 2003) and MERIT40 (Feng et al., 2009). The BRCA1-A complex, excluding BRCA1 is found at stable levels in the cell throughout the cell cycle but BRCA1 is found in very low levels in G1 and rises in S and G2 phases (Chen et al., 1996).

BRCC36, a DUB, removes the K63-linked chains from histones after the BRCA1-A complex is recruited and promotes the interaction between BRCA1 and BARD1 (Shao et al., 2009). It is possible that BRCC36 removes the K63 chains to promote BRCA1 to create

K6 chains, of which the function remains unclear (Morris and Solomon, 2004; Wu-Baer et al., 2003).

Rad51 is recruited to DSBs in a RNF8 dependent manner but it is not dependent on the creation of K63 chains made by RNF168. This may be because Rad51 is recruited by RNF8's ability to create K48-linked chains (Mailand et al., 2007).

When resection is complete a human helicase (yeast homologue to Sgs1) unwinds the DNA to elongate the 3' ssDNA end which is bound by RPA (Cejka et al., 2010). Rad51 replaces RPA on ssDNA (Wang and Haber, 2004) with the help of BRCA2 (Wong et al., 2003) and DSS1 (Gudmundsdottir et al., 2004). It is the interaction between BRCA2 and BRCA1, via PALB2, that recruits DSS1, from the proteasome, and BRCA2 to the DSB (Zhang et al., 2009). The Rad51 filaments stretches the ssDNA to the homologous sequence on the sister chromatid, creating a D-loop (Sung and Robberson, 1995; Yu et al., 2001). Synthesis using the sister chromatid as template can then occur as Rad51 dissociates from the ssDNA. The end of the newly synthesised DNA is then joined at the other side of the resected area to form a HJ. HJs can be resolved by resolvase enzymes, such as Mus81/Mms4 (Hanada et al., 2007), leading to sister chromatid crossover events depending on which plane the HJ is resolved (Schwartz et al., 2012).

Checkpoint response to replication fork stalling

When DNA replication becomes stalled, the cell needs more time to finish DNA replication and repair before moving into mitosis. Cell cycle checkpoints that help to control this progression. The two main checkpoints that control this are the intra-S and S/M phase checkpoints.

The intra-S phase checkpoint stops late origin firing in favour for the stability of stalled forks and synthesis restart. The S/M checkpoint is enforced to stop cells with unreplicated or damaged DNA going into mitosis, and leading to chromosomal aberrations.

When replication forks become stalled they continue to unwind creating excessive ssDNA which is coated with RPA (Byun et al., 2005; Longhese et al., 1996; Zou and Elledge, 2003). RPA presence activates ATR, a checkpoint kinase, and ATRIP. The ATRIP and ATR complex localises onto DNA as does Rad17 (Choi et al., 2010). Rad17 binds to subunits of RFC and loads the PCNA-like complex, such as 9-1-1, onto the stalled replication fork (Zou et al., 2002; Zou et al., 2003). Once loaded the PCNA-like structure enables ATR to phosphorylate Chk1, which is a PCNA-like chromatin-bound substrate (Kobayashi et al., 2004).

Activated ATR leads to a multitude of protein pathways being activated, such as DNA repair, apoptosis and further checkpoint signalling. ATR specifically phosphorylates Chk1, when promoted by other factors such as Claspin (Kumagai and Dunphy, 2000), TopBP1 (Kim et al., December 15, 2005), Rad9, Rad17 (Zou et al., 2002), TIM and TIPIN (Yoshizawa-Sugata and Masai, 2007). This activates Chk1 which phosphorylates CDC25 A-C (Sanchez et al., 1997), inhibiting cyclin E/A-CDK2 and cyclin B-CDK2 activation. Inhibition of CDK prevents loading of the helicase and replisome via Cdc45 (Aparicio et al., 1999). This process leads to an elongation of S phase. Without ATR activity, cells lose the S/M checkpoint which leads to an accumulation of DSBs.

Fork progression is also influenced by the presence of various factors mentioned above. For example defects in TIM (Ünsal-Kaçmaz et al., 2007), Claspin (Osborn and Elledge, 2003),

or TopBP1 slow fork replication rates. TopBP1 slows replication forks by 40% in Xenopus egg extracts (Van Hatten et al., 2002).

Checkpoint response to double-strand breaks

Stalled forks can collapse into DSBs, and this activates the S/M checkpoint until they are completely repaired. As discussed above, stalled forks lead to ssDNA which activates the ATR pathways and consequently the intra-S phase checkpoint, to lengthen the time the cell is in S-phase. When a DSB is sensed the ATM pathway is stimulated alongside the ATR pathways.

MDC1, which is one of the earliest proteins involved in DSB response, is known to associate with Chk2 in the ATM/Chk2 cell cycle checkpoint pathway (Lou et al., 2003b). MDC1 is essential for the recruitment of BRCA1, as without MDC1, BRCA1 does not relocalize and is not hyperphosphorylated (Lou et al., 2003a). This affects the function of BRCA1 and its ability to bind in its several complexes that are needed for DSB repair. BRCA1 is also needed for the phosphorylation of Chk1 following DNA damage (Lou et al., 2003a) which suggests BRCA1 may aid the regulation of the G2/M checkpoint through Chk1 (Yarden et al., 2002). Mre11 has also been shown to further activate the Chk2 which targets the ATR/Chk1 pathway through CDKs and p53 (Lee and Paull, 2004).

It is the activation of Chk1 and Chk2 that, through down-regulation of CDK activity, control the regulation from S-phase through G2 and into mitosis.

Gemcitabine

Gemcitabine is one of several drugs whose target is to cause faulty DNA replication and create DNA damage that will kill the cancer cells. Gemcitabine, 2',2'-difluoro-2'-

deoxycytidine (dFdC) (Bianchi et al., 1994) is similar to the DNA building block deoxycytidine, but it has two fluorine atoms replacing hydrogen on its 2nd carbon in its ribose ring (Hertel et al., 1990).

Gemcitabine is metabolised into two compounds; 5'-diphosphate (dFdCDP) and 5'-triphosphate (dFdCTP) (Cerqueira, Fernandes and Ramos, 2007). dFdCDP has been shown to inhibit ribonucleotide reductase (RNR) by disrupting the kinetics of both of the RNR two protein subunits (R1, R2). RNR catalyzes, dependent on its two active subunits, the reaction that produces deoxyribonucleotides that are the building blocks of DNA. Therefore there is a reduction in dNTPs for DNA synthesis in Gemcitabine treated cells. dFdCTP is similar enough to deoxycytidine 5-triphosphate (dCTP) that they compete for incorporation during DNA synthesis. Once dFdCTP is added onto a synthesising strand, it is only possible to add a single deoxyribonucleotide before the synthesis is inhibited (Cerqueira et al., 2007).

Gemcitabine therefore acts in three ways using its two metabolites; firstly, dFdCDP reduces the amount of free dNTPs for DNA synthesis by inhibiting RNR: secondly, Gemcitabine metabolism increases due to the lack of dNTPs: finally, dFdCTP is incorporated into the DNA which stops further DNA being synthesised (Cerqueira et al., 2007).

Gemcitabine is a FDA and EMEA approved drug treatment for non-small cell lung cancer (Shepherd et al., 1997), pancreatic adenocarcinoma (Plate et al., 2005), breast cancer, ovarian cancer and bladder cancer (Nawrocki et al., 2002). It has been trialled alongside Carboplatin, Cisplatin or Imatinib in pancreatic cancer and in combination with Cisplatin in

breast and non-small cell lung cancer (Cerqueira, Fernandes and Ramos, 2007; Nagourney et al., 2008) .

BRCA1 in breast cancer

BRCA1 (Breast cancer type 1 susceptibility protein), previously mentioned to be important in DSB repair, is a tumour suppressor found on chromosome 17q21 in humans that, when mutated, causes breast cancer. It was isolated through linkage analysis of families with high incidence of early onset breast and ovarian cancer (Hall et al., 1990). An inherited mutation in BRCA1 is recessive; therefore for tumour development a loss of heterozygosity is needed. Inherited breast cancer is estimated to be causative of 5-10% of breast cancer cases, but inheriting a mutation gives the individual a 40-80% risk of developing breast cancer (Wang et al., 2012). There are a multitude of inherited BRCA1 mutations that can be traced through populations such as among Ashkenazi Jews. Most of the mutations found in BRCA1 are protein-truncating mutations and they mostly are in the two most functional domains in BRCA1 (Wang et al., 2012).

The two domains are the N-terminal Zinc RING finger domain and the C-terminal double BRCT domain. The RING domain provides BRCA1 with its E3 ubiquitin ligase activity and interacts with BARD1 (Xia et al., 2003). The BRCT domain binds to many proteins, such as CtIP, p53 and BRCA2 (Drikos et al., 2009).

BRCA1 is involved in many important cellular functions, such a cell cycle checkpoint control and DSB repair. In the DSB repair, as previously discussed, BRCA1 is involved in promoting HR through competing with 53BP1, as well as regulating Mre11 and CtIP end resection, BRCA2 recruitment to DSBs, S and G2/M checkpoint control during DNA

replication. Defects in BRCA1 risk genomic integrity through faulty DNA replication, DNA repair and cell cycle progression. This would lead to chromosomal rearrangements, duplication and deletions of genetic material to daughter cells and eventually to cell death.

Aims of project

Gemcitabine causes fork stalling through its inhibition of RNR and incorporation into the newly synthesized DNA strand. Gemcitabine is currently used to treat cancer because it causes DNA replication to slow and induces DSBs at stalled forks, leading the cells to cell death. It is used in ovarian and breast cancer treatment alongside other drugs such as Cisplatin. Therefore, we decided to measure the response of the HR-defective BRCA1-deficient breast cancer cell line HCC1937.

Our main questions were:-

- Does BRCA1 status affect fork stalling or restart after Gemcitabine treatment?
- Does BRCA1 status affect the survival of cells after Gemcitabine treatment?
- What are the localization foci timings of 53BP1 and Rad51 in BRCA1-defective cells after Gemcitabine treatment?
- Does BRCA1 status affect the induction of p-RPA32 after Gemcitabine treatment?

METHODS

Unless otherwise stated chemicals were obtained from Sigma-Aldridge (St Louis, MO, USA) or Thermo Fisher Scientific (Loughborough, UK)

Unless otherwise stated tissue culture supplies were obtained from Corning (Corning, NY, USA)

Materials

Primary Antibodies
Mouse α-BrdU (Beckton Dickinson, Oxford, UK)
Mouse α-γH2AX (Millipore, Billerica, MA, USA)
Mouse α-Tubulin
Rabbit α-53BP1 (Bethyl Laboratories, Montgomery, TX, USA)
Rabbit α-RPA32-P (Bethyl Laboratories, Montgomery, TX, USA)
Rat α-BrDU (AbD Serotec, Dusseldorf, Germany)

Secondary Antibodies
α-Mouse AlexaFluor 488 (Invitrogen, Grand Island, NY, USA)
α-Mouse HRP (Dako, Glostrup, Denmark)
α-Rabbit AlexaFluor 555 (Invitrogen, Grand Island, NY, USA)
α-Rabbit HRP (Dako, Glostrup, Denmark)
α-Rat AlexaFluor 555 (Invitrogen, Grand Island, NY, USA)

siRNAs
ON-TARGETplus SMARTpool, Human BRCA1 siRNA (672) [L-003461-00-0010] (Thermo Fisher Scientific, Loughborough, UK)
ON-TARGETplus Non-targeting siRNA#1 [D-001810-01-20] (Thermo Fisher Scientific, Loughborough, UK)

Cell Lines
U20S osteosarcoma (Niforou et al., 2008)
HCC1937 with empty pcDNA3 vector (BRCA1-ve cells) (Scully et al., 1999)
HCC1937 with pcDNA3BRCA1 vector (BRCA1+ve cells) (Scully et al., 1999)

Solutions

Spreading buffer
200mM Tris-HCl pH 7.4
50mM EDTA
0.5% SDS

HCl solution

5.2ml 37% Hydrochloric Acid
19.8ml H_2O

Blocking solution
200µl Tween20
2g Bovine Serum Albinum
200ml PBS

UTB buffer
50mM Tris pH7.5
150mM β-mercaptoethanol
8M Urea

PI/RNase solution (per sample)
9µl Propidium Iodide (PI)
0.3µl RNase A
490.7µl PBS

TBSTx10
12.1g Tris
81.8g NaCl
Correct pH to 7.9 with HCl
Make up to 1litre with dH20

Ponceau stain
1g Ponceau S
50ml acetic acid
Make up to 1L with ddH2O

0.2% Methylene Blue Stock Solution
0.2g methylene blue-trihydrate
100ml dH2O

0.025% Methylene Blue Staining Solution
62.5ml of 0.2% Methylene Blue stock solution
437.5ml dH2O

Protocols

Tissue Culture

Cells were maintained in Gibco® by Life Technologies, Iscove's Modified Dulbecco's Medium with added L-Glutamine and 25mM HEPES. Grown with 15% FCS and Penicillin/Streptomycin and grown at 37°C, 5% CO_2. Routine passages were done

regularly depending on cell confluence. When cells reached 90% confluence they were passaged at a 1:3 dilution.

Clonogenics/Cell survival assay

Cells were seeded in 6 well plates at two total cell numbers for each drug concentration and left overnight to adhere. The following day cells were treated for 2hrs with the desired Gemcitabine concentration. The cells were washed twice with warm PBS and released into fresh media. The cells were checked regularly to see if the surviving colonies had reached ~30 cells. When the majority of colonies reached this size, they were fixed and stained with 0.025% Methylene Blue solution. The media was taken off the cells and they were washed twice with PBS. Methylene blue was added to the well to fix and stain the cells for 10 minutes. This was washed off and the plates are left to dry before the colonies in each condition, were counted.

Fibre assay using CldU/IdU labelling

1) Labelling. Cells were seeded overnight in 6 well plates. CldU was added to cells at a final concentration of 25μM and incubated for 20 minutes. IdU was added to the cells at a final concentration of 250μM and incubated for 20 minutes. The cells were washed with ice cold PBS and trypsinised and collected in PBS. Cells were diluted to a concentration of $5x10^5$/ml in PBS. Cells that were treated with Gemcitabine followed a different labelling protocol. CldU (25μM) was added to cells for 20 minutes and Gemcitabine was added, at the desired concentration, and incubated for 30 minutes, still in CldU. IdU (250μM) was then added for either 2 or 4 hours and cells were harvested with PBS as described before.

2) Spreading. 2µl of a sample was pipeted onto a microscope slide and left to dry for 5-7 minutes or until the sample was 'sticky' but not dry. 7µl of spreading buffer was added and stirred into the sample, to lyse the cells and degrade protein structures, and incubated at RT for 2 minutes. The slides were tilted so the sample runs down the slide slowly, taking around 3-5 minutes to get to the bottom edge of the slide. The slides were air dried before being fixed in Methanol/Acetic Acid (3:1) for 10 minutes. These were air dried and stored in the fridge.
3) Immunostaining. Slides were washed twice with water for 5 minutes to rehydrate the slides. The slides were rinsed with HCl solution and incubated in HCl solution for 80 minutes. The slides were rinsed twice with PBS and washed twice with blocking solution (5-10 minutes each) before incubating at RT in blocking solution for 30-60 minutes. 115µl of primary antibody mix was added to the slides, covered with a large coverslip and incubated for 1hr. Primary antibody solution contained Rat αBrDU (1:1000) and Mouse αBrdU (1:500) in blocking solution. Slides were rinsed three times with PBS and fixed with 4% paraformaldehyde/PBS for 10 minutes. Slides were rinsed three times with PBS and washed three times with blocking solution. 115µl of secondary antibody mix was added to the slides, covered with a large coverslip and incubated for 2hrs. Secondary antibody solution contained αRat AlexaFluor 555 and αMouse AlexaFluor 488 (both 1:500) in blocking solution. Slides were rinsed twice with PBS, washed three times with blocking solution and washed twice with PBS. Slides were mounted with mounting medium and a large coverslip and stored at -20^{o}C.

Fibres were either counted for structure type or fibre length was counted by pixels using ImageJ software. This was achieved by imaging a scale bar on a microscope slide and using this image to identify a conversion factor from µMs to pixels to kilobase pairs of DNA.

Foci protocol

Cells were plated overnight on coverslips in a six well plate. Media was removed and cells were fixed for 10 minutes in 4% paraformaldehyde/PBS. Cells were washed in PBS and stored in PBS in the fridge. Cells were permeablised with 0.25% Triton X100/ PBS solution at RT for 5 minutes before being washed twice with PBS and washed three times with blocking solution. 80µl of Mouse α-γH2AX antibody (1:1000) was added to the coverslip and incubated for 1hr at RT. Cells were washed twice with PBS and washed three times with blocking solution. 80µl of α-mouse 488 antibody (1:500) was added to the coverslip and incubated in the dark for 2hrs at RT. Cells were washed twice with PBS and washed three times with blocking solution. 80µl of Rabbit α-53BP1 antibody (1:3000) was added to the coverslip and incubated for overnight at 4^{o}C. Cells were washed twice with PBS and washed three times with blocking solution. 80µl of α-rabbit 555 antibody (1:500) was added to the coverslip and incubated in the dark for 2hrs at RT. Cells were washed twice with PBS and mounted with Mounting Medium containing DAPI stain onto microscope slides and stored at 4^{o}C.

γH2AX staining was quantified using the overall signal of green in RGB photo using ImageJ. This was normalised by comparing the quantified green signal of the same cells imaged for DAPI stain.

FACS protocol

Cells were grown in a T25 flask until confluent under normal tissue culture conditions. Cells were treated to create the following conditions:-

- CPT- Camptothecin at 1µM for 1hr with 50µM of Mirin (Tocris Bioscience, Bristol, UK) throughout or with 10µl of DMSO throughout.
- Gemcitabine- Gemcitabine at 6µM for 2hr with 50µM of Mirin throughout or with 10µl of DMSO throughout.

Cells were released into fresh media and harvested either immediately (CPT), or after 2 or 48 hours (Gemcitabine). To harvest the cells, they were trypinised (Invitrogen, Grand Island, NY, USA) and resuspended in 1ml ice cold PBS before centrifuging at 5,000rpm for 5 minutes. The cells were resuspended in ice cold 70% EtOH and vortexed. They were then stored at 4^{o}C until they were washed before being PI stained.

Cells were centrifuged at 2,500rpm for 4 minutes at 4^{o}C and the supernatant was gradually removed. Cells were washed with PBS and centrifuged again. Cells were resuspended in PBS for 1hr at RT before being centrifuged again. Finally, cells were resuspended in 500µl of PI/RNase solution and incubated for at least 1hr at 4^{o}C in FACs tubes. Samples were stored for up to 7 days.

Western Blotting

Samples were plated overnight and treated with various drugs for the correct conditions. Harvested cells were counted and resuspended in UTB buffer to the concentration of ~$5x10^{6}$cells/ml and kept on ice. Samples were sonicated twice for 10 seconds at 4.5 input power and cooled with ice before centrifuged at full speed for 10 minutes at 4^{o}C. The supernatant was transferred to a new tube and loading buffer was added at a ratio of 1:4. Samples and protein marker (New England BioLabs, Hitchin, UK) were boiled before 20µl

of sample was loaded into a 12% acrylamide gel. The gel was then run for 80 minutes at 150V before being transferred onto transfer membrane for 90 minutes at 100V. The transfer membranes (GE Healthcare UK, Little Chalfont, UK) were stained with ponceau stain and cut at 46kDa, 27kDa and 5kDA. Membranes were then blocked in 5% Milk/TBST for 1hr at RT, before being separated and put into the first antibody and incubated overnight at 4^{o}C. The first antibodies were Mouse α-Tubulin (1:2000), Rabbit α-RPA32-P (1:500) and Mouse α-γH2AX (1:1000). Membranes were washed three times in TBST for 5 minutes before being blocked in 5% Milk/TBST for 20 minutes at RT. Membranes were placed into the corresponding secondary antibody and incubated at RT for 90 minutes. Secondary antibodies were α-Mouse and α-Rabbit, both conjugated to HRP and both at 1:5000 concentration. The membranes were washed three times in TBST for 5 minutes and added to an ECL wash (Thermo Fisher Scientific, Loughborough, UK) and developed.

	Separating Gel (12%) 20ml	Stacking Gel (5%) 10ml
Water	6.6ml	6ml
1.5M Tris pH 8.8	5ml	-
1M Tris pH 6.7	-	2.5ml
Acrylamide (30%)	8ml	1.34ml
SDS (10%)	200µl	100µl
APS	200µl	100µl
TEMED	18µl	10µl

Table 1- *Recipes of acrylamide gels used for western blotting.*

siRNA transfection protocol

Tube1: diluted siRNA (µl/well)	Tube2: diluted DharmaFECT (µl/well)
20µM of siRNA = 4µl	DharmaFECT 1 reagent = 4µl
OptiMem medium = 196µl	OptiMem medium = 196µl

Table 2- *Recipe of siRNA transfection reagents*

Volumes above based on single wells of a 6-well plate.

Seed cells 12hours before transfecting. Ingredients are added with desired siRNA into tube 1 and 2 and incubated for 5 minutes at RT. Tube 1 and Tube 2 are then added to each other slowly and incubated for 20 minutes at RT. The final solution is then added to each well in the 6-well plate to make up the medium (antibiotic-free) to 2ml. Media is changed ~16 hours after transfection. siRNA is considered to work ~48-72 hours after transfection. DharmaFECT 1 was purchased from Thermo Fisher Scientific (Loughborough, UK) and OptimMEM was purchased from Invitrogen (Grand Island, NY, USA).

RESULTS

Fork stalling and BRCA1 status

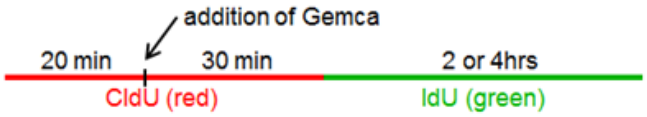

Figure 1 – *Diagram of the CldU and IdU labelling for Gemcitabine (Gemca) treated conditions in the fork stalling DNA fibre experiment.*

The DNA fibre technique uses double labelling with thymidine analogues (CldU and IdU) to assess the level of DNA replication fork stalling in the presence of inhibitors of DNA replication. HCC1937 BRCA1-proficient and -deficient cells were labelled to investigate the influence of BRCA1 status on Gemcitabine-induced fork stalling. 20 minutes into the 1st label (CldU, 50 minutes total), a dose of 2µM Gemcitabine was added and remained present throughout the 2nd label (IdU, two or four hours) (Figure 1). Control cells were untreated and both labels were added for 20 minutes consecutively. Images of the fibres were analysed for replicative structures (Figure 3) defined by the two labels (Figure 2). The experiment was repeated with a 6µM dose of Gemcitabine (Figure 4 & 5) as HCC1937 cells showed some resistance to the replication inhibitory effects at the lower concentration. The percentage of CldU-only labelled tracks, a measure of stalled forks, increased in the 2µM Gemcitabine treated cells compared with control, and the increase was greater in the 4 hour IdU treatment (Figure 3). After Gemcitabine treatment, the BRCA1-deficient cells showed a higher level of fork stalling compared to control than the BRCA1-proficient cells. In the 6µM Gemcitabine experiment a similar result was seen

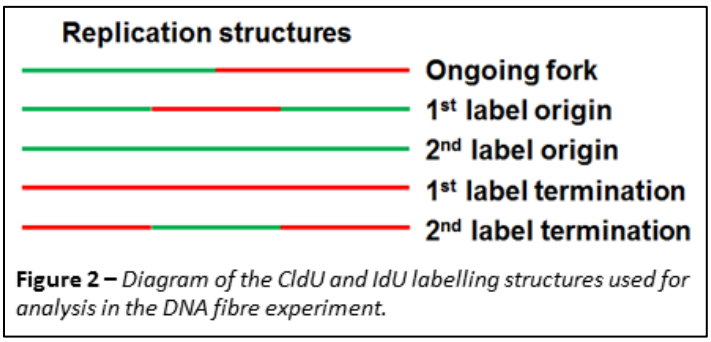

Figure 2 – *Diagram of the CldU and IdU labelling structures used for analysis in the DNA fibre experiment.*

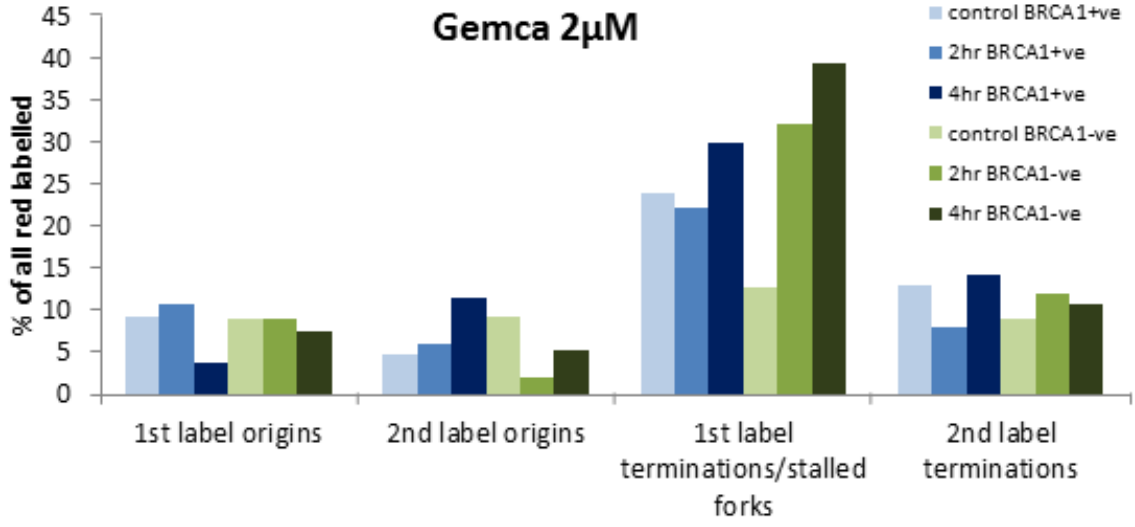

Figure 3 – *Percentage of each replication structure seen in images from the fork stalling DNA fibre experiment using HCC1937 BRCA1 +ve and –ve cells. The conditions are Control (untreated), 2hr (2µM Gemcitabine treated cells with 2hr IdU labelling) and 4hr (2µM Gemcitabine treated cells with 4hr IdU labelling).*

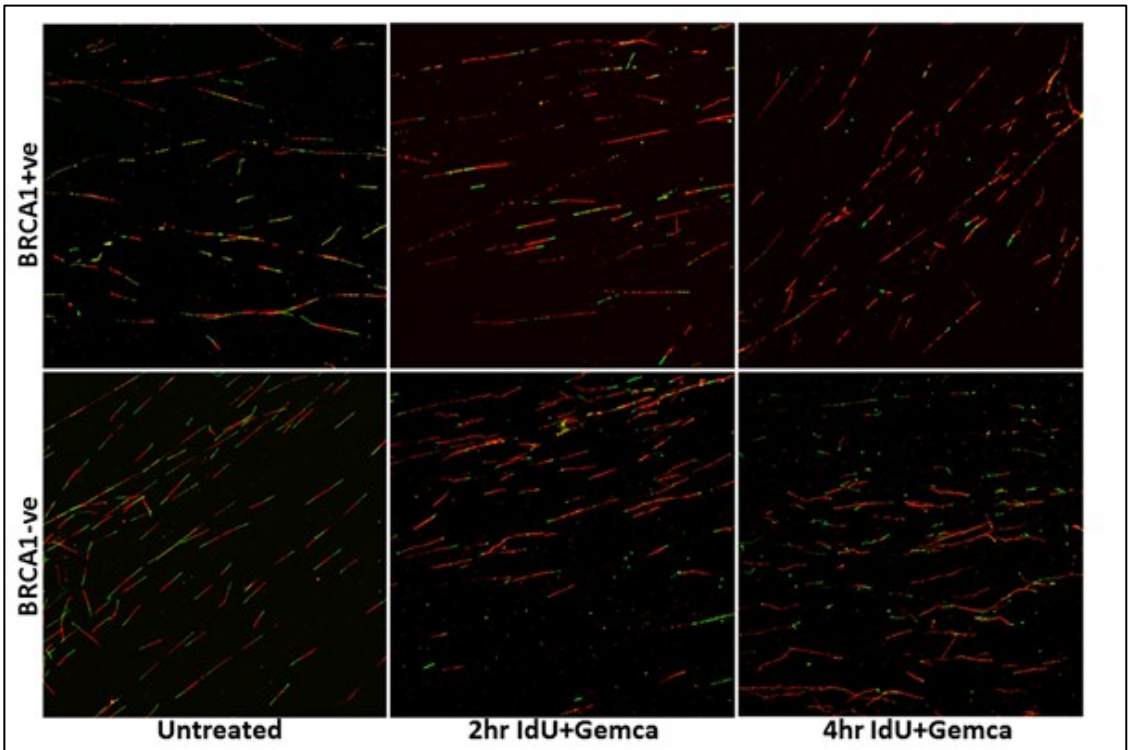

Figure 4 – *Images from the fork stalling DNA fibre experiment using HCC1937 BRCA1 +ve and –ve cells. The conditions are Control (untreated), 2hr (6µM Gemcitabine treated cells with 2hr IdU labelling) and 4hr (6µM Gemcitabine treated cells with 4hr IdU labelling).*

(Figure 5). The overall increase shows the DNA replication fork stalling by Gemcitabine occurs in HCC1937 cells. BRCA1-deficient cells have a lower rate of fork stalling in the absence of Gemcitabine (Supplementary Figure 1). The increased level of fork stalling seen in the BRCA1-deficient Gemcitabine treated cells suggests that BRCA1 may be involved in fork progression in the presence of Gemcitabine. This can been seen in the images of the fibres (Figure 4). The increase in CldU-only tracks seen in the 4 hour IdU treatment compared to the 2 hour IdU treatment is indicative of nucleotide degradation of the second label (see Discussion).

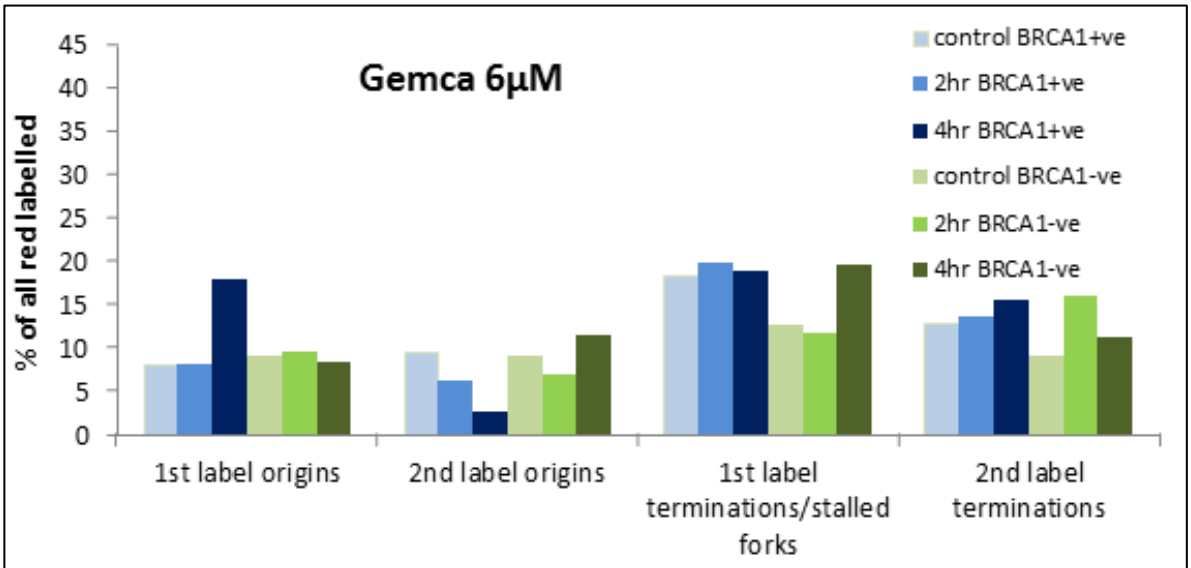

Figure 5 – *Percentage of each replication structure seen in images from the fork stalling DNA fibre experiment using HCC1937 BRCA1 +ve and –ve cells. The conditions are Control (untreated), 2hr (6µM Gemcitabine treated cells with 2hr IdU labelling) and 4hr (6µM Gemcitabine treated cells with 4hr IdU labelling).*

Using the same DNA fibre experimental images, the length (in pixels) of the labels for each fibre were measured and converted into µM and kilobase pairs (kb) to quantify the rate of DNA replication with and without Gemcitabine treatment in both BRCA1 cell types. The rate of fork speed in the 1st label (CldU) was decreased with Gemcitabine treatment in both

cell types, but BRCA1-deficient cells showed a greater decrease in replication rate compare to BRCA1-proficient cells (Figure 6a). The rate of fork speed in the 2nd label (IdU) was decreased to less than 10% of the untreated control IdU fork speed after 2hrs IdU labelling and to below 4% after 4hr IdU labelling (Figure 6b). The BRCA1-deficient cells showed a greater decrease in fork speed in the 2hr IdU labelling in compared to BRCA1-proficient cells, but this difference was not as great in the 4hr IdU labelling. These results show that BRCA1-deficient cells show a greater sensitivity to Gemcitabine treatment in both 1st and 2nd label fork speed rates, than BRCA1-proficient cells.

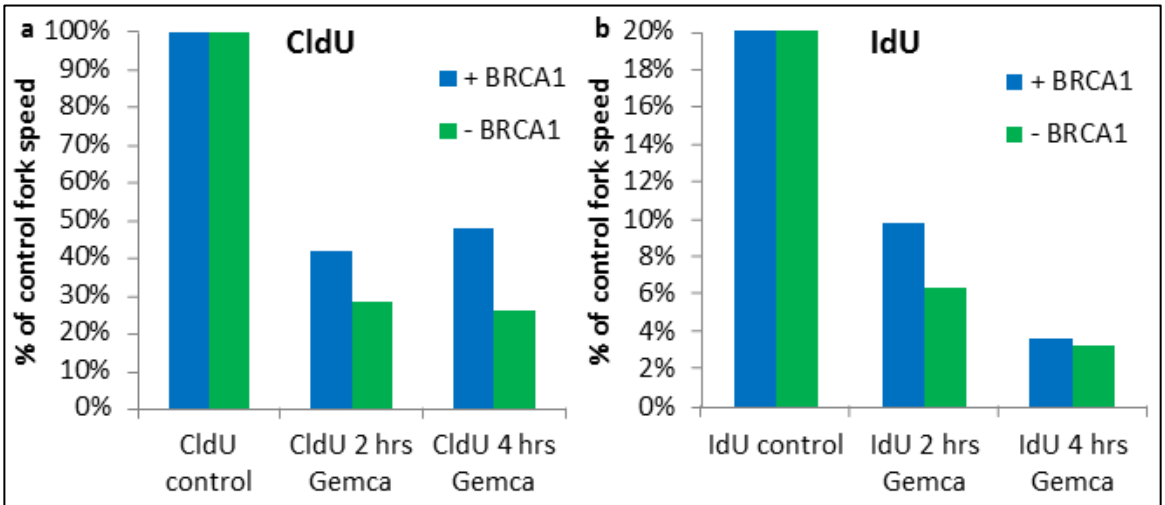

Figure 6 – *Graphs show the average fork speeds as a percentage of untreated control. (a) fork speed of CldU, 1st label, and (b) fork speed of IdU, 2nd label, from the fork stalling DNA fibres experiment in HCC1937 BRCA1 +ve and –ve cells that are untreated (Control) or treated (6µM Gemca for 2 hours) and released for 2 or 4 hours. The Y axis of (b) is shortened to highlight the difference between BRCA1+ve and –ve.*

When looking at the kilobases of replicated DNA throughout the time course (Figure 7) we can see that BRCA1-proficient cells slow the amount of DNA replicated 20 minutes after addition of Gemcitabine and appear to stall replication completely around 150 minutes. BRCA1-deficient cells appear to slow replication at 20 minutes although more DNA appears to have been replicated, and also stall replication forks completely by 150 minutes.

The reduction of the total amount of DNA replicated in BRCA1-deficient cells early during Gemcitabine treatment, may be indicative of DNA degradation. The final length of replicated DNA in the BRCA1-proficient cells is slightly shorter than at the previous time point (150 minutes), which may also be indicative of DNA degradation of stalled forks. The greater difference in BRCA1-proficient and –deficient total amount of replicated DNA before fork stalling suggests that BRCA1-deficient cells have a higher speed of replication than BRCA1-proficient cells.

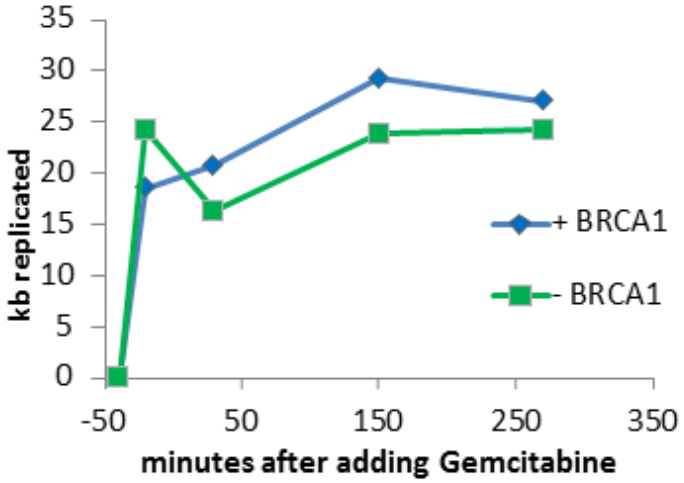

Figure 7 – *Graph shows the kilobases of DNA replication in HCC1937 BRCA1 +ve and –ve cells throughout the fork stalling DNA fibre experiment.*

The DNA fibre experiment was repeated in BRCA1 siRNA (BRCA1-ve) or non-targeted control (NTC) siRNA (BRCA1+ve) U2OS cells with the same labelling protocol and treatment with 2μM Gemcitabine (Treated, T) or untreated (Control, C) (Supplementary Figure 2). The treatment followed the time course and labelling in the previous experiment, (Figure 1) but without the 4hr IdU treatment. Spread fibres were stained using the same protocol as before and analysed for DNA replication structures. Both Gemcitabine-treated cell lines showed increased levels of fork stalling compared to the untreated control (Figure 8) and slightly more fork stalling in the BRCA1 siRNA-treated cells, than the NTC siRNA-treated cells. This suggests Gemcitabine does stall forks effectively in U2OS cells and the

increase in fork stalling in the BRCA1-deficient cells also occurs in a BRCA1 siRNA knockdown and therefore it supports the idea of BRCA1 status affecting fork stalling.

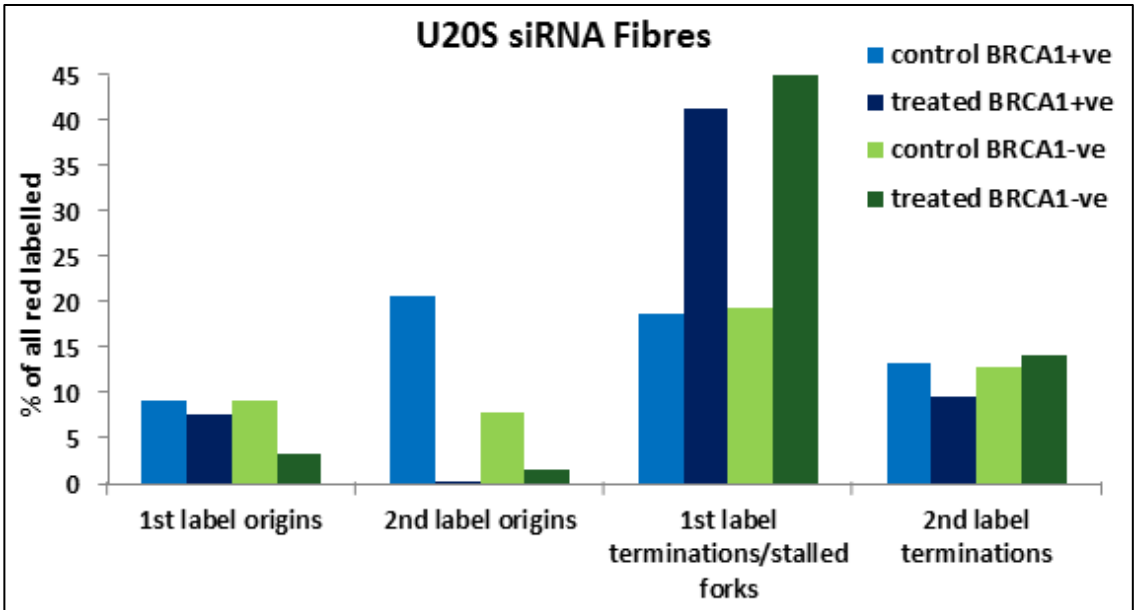

Figure 8 – *Percentage of each replication structure seen in images from the fork stalling DNA fibre experiment using BRCA1 or NTC siRNA treated U2OS cells. The conditions are control (untreated) and treated (2µM Gemcitabine treated cells with 2hr IdU labelling).*

Fork restart and BRCA1 status

The DNA fibre experiment can also be used to assess the level of fork restart after fork stalling induced by inhibitors of DNA replication. A dose of 2µM Gemcitabine was used to treat HCC1937 BRCA1-proficient and -deficient cells from 20 minutes into the 1st label (140 minutes total), and the Gemcitabine is washed out before adding the 2nd label (two hours) (Figure 9). Control cells were untreated and both labels were added for 20 minutes consecutively. DNA fibre images were analysed for replicative structures defined by the two labels (Figure 10 &

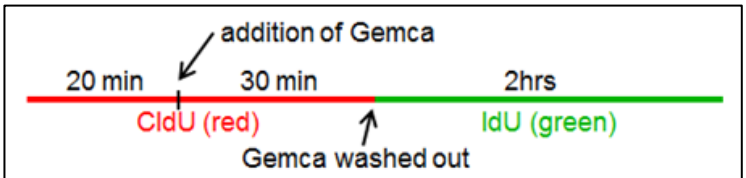

Figure 9 – *Diagram of the CldU and IdU labelling for Gemcitabine (Gemca) treated conditions in the fork restart DNA fibre experiment.*

Supplementary Figure 3). The fibres show levels of replication fork stalling similar to during Gemcitabine treatment and a slight increase in fork stalling in BRCA1-deficient cells as shown in the DNA fibres fork stalling experiment. Fork stalling persists for two hours after release from Gemcitabine suggesting the DNA replication inhibition is prolonged after Gemcitabine is removed. This suggests BRCA1 has no role in fork restart of Gemcitabine stalled forks.

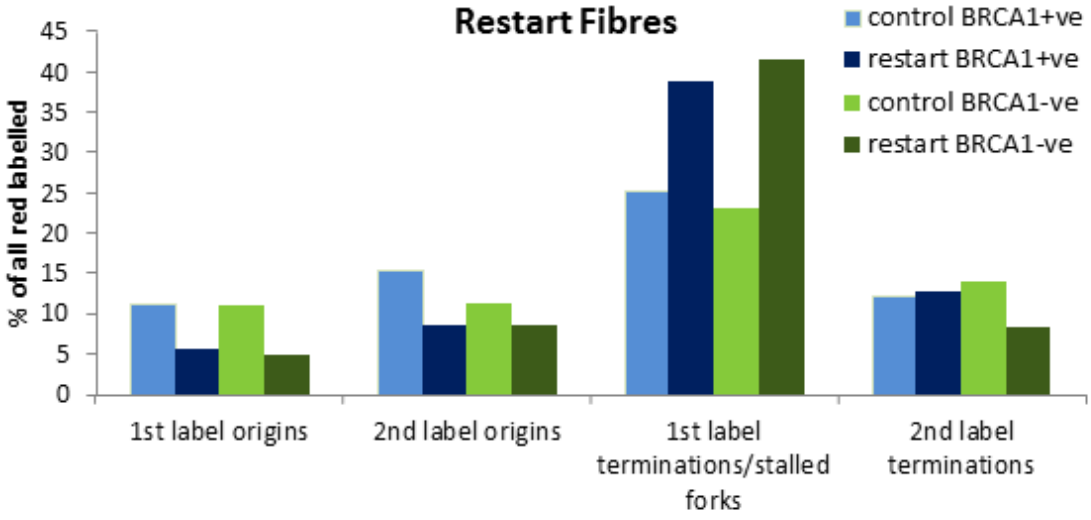

Figure 10 – *Percentage of each replication structure seen in images from the fork restart DNA fibre experiment using HCC1937 BRCA1 +ve and –ve cells. The conditions are control (untreated) and restart (2μM Gemcitabine treated cells with 2hr IdU labelling without Gemca).*

BRCA1 status effects on 53BP1 and ɣH2AX immunofluorescent staining

DNA damage from Gemcitabine treatment was measured using 53BP1 and ɣH2AX foci. 53BP1 foci indicate the presence of, specifically, DSBs and ɣH2AX is present at sites of DNA damage including stalled forks and DSBs.

HCC1937 BRCA1-proficient and –deficient cells were treated with Gemcitabine (2 or 6μM) or DMSO for two hours and released into fresh media for several time periods to allow DSBs to be induced and DNA repair response mechanisms to occur. Cells were

fixed, permeabilized and immunofluorescence stained for the presence of 53BP1 and γH2AX.

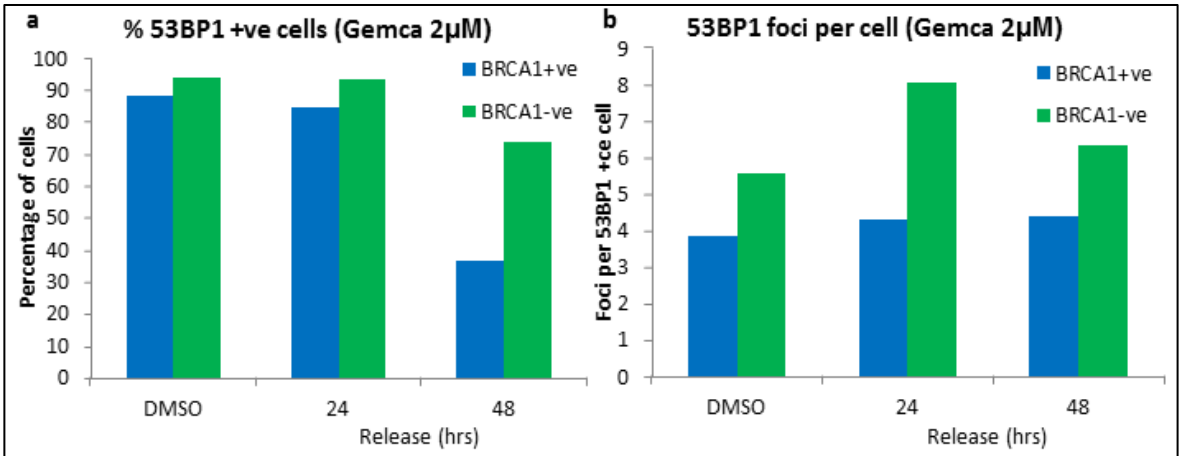

Figure 11 – *(a) Percentage of total cells with 53BP1 foci and, (b) the average number of 53BP1 foci per 53BP1 foci positive cell, in HCC1937 BRCA1 +ve and –ve cells untreated (DMSO) or treated with 2hr dose of Gemcitabine (2μM) and fixed after 24 or 48 hours release.*

In the 2μM Gemcitabine foci experiment, there were more cells that had 53BP1 foci (Figure 11a) and more foci in each 53BP1 positive cell (Figure 11b) after release from treatment (24 & 48 hours) in the BRCA1-deficient cells compared to BRCA1-proficient cells. However, there was little or no increase in the number of 53BP1 foci compared to the

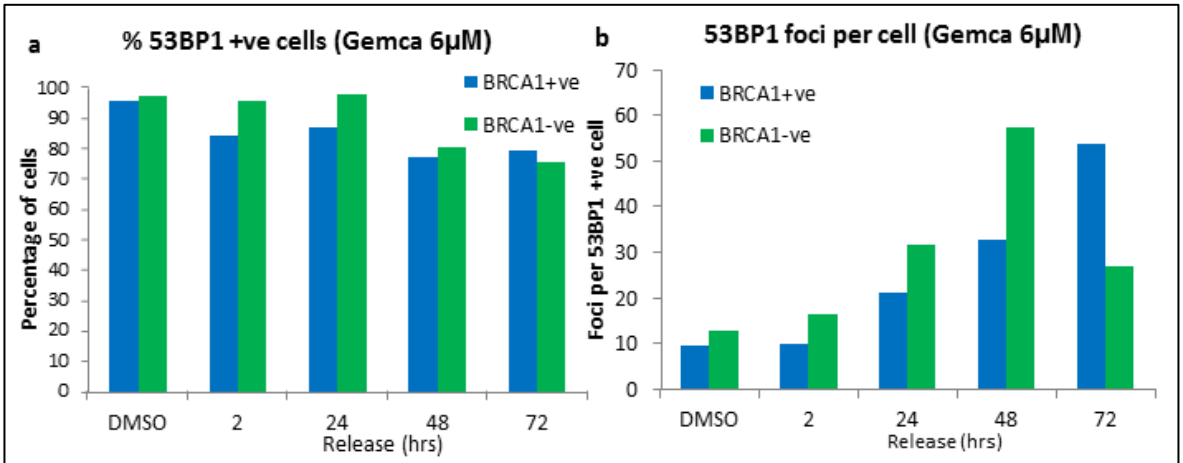

Figure 12 – *(a) Percentage of total cells with 53BP1 foci and, (b) the average number of 53BP1 foci per 53BP1 foci positive cell in HCC1937 BRCA1 +ve and –ve cells untreated (DMSO) or treated with 2hr dose of Gemcitabine (6μM) and fixed after 2, 24, 48 or 72 hours release.*

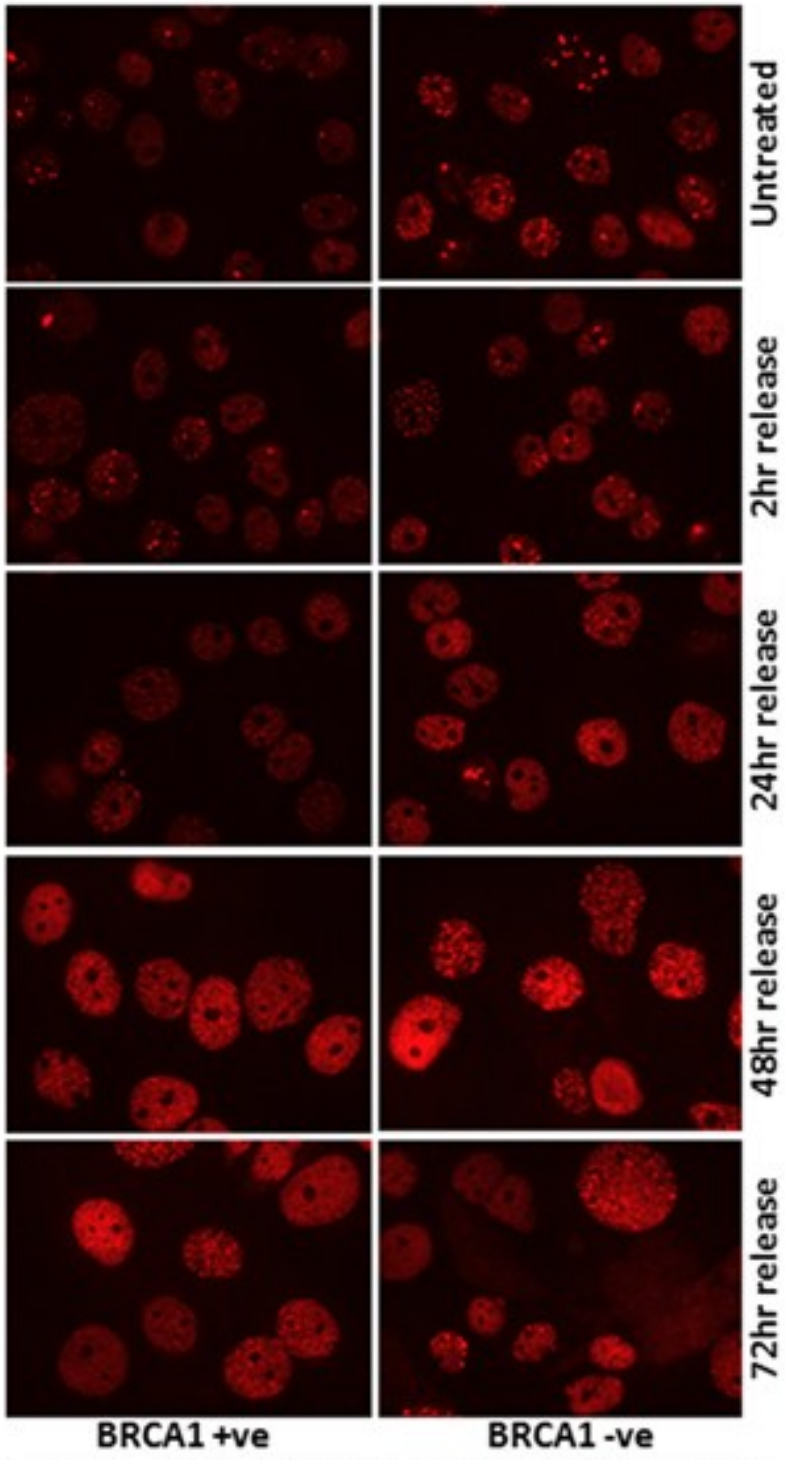

Figure 13 – *Pictures of 53BP1 (red) staining in HCC1937 BRCA1 +ve and –ve cells untreated or treated with 2hr dose of Gemcitabine (6μM) and fixed after 2, 24, 48 or 72 hours release.*

control (DMSO), suggesting that the 2μM Gemcitabine treatment did not induce many DSBs in HCC1937 cells. When the dose of Gemcitabine was increased to 6μM, the number of 53BP1 foci per positive cell increased dramatically over time, suggesting that DSBs were induced by the treatment (Figure 12b & 13). The difference between the percentages of BRCA1-deficient 53BP1-positive cells compared to BRCA1-proficient 53BP1-positive cells was similar after 6μM Gemcitabine treatment as it was in the 2μM Gemcitabine treatment

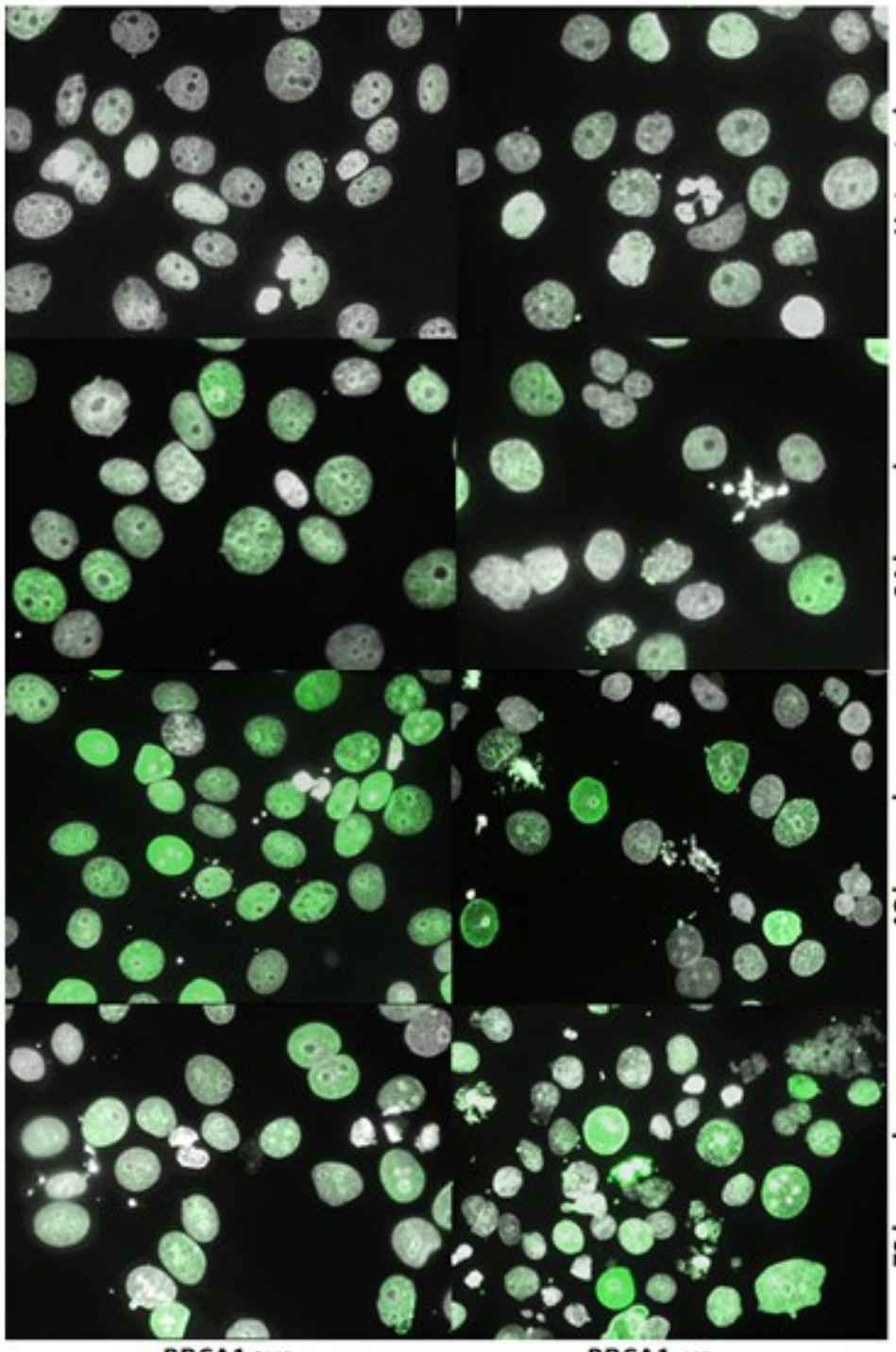

Figure 14 – *Pictures of DAPI (grey) and γH2AX (green) staining in HCC1937 BRCA1 +ve and –ve cells untreated or treated with 2hr dose of Gemcitabine (6μM) and fixed after 24, 48 or 72 hours release.*

(Figure 12a & 13). A decrease in the 53BP1 positive cells, at late time points, was seen in in both experiments, possibly because of high cell death due to the amount of damage (Figure 14). The number of 53BP1 foci increased in the BRCA1-proficient cell line until 72 hours, but in the BRCA1-deficient cell line the number of foci increased more strongly until it peaked at 48 hours (Figure 12b). The reduction in foci in the BRCA1-deficient cells at 72 hours may be due to high levels of cell death (Figure 14).

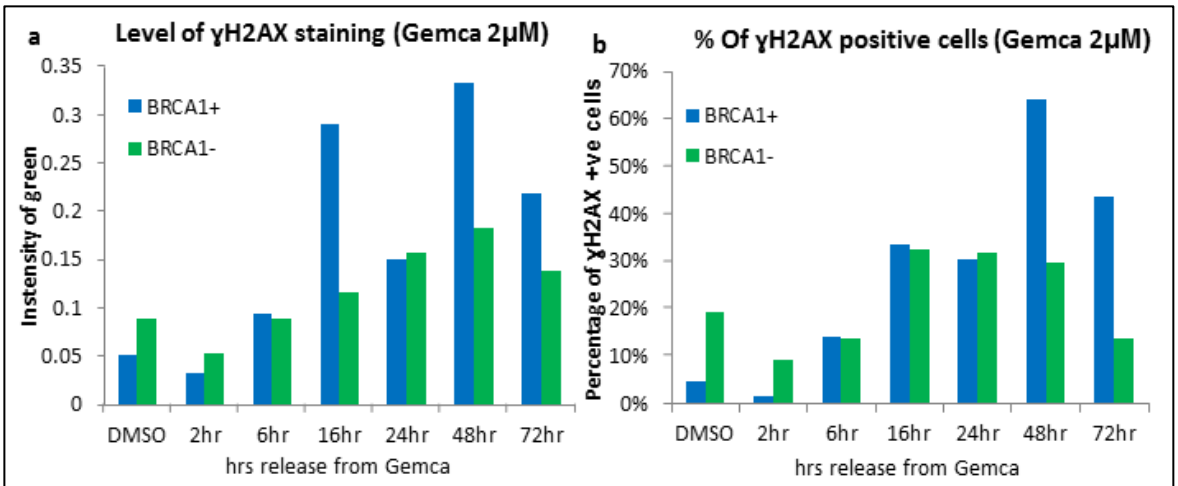

Figure 15 – *(a) Level of γH2AX staining and, (b) the percentage of γH2AX positive cells in HCC1937 BRCA1 +ve and –ve cells untreated (DMSO) or treated with 2hr dose of Gemcitabine (2μM) and fixed after 2, 6, 16, 24, 48 or 72 hours release.*

In the 2μM Gemcitabine foci experiment, the levels of γH2AX staining did increase but were not consistent (Figure 15a & b). These cells were measured for their γH2AX staining in two ways: firstly, the level of staining was measured by the concentration of green fluorescence in ImageJ (http://rsbweb.nih.gov/ij/) (Figure 15a); and secondly, by counting the number of cells positive for γH2AX staining (Figure 15b). This was attempted because the base level of γH2AX staining was high and counting positive cells did not account for the changes in staining intensity. Both methods showed similar results and are interchangeable. The 6μM Gemcitabine foci experiment had two controls; DMSO, which

was fixed immediately after release, and C24, which was treated with DMSO and fixed after 24 hours release (Figure 16). C24 was used to show the background level of γH2AX staining was consistent throughout

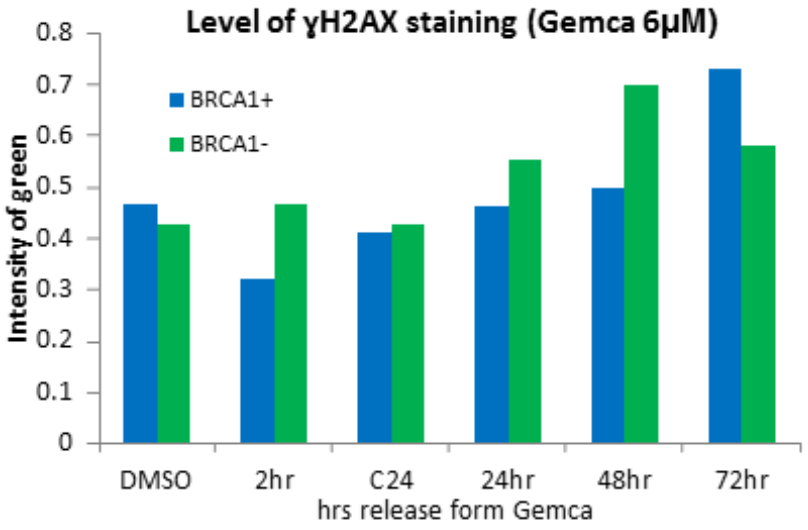

Figure 16 – *Level of γH2AX staining in HCC1937 BRCA1 +ve and –ve cells untreated and fixed immediately (DMSO) or after 24 hours (C24), or treated with 2hr dose of Gemcitabine (6μM) and fixed after 2, 24, 48 or 72 hours release.*

the time course, and a feature of the cells, not an effect of seeding the cells. BRCA1-proficient cells showed an increase in γH2AX staining, peaking at 72 hours, similar to the 53BP1 foci level. The BRCA1-deficient cells showed a peak in γH2AX staining at 48 hours, similar to the 53BP1 foci level (Figure 16 and Figure 14). This suggests the peaks in 53BP1 foci and presence of γH2AX after Gemcitabine treatment correlate. It also suggests, as they are both markers for DSBs, that DSBs are induced earlier (48 hours) in BRCA1-deficient cells than they are in BRCA1-proficient cells (72 hours). This suggests BRCA1 is involved in the prevention of DSBs at stalled replication forks.

Levels of phospho-RPA induced by Gemcitabine treatment and BRCA1 status

Phospho-RPA covers ssDNA and therefore, can be used to measure of the induction of ssDNA at stalled replication forks. HCC1937 BRCA1-proficient and –deficient cells were not treated (Control), treated with 6μM Gemcitabine for 2 hours and released for 2 or 48 hours in the presence of Mirin or DMSO, or treated for 1 hour with 1μM Camptothecin

(CPT) in the presence of Mirin or DMSO. Protein samples for Western blot were generated using sonication. Membranes were probed for Tubulin, phospho-RPA, and γH2AX (Figure 17).

Control samples showed a slightly higher level of phosphorylated RPA in BRCA1-deficient samples and all samples had a high baseline of γH2AX that agrees with the high level of immunofluorescent γH2AX staining previously discussed. The CPT treatment was used as a test for DNA resection and inhibition of resection by Mirin, which is an inhibitor of Mre11-dependent resection (Garner et al., 2009; Sartori et al., 2007; Wall et al., 1966). DMSO treatment was used as a

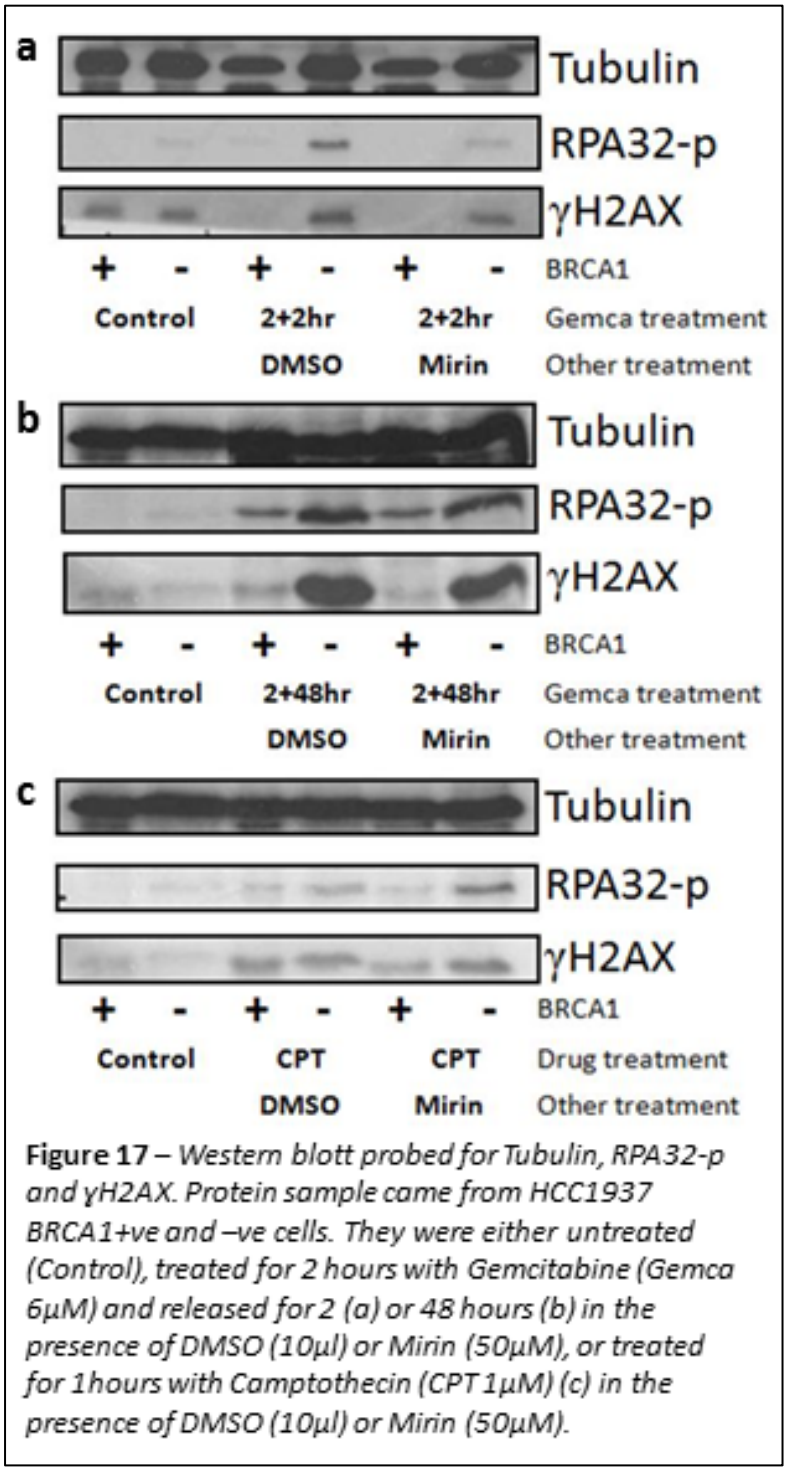

Figure 17 – *Western blott probed for Tubulin, RPA32-p and γH2AX. Protein sample came from HCC1937 BRCA1+ve and –ve cells. They were either untreated (Control), treated for 2 hours with Gemcitabine (Gemca 6μM) and released for 2 (a) or 48 hours (b) in the presence of DMSO (10μl) or Mirin (50μM), or treated for 1hours with Camptothecin (CPT 1μM) (c) in the presence of DMSO (10μl) or Mirin (50μM).*

control because Mirin was dissolved in DMSO. Cells treated with CPT showed higher levels of γH2AX after treatment, as expected. Phospho-RPA was equally induced in BRCA1-proficient and –deficient cells, suggesting that BRCA1-deficient HCC1937 cells are proficient in resection. Phospho-RPA was not decreased by Mirin treatment in BRCA1-deficient cells, suggesting that ssDNA generation after CPT treatment is Mre11-independent in absence of BRCA1 (Figure 17c).

In the 2 hour release (2+2hr) BRCA1-deficient cells have higher levels of phospho-RPA than BRCA1-proficient cells. This is decreased in the Mirin treatment, suggesting the phospho-RPA is partially caused by Mre11-dependent resection after Gemcitabine has stalled DNA replication forks (Figure 17a). After 48 hours release (2+48hr) BRCA1-deficient cells have much higher levels of phospho-RPA than BRCA1-proficient cells, and this is also increased after 2 hours release (Figure 17b). There is no noticeable difference between the levels of phospho-RPA between DMSO and Mirin treated cells, in either cell line after 48 hours release, suggesting that the phospho-RPA is not Mre11-dependent at later time points. We conclude from our 53BP1 and γH2AX immunofluorescence data that high levels of DSBs have formed in the BRCA1-deficient cell line after 48 hours release, which would be supported by the presence of the high level of γH2AX in the cells released for 48 hours. The high levels of phospho-RPA in BRCA1-deficient cells in both the 2 and 48 hours release, also suggest that BRCA1-deficient cells have more damaged DNA compared to BRCA1-proficient cells, before and after Gemcitabine treatment.

BRCA1 status and S phase accumulation

Replication inhibitors cause S phase accumulation because DNA damage and stalled forks cause activation of cell cycle checkpoints to stop cells going into G2 phase and mitosis with

unreplicated DNA. This is an important control experiment because Gemcitabine DNA damage is S-phase dependent.

Cells were grown and treated with the same treatment combination as for the Western blots (without the CPT conditions), fixed, and stained with PI to label the DNA content of the cells. The FACS (Fluorescent-activated cell sorting) was set up to process 20,000 events and the cells which show the appropriate DNA content for cells in G1, S and G2 phases of the cell cycle (Supplementary Figure 4) were analysed. Replication inhibitors cause G1 (or early S phase) accumulation.

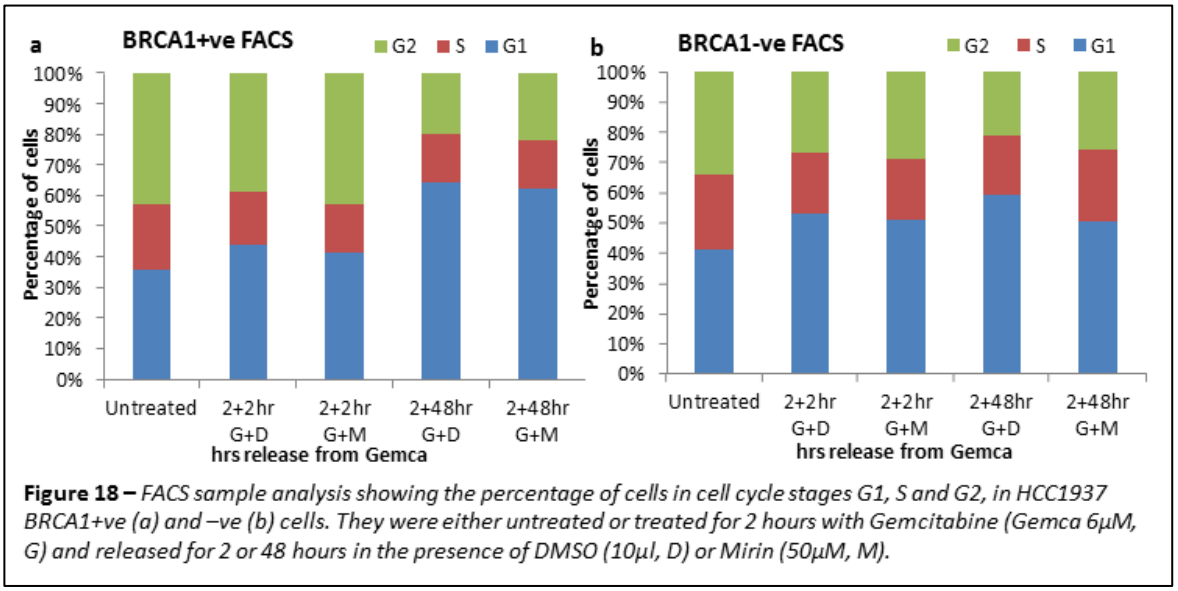

Figure 18 – *FACS sample analysis showing the percentage of cells in cell cycle stages G1, S and G2, in HCC1937 BRCA1+ve (a) and –ve (b) cells. They were either untreated or treated for 2 hours with Gemcitabine (Gemca 6µM, G) and released for 2 or 48 hours in the presence of DMSO (10µl, D) or Mirin (50µM, M).*

BRCA1-deficient cells accumulate in S-Phase from 2 hours release after Gemcitabine treatment, whereas BRCA1-proficient cells do not accumulate until 48 hours release form Gemcitabine (Figure 18). This may be because BRCA1-proficient cells still have a functional G2/M checkpoint. There are more BRCA1-deficient cells in S phase in all treatments compared to respective treatments in BRCA1-proficient cells. This could be indicative of BRCA1-proficient cells accumulating in early S phase later.

BRCA1 status and colony survival

HCC1937 BRCA1-proficient and –deficient cell lines were plated at two different cell densities for each treatment concentration and treated with various concentrations of Gemcitabine for 2 hours to assess the sensitivity of these cell lines to this treatment. Gemcitabine was removed and cells were grown in fresh medium for between 10-28 days. The colonies that survived were counted and compared to the plating survival rate of untreated cells.

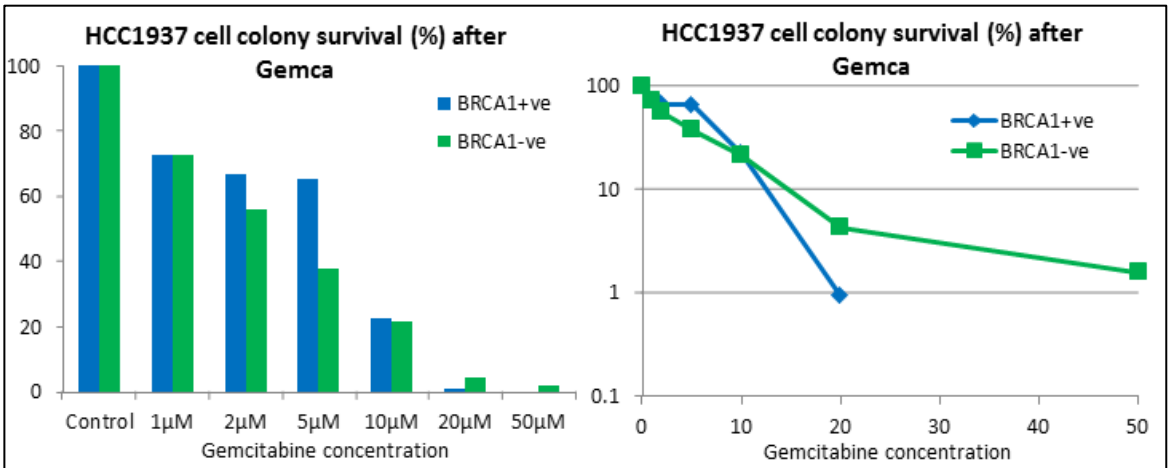

Figure 19 – *(a) histogram and (a) line graph showing the percentage of clonogenic survival colonies of HCC1937 BRCA1+ve and –ve cells, for untreated (Control) or cells after treatment with 2 hour dose of Gemcitabine at 1μM, 2μM, 5μM, 10μM, 20μM and 50μM. (a) and (b) are two ways of showing the same data.*

BRCA1-deficient cells have fewer colonies that survive doses of Gemcitabine between 1μM and 10μM, than BRCA1-proficient cells (Figure 19). This seems to be in contrast to the 20μM concentration, but the higher concentration (over 20μM) data are incomplete and need to be repeated. This suggests that BRCA1-deficient cells are more sensitive to Gemcitabine at concentrations up to 10μM, with the greatest difference at 5μM. This suggests BRCA1 status affects cellular sensitivity to Gemcitabine.

DISCUSSION

Here we have shown that BRCA1-proficient cells show less Gemcitabine induced fork stalling and slowed replication forks progress faster, which suggests BRCA1 to be involved in slowed fork progression leading to the stalling of forks. The total length of newly synthesised DNA decreases during Gemcitabine treatment in BRCA1-deficient cells, which may be indicative of DNA degradation. The absence of BRCA1 leads to earlier induction of 53BP1 foci and to higher levels of γH2AX foci and phospho-RPA after Gemcitabine treatment. Finally, BRCA1-deficient cells are slightly more sensitive to Gemcitabine at concentrations under 10μM.

There was increased fork stalling (CldU-only tracks) during Gemcitabine treatment in BRCA1-deficient cells, and the percentage of CldU-only tracks increased with longer incubations in Gemcitabine and IdU. There was also a decrease in the total length of DNA replicated in BRCA1-deficient cells early during Gemcitabine treatment. Both these observations may be indicative of DNA degradation during Gemcitabine-induced fork stalling. After prolonged Gemcitabine treatment, the final length of replicated DNA in the BRCA1-proficient cells was also slightly shorter than at the first time of stalling, which may also be indicative of DNA degradation of stalled forks at later time points. The higher amount of total replicated DNA in BRCA1–deficient cells before fork stalling suggests that BRCA1-deficient cells have a higher speed of replication than BRCA1-proficient cells in the absence of Gemcitabine. The dramatic level of DNA degradation in the BRCA1-deficient cells and the lesser amount in the BRCA1-proficient cells suggests that the presence of BRCA1 protects against DNA degradation.

This alongside the presence of Mirin-sensitive phospho-RPA after Gemcitabine fork stalling in BRCA1-deficient cells, also supports BRCA1 having a role in protecting stalled forks but specifically from Mre11 degradation, which is supported by Schlacher, 2012 (Schlacher et al., 2012). The earlier induction of increased levels of 53BP1, phospho-RPA and γH2AX at 48 hours in the absence of BRCA1 further suggests BRCA1 is protecting Gemcitabine slowed or stalled forks, and this protection delays the collapse into DSBs. The increased phospho-RPA levels (with and without Mirin treatment) may also be related to the formation of DSBs when BRCA1 is absent. We conclude that there is no change the phospho-RPA level after Mirin treatments because in response to DSBs, phospho-RPA levels may be generated by mechanisms other than Mre11-dependent resection.

As the replication fork speed is higher in untreated BRCA1-deficient cells, and the G2/M checkpoint is less effective in causing G1 accumulation with functional BRCA1, it may be because BRCA1-deficient cells cycle faster and without intact checkpoints that more DNA damage accumulates. This could also explain the earlier induction and higher levels of 53BP1 and γH2AX in BRCA1-deficient cells.

BRCA1-proficient cells are slightly more resistant to Gemcitabine at concentrations under 10μM. This resistance may be because cells accumulated less DNA damage than BRCA1-defective cells. Above 10μM concentration, BRCA1-proficent cells are more sensitive to Gemcitabine. The molecular explanation behind this is unclear, but it may be because BRCA1 presence allows G2/M checkpoint to be active and may thereby protect cells from DNA damage-induced apoptosis.

BRCA1 has been shown to be important in preventing stalled replication forks from accumulating DNA damage and it is, therefore, interesting to remember that BRCA1 is also

functional in DSB repair. BRCA1's function in supporting stalled forks is upstream of DSB formation and therefore BRCA1 must accumulate before DSB repair response signalling that recruits BRCA1. The specific biological function of BRCA1 at stalled replication forks is not clear, but from these results, BRCA1 is involved in supporting (perhaps physically) the replisome at stalled forks during replication inhibition. Some replisome proteins, such as the alternative clamp, clamp loader and the special polymerases, are exchanged at stalled forks for progression and it is not unreasonable that proteins are recruited to support the fork and replisome during these changes. During the repair of DSBs, the broken and resected DNA needs to be protected and supported, and recruited proteins do not all have direct roles in repairing the DNA strands but some are for maintaining structure of recruited proteins. Therefore, it is not surprising that some of these recruited HR proteins are also associated with protecting stalled forks, such as BRCA2 and Rad51 (Lomonosov et al., 2003; Petermann et al., 2010). BRCA2 and Rad51 are associated with protecting stalled forks, in contrast to BRCA1, BRCA2 and Rad51 promote fork stalling during Gemcitabine treatment and do not appear to protect Gemcitabine-stalled forks from becoming DSBs (RM. Jones, personal communication).

Some BRCA1-deficient cell lines have been reported to be resection-defective, but the observed Mirin-sensitive induction of phospho-RPA after Gemcitabine treatment suggest that Mre11-dependent resection is not defective and the effects of absent BRCA1 could induce Mre11- and CtIP-dependent resection. The BRCA1-dependent protection of stalled forks from Mre11 resection suggests that BRCA1 may prevent, or compete with, Mre11 from accessing stalled forks via its supportive role. BRCA1 is known, with 53BP1, to be important for the choice between NHEJ and HR, and BRCA1 regulates HR resection by

CtIP and Mre11. BRCA2 and Rad51 are also reported to protect stalled forks from Mre11 resection (Schlacher et al, Cell 2011; Hashimoto Y., Chaudhuri AR. et al, NSMB 2010). BRCA1 may function to regulate Mre11 and, potentially, be influential in the choice of repair method at stalled forks (Schlacher et al, Cancer Cell 2012). But our results suggest BRCA1 does not increase replication fork restart before DSBs are induced.

The data I have shown are from single experiments and using the HCC1937 cell line, or U2OS cell line. Further repeats of these experiments are needed, in both HCC1937 and U2OS cells lines and in other non-cancerous breast and cancerous cell lines. It would also be interesting to see if similar results were obtained in ovarian cancer cell lines from a patient with an inherited BRCA1 mutation. It could also be investigated if the results would alter with other mutations in BRCA1, other than the truncated (5382insC) mutant in HCC1937, to see which motif in BRCA1 is important for the described phenotype.

53BP1 data could also be supported by performing pulse-field gel electrophoresis with identical samples, confirming the presence and timing of DSBs.

Further experiments could look at the timing of BRCA1 in the protection of slowed or stalled forks, with reference to known stalled fork proteins, such as BRCA2, PARP1, Mre11 and Rad51. The order in which they are recruited may give an indication as to the molecular reason BRCA1 protects stalled forks from Mre11 resection, how DSBs are prevented and how replication restart or DNA repair is organised.

The accumulation of damage and high level of DNA damage signals in a BRCA1-deficient cell line is reflective of BRCA1's multiple important cellular functions. It is because of its importance that when mutations in BRCA1 are inherited the risk of developing breast and ovarian cancer is greatly increased. It is important to research the functions and functional

regions of BRCA1 to try to understand it how it causes transformation and to predict the effectiveness of cancer therapies. These results suggest the concentration of Gemcitabine at the tumour would be important to the resistance of normal and cancer cells and this would need further research to define an optimum concentration. The increased levels of accumulated damage and less resistance of BRCA1-defective cells to lower concentrations of Gemcitabine treatment, suggests that Gemcitabine may be an effective treatment for BRCA1 negative cancers.

SUPPLEMENTARY FIGURES

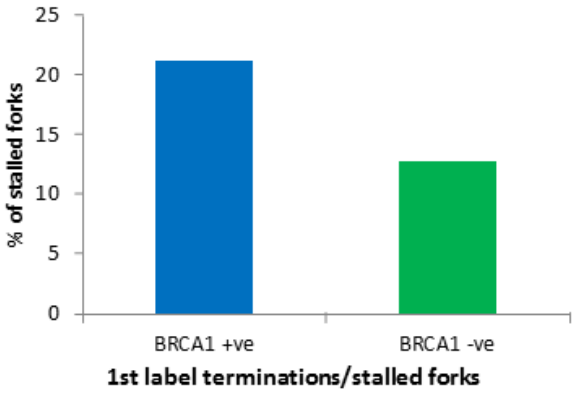

Figure 1 – *Graph shows percentage of stalled replication forks in untreated HCC1937 BRCA1 +ve and –ve cells from the fork stalling DNA fibre experiment.*

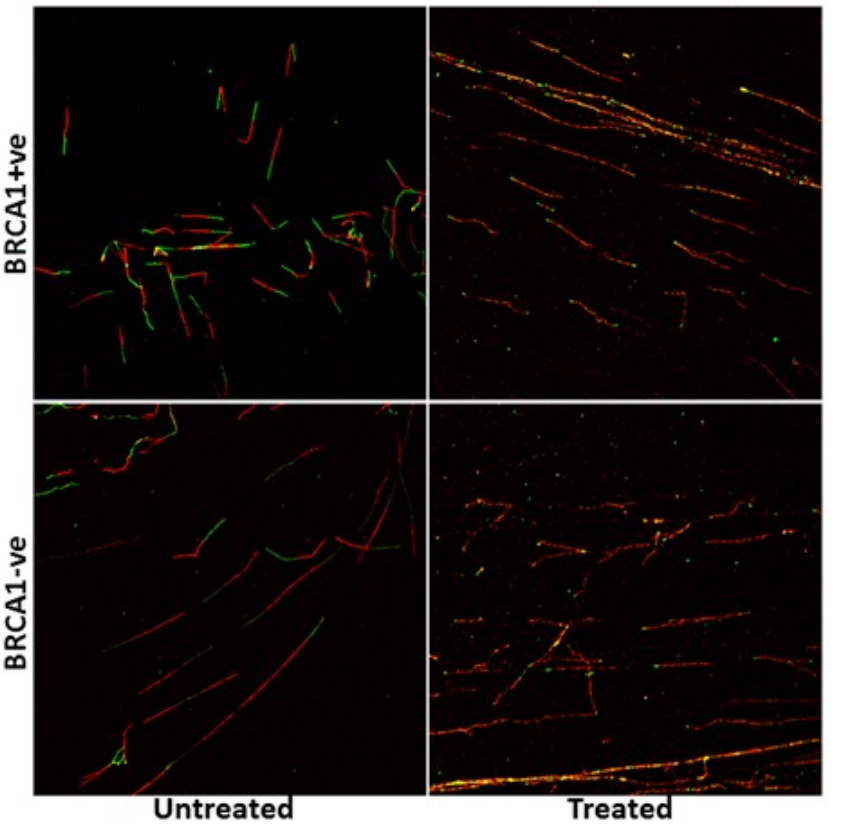

Figure 2 – *Images from the fork stalling DNA fibre experiment using BRCA1 or NTC siRNA treated U2OS cells. The conditions are untreated and treated (2µM Gemcitabine treated cells with 2hr IdU labelling).*

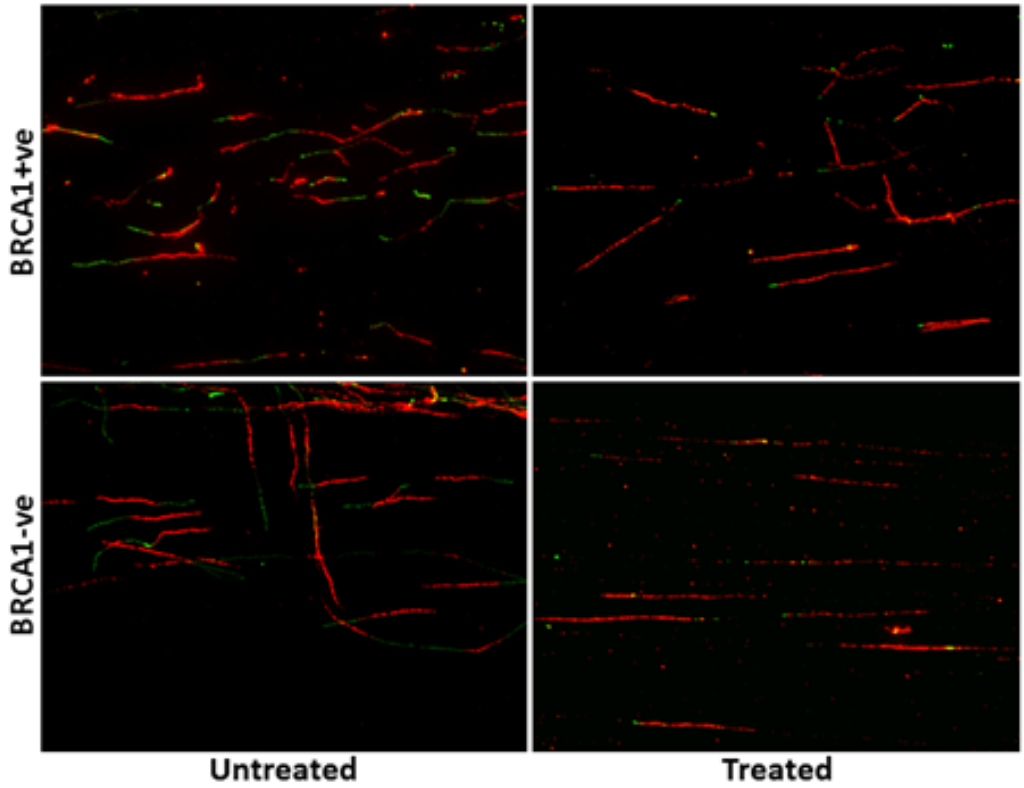

Figure 3 – *Images from the fork restart DNA fibre experiment using HCC1937 BRCA1 +ve and –ve cells. The conditions are untreated and treated (2µM Gemcitabine treated cells with 2hr IdU labelling without Gemca).*

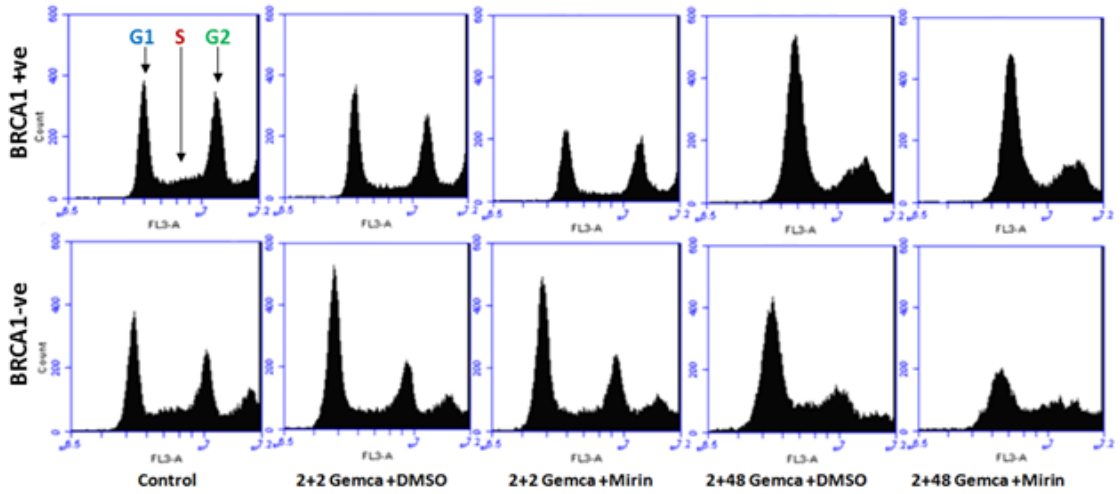

Figure 4 – *FACS sample graphs showing the amount of cells to level of PI staining in HCC1937 BRCA1+ve and –ve cells. Level of PI staining relates to DNA content of each cell and this is specific to phases of the cell cycle. They were either untreated or treated for 2 hours with Gemcitabine (Gemca 6µM) and released for 2 or 48 hours in the presence of DMSO (10µl) or Mirin (50µM).The left peak is indicative of cells in G1 phase, the right peak is indicative of cells in G2 phase and the cells in between the two peaks are indicative of cells in S phase. The peaks to the right of G2 are most likely doublet cells.*

BIBLIOGRAPHY

Abraham, R.T. (2001) Cell cycle checkpoint signaling through the ATM and ATR kinases. **Genes & development,** 15 (17): 2177-2196.

Acs, K., Luijsterburg, M.S., Ackermann, L., et al. (2011) The AAA-ATPase VCP/p97 promotes 53BP1 recruitment by removing L3MBTL1 from DNA double-strand breaks. **Nat Struct Mol Biol,** 18 (12): 1345-1350.

Aparicio, O.M., Stout, A.M. and Bell, S.P. (1999) Differential assembly of Cdc45p and DNA polymerases at early and late origins of DNA replication. **Proceedings of the National Academy of Sciences,** 96 (16): 9130-9135.

Bartek, J., Lukas, C. and Lukas, J. (2004) Checking on DNA damage in S phase. **Nature reviews. Molecular cell biology,** 5 (10): 792-804.

Bekker-Jensen, S., Danielsen, J.R., Fugger, K., et al. (2010) HERC2 coordinates ubiquitin-dependent assembly of DNA repair factors on damaged chromosomes. **Nature cell biology,** 12 (1): 80-86.

Bekker-Jensen, S. and Mailand, N. (2010) Assembly and function of DNA double-strand break repair foci in mammalian cells. **DNA Repair,** 9 (12): 1219-1228.

Bell, S.P., Mitchell, J., Leber, J., et al. (1995) The multidomain structure of Orc1 p reveals similarity to regulators of DNA replication and transcriptional silencing. **Cell,** 83 (4): 563-568.

Bell, S.P. and Stillman, B. (1992) ATP-dependent recognition of eukaryotic origins of DNA replication by a multiprotein complex. **Nature,** 357 (6374): 128-134.

Bencokova, Z., Kaufmann, M.R., Pires, I.M., et al. (2009) ATM Activation and Signaling under Hypoxic Conditions. **Molecular and cellular biology,** 29 (2): 526-537.

Bianchi, V., Borella, S., Calderazzo, F., et al. (1994) Inhibition of ribonucleotide reductase by 2'-substituted deoxycytidine analogs: possible application in AIDS treatment. **Proceedings of the National Academy of Sciences,** 91 (18): 8403-8407.

Boddy, M.N., Gaillard, P.L., McDonald, W.H., et al. (2001) Mus81-Eme1 Are Essential Components of a Holliday Junction Resolvase. **Cell,** 107 (4): 537-548.

Botuyan, M.V., Lee, J., Ward, I.M., et al. (2006) Structural Basis for the Methylation State-Specific Recognition of Histone H4-K20 by 53BP1 and Crb2 in DNA Repair. **Cell,** 127 (7): 1361-1373.

Brewer, B.J. and Fangman, W.L. (1988) A replication fork barrier at the 3' end of yeast ribosomal RNA genes. **Cell,** 55 (4): 637-643.

Brill, S.J. and Stillman, B. (1989) Yeast replication factor-A functions in the unwinding of the SV40 origin of DNA replication. **Nature,** 342 (6245): 92-95.

Bryant, H.E., Petermann, E., Schultz, N., et al. (2009) PARP is activated at stalled forks to mediate Mre11-dependent replication restart and recombination. **The EMBO journal,** 28 (17): 2601-2615.

Buis, J., Stoneham, T., Spehalski, E., et al. (2012) Mre11 regulates CtIP-dependent double-strand break repair by interaction with CDK2. **Nat Struct Mol Biol,** 19 (2): 246-252.

Bunting, S.F., Callen, E., Wong, N., et al. (2010) 53BP1 Inhibits Homologous Recombination in Brca1-Deficient Cells by Blocking Resection of DNA Breaks. **Cell,** 141 (2): 243-254.

Burma, S., Chen, B.P., Murphy, M., et al. (2001) ATM Phosphorylates Histone H2AX in Response to DNA Double-strand Breaks. **Journal of Biological Chemistry,** 276 (45): 42462-42467.

Byun, T.S., Pacek, M., Yee, M., et al. (2005) Functional uncoupling of MCM helicase and DNA polymerase activities activates the ATR-dependent checkpoint. **Genes & development,** 19 (9): 1040-1052.

Cadoret, J., Meisch, F., Hassan-Zadeh, V., et al. (2008) Genome-wide studies highlight indirect links between human replication origins and gene regulation. **Proceedings of the National Academy of Sciences,** 105 (41): 15837-15842.

Campbell, S.J., Edwards, R.A., Leung, C.C.Y., et al. (2012) Molecular Insights into the Function of RING Finger (RNF)-containing Proteins hRNF8 and hRNF168 in Ubc13/Mms2-dependent Ubiquitylation. **Journal of Biological Chemistry,** 287 (28): 23900-23910.

Cejka, P., Cannavo, E., Polaczek, P., et al. (2010) DNA end resection by Dna2-Sgs1-RPA and its stimulation by Top3-Rmi1 and Mre11-Rad50-Xrs2. **Nature,** 467 (7311): 112-116.

Cerqueira, N.M., Fernandes, P.A. and Ramos, M.J. (2007) Ribonucleotide reductase: a critical enzyme for cancer chemotherapy and antiviral agents. **Recent Pat Anticancer Drug Discov**. Jan;2(1):11-29.

Cerqueira, N.M.F.S.A., Fernandes, P.A. and Ramos, M.J. (2007) Understanding Ribonucleotide Reductase Inactivation by Gemcitabine. **Chemistry - A European Journal,** 13 (30): 8507-8515.

Chapman, J.R. and Jackson, S.P. (2008) Phospho-dependent interactions between NBS1 and MDC1 mediate chromatin retention of the MRN complex at sites of DNA damage. **EMBO reports,** 9 (8): 795-801.

Chen, L., Nievera, C.J., Lee, A.Y., et al. (2008) Cell Cycle-dependent Complex Formation of BRCA1·CtIP·MRN Is Important for DNA Double-strand Break Repair. **Journal of Biological Chemistry,** 283 (12): 7713-7720.

Chen, Y., Farmer, A.A., Chen, C., et al. (1996) BRCA1 Is a 220-kDa Nuclear Phosphoprotein That Is Expressed and Phosphorylated in a Cell Cycle-dependent Manner. **Cancer research,** 56 (14): 3168-3172.

Choi, J., Lindsey-Boltz, L.A., Kemp, M., et al. (2010) Reconstitution of RPA-covered single-stranded DNA-activated ATR-Chk1 signaling. **Proceedings of the National Academy of Sciences,** 107 (31): 13660-13665.

Costanzo, V., Robertson, K., Bibikova, M., et al. (2001) Mre11 Protein Complex Prevents Double-Strand Break Accumulation during Chromosomal DNA Replication. **Molecular cell,** 8 (1): 137-147.

Daboussi, F., Courbet, S., Benhamou, S., et al. (2008) A homologous recombination defect affects replication-fork progression in mammalian cells. **Journal of cell science,** 121 (2): 162-166.

Davies, S.L., North, P.S. and Hickson, I.D. (2007) Role for BLM in replication-fork restart and suppression of origin firing after replicative stress. **Nat Struct Mol Biol,** 14 (7): 677-679.

Doil, C., Mailand, N., Bekker-Jensen, S., et al. (2009) RNF168 Binds and Amplifies Ubiquitin Conjugates on Damaged Chromosomes to Allow Accumulation of Repair Proteins. **Cell,** 136 (3): 435-446.

Dong, Y., Hakimi, M., Chen, X., et al. (2003) Regulation of BRCC, a Holoenzyme Complex Containing BRCA1 and BRCA2, by a Signalosome-like Subunit and Its Role in DNA Repair. **Molecular cell,** 12 (5): 1087-1099.

Drikos, I., Nounesis, G. and Vorgias, C.E. (2009) Characterization of cancer-linked BRCA1-BRCT missense variants and their interaction with phosphoprotein targets. **Proteins: Structure, Function, and Bioinformatics,** 77 (2): 464-476.

Erdile, L.F., Heyer, W.D., Kolodner, R., et al. (1991) Characterization of a cDNA encoding the 70-kDa single-stranded DNA-binding subunit of human replication protein A and the role of the protein in DNA replication. **Journal of Biological Chemistry,** 266 (18): 12090-12098.

Feng, L., Wang, J. and Chen, J. (2010) The Lys63-specific deubiquitinating enzyme BRCC36 is regulated by two scaffold proteins localizing in different subcellular compartments. **Journal of Biological Chemistry,** 285 (40): 30982-30988.

Feng, L., Huang, J. and Chen, J. (2009) MERIT40 facilitates BRCA1 localization and DNA damage repair. **Genes & development,** 23 (6): 719-728.

Franchitto, A., Pirzio, L.M., Prosperi, E., et al. (2008) Replication fork stalling in WRN-deficient cells is overcome by prompt activation of a MUS81-dependent pathway. **The Journal of cell biology,** 183 (2): 241-252.

Gambus, A., Jones, R.C., Sanchez-Diaz, A., et al. (2006) GINS maintains association of Cdc45 with MCM in replisome progression complexes at eukaryotic DNA replication forks. **Nature cell biology,** 8 (4): 358-366.

Gari, K., Decaillet, C., Stasiak, A.Z., et al. (2008) The Fanconi Anemia Protein FANCM Can Promote Branch Migration of Holliday Junctions and Replication Forks. **Molecular cell,** 29 (1): 141-148.

Garner, K.M., Pletnev, A.A. and Eastman, A. (2009) Corrected structure of mirin, a small-molecule inhibitor of the Mre11-Rad50-Nbs1 complex. **Nat Chem Biol,** 5 (3): 129-130.

Gudmundsdottir, K., Lord, C.J., Witt, E., et al. (2004) DSS1 is required for RAD51 focus formation and genomic stability in mammalian cells. **EMBO reports,** 5 (10): 989-993.

Guo, C., Fischhaber, P.L., Luk-Paszyc, M., et al. (2003) Mouse Rev1 protein interacts with multiple DNA polymerases involved in translesion DNA synthesis. **The EMBO journal,** 22 (24): 6621-6630.

Haince, J., McDonald, D., Rodrigue, A., et al. (2008) PARP1-dependent Kinetics of Recruitment of MRE11 and NBS1 Proteins to Multiple DNA Damage Sites. **Journal of Biological Chemistry,** 283 (2): 1197-1208.

Hall, J., Lee, M., Newman, B., et al. (1990) Linkage of early-onset familial breast cancer to chromosome 17q21. **Science,** 250 (4988): 1684-1689.

Hanada, K., Budzowska, M., Davies, S.L., et al. (2007) The structure-specific endonuclease Mus81 contributes to replication restart by generating double-strand DNA breaks. **Nat Struct Mol Biol,** 14 (11): 1096-1104.

Hashimoto, Y., Chaudhuri, A.R., Lopes, M., et al. (2010) Rad51 protects nascent DNA from Mre11-dependent degradation and promotes continuous DNA synthesis. **Nat Struct Mol Biol,** 17 (11): 1305-1311.

Hertel, L.W., Boder, G.B., Kroin, J.S., et al. (1990) Evaluation of the Antitumor Activity of Gemcitabine (2′,2′-Difluoro-2′-deoxycytidine). **Cancer research,** 50 (14): 4417-4422.

Hoege, C., Pfander, B., Moldovan, G., et al. (2002) RAD6-dependent DNA repair is linked to modification of PCNA by ubiquitin and SUMO. **Nature,** 419 (6903): 135-141.

Huen, M.S.Y., Grant, R., Manke, I., et al. (2007) RNF8 Transduces the DNA-Damage Signal via Histone Ubiquitylation and Checkpoint Protein Assembly. **Cell,** 131 (5): 901-914.

Ilves, I., Petojevic, T., Pesavento, J.J., et al. (2010) Activation of the MCM2-7 Helicase by Association with Cdc45 and GINS Proteins. **Molecular cell,** 37 (2): 247-258.

Jackson, D.A. and Pombo, A. (1998) Replicon Clusters Are Stable Units of Chromosome Structure: Evidence That Nuclear Organization Contributes to the Efficient Activation and Propagation of S Phase in Human Cells. **The Journal of cell biology,** 140 (6): 1285-1295.

Jones, R.M. and Petermann, E. (2012) Replication fork dynamics and the DNA damage response. **Biochemical Journal.** 443(1):13-26.

Katou, Y., Kanoh, Y., Bando, M., et al. (2003) S-phase checkpoint proteins Tof1 and Mrc1 form a stable replication-pausing complex. **Nature,** 424 (6952): 1078-1083.

Kim, J., McAvoy, S.A., Smith, D.I., et al. (December 15, 2005) Human TopBP1 Ensures Genome Integrity during Normal S Phase. **Molecular and cellular biology,** 25 (24): 10907-10915.

Kobayashi, M., Hirano, A., Kumano, T., et al. (2004) Critical role for chicken Rad17 and Rad9 in the cellular response to DNA damage and stalled DNA replication. **Genes to Cells,** 9 (4): 291-303.

Krude, T., Jackman, M., Pines, J., et al. (1997) Cyclin/Cdk-Dependent Initiation of DNA Replication in a Human Cell-Free System. **Cell,** 88 (1): 109-119.

Kumagai, A. and Dunphy, W.G. (2000) Claspin, a Novel Protein Required for the Activation of Chk1 during a DNA Replication Checkpoint Response in Xenopus Egg Extracts. **Molecular cell,** 6 (4): 839-849.

Lambert, S., Watson, A., Sheedy, D.M., et al. (2005) Gross Chromosomal Rearrangements and Elevated Recombination at an Inducible Site-Specific Replication Fork Barrier. **Cell,** 121 (5): 689-702.

Lee, J. and Paull, T.T. (2004) Direct Activation of the ATM Protein Kinase by the Mre11/Rad50/Nbs1 Complex. **Science,** 304 (5667): 93-96.

Lee, S.H., Kwong, A.D., Pan, Z.Q., et al. (1991) Studies on the activator 1 protein complex, an accessory factor for proliferating cell nuclear antigen-dependent DNA polymerase delta. **Journal of Biological Chemistry,** 266 (1): 594-602.

Lehmann, A.R., Niimi, A., Ogi, T., et al. (2007) Translesion synthesis: Y-family polymerases and the polymerase switch. **DNA Repair,** 6 (7): 891-899.

Lei, M., Kawasaki, Y., Young, M.R., et al. (1997) Mcm2 is a target of regulation by Cdc7–Dbf4 during the initiation of DNA synthesis. **Genes & development,** 11 (24): 3365-3374.

Li, C., Vassilev, A. and DePamphilis, M.L. (2004) Role for Cdk1 (Cdc2)/Cyclin A in Preventing the Mammalian Origin Recognition Complex's Largest Subunit (Orc1) from Binding to Chromatin during Mitosis. **Molecular and cellular biology,** 24 (13): 5875-5886.

Liu, Z., Wu, J. and Yu, X. (2007) CCDC98 targets BRCA1 to DNA damage sites. **Nat Struct Mol Biol,** 14 (8): 716-720.

Lobachev, K., Rattray, A. and Narayanan, V. (2007) Hairpin- and cruciform-mediated chromosome breakage: causes and consequences in eukaryotic cells. **Front Biosci**. 12:4208-20.

Lok, G.T., Sy, S.M.-., Dong, S., et al. (2012) Differential regulation of RNF8-mediated Lys48- and Lys63-based poly-ubiquitylation. **Nucleic acids research,** 40 (1): 196-205.

Lomonosov, M., Anand, S., Sangrithi, M., et al. (2003) Stabilization of stalled DNA replication forks by the BRCA2 breast cancer susceptibility protein. **Genes & development,** 17 (24): 3017-3022.

Longhese, M.P., Neecke, H., Paciotti, V., et al. (1996) The 70 kDa Subunit of Replication Protein A is Required for the G1/S and Intra-S DNA Damage Checkpoints in Budding Yeast. **Nucleic acids research,** 24 (18): 3533-3537.

Lou, Z., Chini, C.C.S., Minter-Dykhouse, K., et al. (2003) Mediator of DNA Damage Checkpoint Protein 1 Regulates BRCA1 Localization and Phosphorylation in DNA Damage Checkpoint Control. **Journal of Biological Chemistry,** 278 (16): 13599-13602.

Lou, Z., Minter-Dykhouse, K., Wu, X., et al. (2003) MDC1 is coupled to activated CHK2 in mammalian DNA damage response pathways. **Nature,** 421 (6926): 957-961.

Mailand, N., Bekker-Jensen, S., Faustrup, H., et al. (2007) RNF8 Ubiquitylates Histones at DNA Double-Strand Breaks and Promotes Assembly of Repair Proteins. **Cell,** 131 (5): 887-900.

Manders, E.M., Stap, J., Brakenhoff, G.J., et al. (1992) Dynamics of three-dimensional replication patterns during the S-phase, analysed by double labelling of DNA and confocal microscopy. **Journal of cell science,** 103 (3): 857-862.

Matsumoto, T., Eki, T. and Hurwitz, J. (1990) Studies on the initiation and elongation reactions in the simian virus 40 DNA replication system. **Proceedings of the National Academy of Sciences,** 87 (24): 9712-9716.

McGarry, T.J. and Kirschner, M.W. (1998) Geminin, an Inhibitor of DNA Replication, Is Degraded during Mitosis. **Cell,** 93 (6): 1043-1053.

Mechali, M. (2001) DNA replication origins: from sequence specificity to epigenetics. **Nature reviews. Genetics,** 2 (8): 640-645.

Mimitou, E.P. and Symington, L.S. (2010) Ku prevents Exo1 and Sgs1-dependent resection of DNA ends in the absence of a functional MRX complex or Sae2. **The EMBO journal,** 29 (19): 3358-3369.

Mimura, S. and Takisawa, H. (1998) Xenopus Cdc45-dependent loading of DNA polymerase [alpha] onto chromatin under the control of S-phase cdk. **The EMBO journal,** 17 (19): 5699-5707.

Mirkin, E.V. and Mirkin, S.M. (March 2007) Replication Fork Stalling at Natural Impediments. **Microbiology and Molecular Biology Reviews,** 71 (1): 13-35.

Morris, J.R. (2010) More Modifiers Move on DNA Damage. **Cancer research,** 70 (10): 3861-3863.

Morris, J.R. and Solomon, E. (2004) BRCA1 : BARD1 induces the formation of conjugated ubiquitin structures, dependent on K6 of ubiquitin, in cells during DNA replication and repair. **Human molecular genetics,** 13 (8): 807-817.

Murakami, Y., Eki, T. and Hurwitz, J. (1992) Studies on the initiation of simian virus 40 replication in vitro: RNA primer synthesis and its elongation. **Proceedings of the National Academy of Sciences,** 89 (3): 952-956.

Murante, R.S., Rumbaugh, J.A., Barnes, C.J., et al. (1996) Calf RTH-1 Nuclease Can Remove the Initiator RNAs of Okazaki Fragments by Endonuclease Activity. **Journal of Biological Chemistry,** 271 (42): 25888-25897.

Myers, J.S. and Cortez, D. (2006) Rapid Activation of ATR by Ionizing Radiation Requires ATM and Mre11. **Journal of Biological Chemistry,** 281 (14): 9346-9350.

Nagourney, R.A., Flam, M., Link, J., et al. (2008) Carboplatin plus Gemcitabine Repeating Doublet Therapy in Recurrent Breast Cancer. **Clinical Breast Cancer,** 8 (5): 432-435.

Nam, E.A. and Cortez, D. (2011) ATR signalling: more than meeting at the fork. **Biochem J**. 436(3):527-36.

Nawrocki, S., Skacel, T. and Skoneczna, I. (2002) Pharmacotherapy of bladder cancer: practice and prospects. **Expert opinion on pharmacotherapy,** 3 (6): 671-679.

Nethanel, T., Reisfeld, S., Dinter-Gottlieb, G., et al. (1988) An Okazaki piece of simian virus 40 may be synthesized by ligation of shorter precursor chains. **Journal of virology,** 62 (8): 2867-2873.

Niforou, K.N., Anagnostopoulos, A.K., Vougas, K., et al. (2008) The Proteome Profile of the Human Osteosarcoma U2OS Cell Line. **Cancer Genomics - Proteomics,** 5 (1): 63-77.

Nishitani, H., Lygerou, Z., Nishimoto, T., et al. (2000) The Cdt1 protein is required to license DNA for replication in fission yeast. **Nature,** 404 (6778): 625-628.

Odsbu, I., Morigen, and Skarstad, K. (2009) A Reduction in Ribonucleotide Reductase Activity Slows Down the Chromosome Replication Fork but Does Not Change Its Localization. **PLoS ONE,** 4 (10): e7617.

Osborn, A.J. and Elledge, S.J. (2003) Mrc1 is a replication fork component whose phosphorylation in response to DNA replication stress activates Rad53. **Genes & development,** 17 (14): 1755-1767.

Pacek, M. and Walter, J.C. (2004) A requirement for MCM7 and Cdc45 in chromosome unwinding during eukaryotic DNA replication. **The EMBO journal,** 23 (18): 3667-3676.

Pelizon, C., Madine, M.A., Romanowski, P., et al. (2000) Unphosphorylatable mutants of Cdc6 disrupt its nuclear export but still support DNA replication once per cell cycle. **Genes & development,** 14 (19): 2526-2533.

Petermann, E. and Caldecott, K.W. (2006) Evidence That the ATR/Chk1 Pathway Maintains Normal Replication Fork Progression during Unperturbed S Phase. **cc,** 5 (19): 2203-2209.

Petermann, E. and Helleday, T. (2010) Pathways of mammalian replication fork restart. **Nat Rev Mol Cell Biol.** 11(10):683-7.

Petermann, E., Orta, M.L., Issaeva, N. et al. (2010) Hydroxyurea-Stalled Replication Forks Become Progressively Inactivated and Require Two Different RAD51-Mediated Pathways for Restart and Repair. **Molecular Cell.** 37(4):492-502.

Plans, V., Scheper, J., Soler, M., et al. (2006) The RING finger protein RNF8 recruits UBC13 for lysine 63-based self polyubiquitylation. **Journal of cellular biochemistry,** 97 (3): 572-582.

Plate, J.M.D., Plate, A.E., Shott, S. et al. (2005) Effect of gemcitabine on immune cells in subjects with adenocarcinoma of the pancreas. **Cancer Immunol Immunother**. 54(9):915-25.

Postow, L., Ghenoiu, C., Woo, E.M., et al. (2008) Ku80 removal from DNA through double strand break–induced ubiquitylation. **The Journal of cell biology,** 182 (3): 467-479.

Rezazadeh, S. (2012) RecQ helicases; at the crossroad of genome replication, repair, and recombination. **Mol Biol Rep** 39(4):4527-43.

Roy, R., Chun, J. and Powell, S.N. (2012) BRCA1 and BRCA2: different roles in a common pathway of genome protection. **Nat Rev Cancer,** 12 (1): 68-78.

Sanchez, Y., Wong, C., Thoma, R.S., et al. (1997) Conservation of the Chk1 Checkpoint Pathway in Mammals: Linkage of DNA Damage to Cdk Regulation Through Cdc25. **Science,** 277 (5331): 1497-1501.

Santamaría, D., Viguera, E., Martínez-Robles, M.L., et al. (2000) Bi-directional replication and random termination. **Nucleic acids research,** 28 (10): 2099-2107.

Sarkies, P., Murat, P., Phillips, L.G., et al. (2012) FANCJ coordinates two pathways that maintain epigenetic stability at G-quadruplex DNA. **Nucleic acids research,** 40 (4): 1485-1498.

Sartori, A.A., Lukas, C., Coates, J., et al. (2007) Human CtIP promotes DNA end resection. **Nature,** 450 (7169): 509-514.

Schlacher, K., Christ, N., Siaud, N., et al. (2011) Double-Strand Break Repair-Independent Role for BRCA2 in Blocking Stalled Replication Fork Degradation by MRE11. **Cell,** 145 (4): 529-542.

Schlacher, K., Wu, H. and Jasin, M. (2012) A Distinct Replication Fork Protection Pathway Connects Fanconi Anemia Tumor Suppressors to RAD51-BRCA1/2. **Cancer Cell,** 22 (1): 106-116.

Schwartz, E.K., Wright, W.D., Ehmsen, K.T., et al. (2012) Mus81-Mms4 Functions as a Single Heterodimer To Cleave Nicked Intermediates in Recombinational DNA Repair. **Molecular and cellular biology,** 32 (15): 3065-3080.

Sclafani, R.A. (2000) Cdc7p-Dbf4p becomes famous in the cell cycle. **Journal of cell science,** 113 (12): 2111-2117.

Sclafani, R.A. and Holzen, T.M. (2007) Cell Cycle Regulation of DNA Replication. **Annual Review of Genetics,** 41 (1): 237-280.

Scully, R., Ganesan, S., Vlasakova, K., et al. (1999) Genetic Analysis of BRCA1 Function in a Defined Tumor Cell Line. **Molecular cell,** 4 (6): 1093-1099.

Shao, G., Lilli, D.R., Patterson-Fortin, J., et al. (2009) The Rap80-BRCC36 de-ubiquitinating enzyme complex antagonizes RNF8-Ubc13-dependent ubiquitination events at DNA double strand breaks. **Proceedings of the National Academy of Sciences,** 106 (9): 3166-3171.

Shepherd, F.A., Abratt, R.P., Anderson, H. et al. (1997) Gemcitabine in the treatment of elderly patients with advanced non-small cell lung cancer. **Seminars in Oncology** 24:50-55

Sidorova, J.M., Li, N., Folch, A. et al. (2008) The RecQ helicase WRN is required for normal replication fork progression after DNA damage or replication fork arrest. **Cell Cycle.** 7(6):796-807.

Sobeck, A., Stone, S., Costanzo, V., et al. (2006) Fanconi Anemia Proteins Are Required To Prevent Accumulation of Replication-Associated DNA Double-Strand Breaks. **Molecular and cellular biology,** 26 (2): 425-437.

Sonoda, E., Sasaki, M.S., Buerstedde, J., et al. (1998) Rad51-deficient vertebrate cells accumulate chromosomal breaks prior to cell death. **The EMBO journal,** 17 (2): 598-608.

Stewart, G.S., Panier, S., Townsend, K., et al. (2009) The RIDDLE Syndrome Protein Mediates a Ubiquitin-Dependent Signaling Cascade at Sites of DNA Damage. **Cell,** 136 (3): 420-434.

Stucki, M., Clapperton, J.A., Mohammad, D., et al. (2005) MDC1 Directly Binds Phosphorylated Histone H2AX to Regulate Cellular Responses to DNA Double-Strand Breaks. **Cell,** 123 (7): 1213-1226.

Stukenberg, P.T., Studwell-Vaughan, P.S. and O'Donnell, M. (1991) Mechanism of the sliding beta-clamp of DNA polymerase III holoenzyme. **Journal of Biological Chemistry,** 266 (17): 11328-11334.

Subramanian, P., Nelson, D. and Chinault, A.C. (1996) Large domains of apparent delayed replication timing associated with triplet repeat expansion at FRAXA and FRAXE. **Am J Hum Genet.** 59(2):407-16.

Sung, P. and Robberson, D.L. (1995) DNA strand exchange mediated by a RAD51-ssDNA nucleoprotein filament with polarity opposite to that of RecA. **Cell,** 82 (3): 453-461.

Takayama, Y., Kamimura, Y., Okawa, M., et al. (2003) GINS, a novel multiprotein complex required for chromosomal DNA replication in budding yeast. **Genes & development,** 17 (9): 1153-1165.

Tanaka, S. and Diffley, J.F.X. (2002) Interdependent nuclear accumulation of budding yeast Cdt1 and Mcm2-7 during G1 phase. **Nature cell biology,** 4 (3): 198-207.

Tanaka, S., Umemori, T., Hirai, K., et al. (2007) CDK-dependent phosphorylation of Sld2 and Sld3 initiates DNA replication in budding yeast. **Nature,** 445 (7125): 328-332.

Tanaka, T., Knapp, D. and Nasmyth, K. (1997) Loading of an Mcm Protein onto DNA Replication Origins Is Regulated by Cdc6p and CDKs. **Cell,** 90 (4): 649-660.

Taylor, E.M., Cecillon, S.M., Bonis, A., et al. (2010) The Mre11/Rad50/Nbs1 complex functions in resection-based DNA end joining in Xenopus laevis. **Nucleic acids research,** 38 (2): 441-454.

Timson, J. (1975) Hydroxyurea**. Mutat Res**. 32(2):115-32.

Tittel-Elmer, M., Alabert, C., Pasero, P., et al. (2009) The MRX complex stabilizes the replisome independently of the S phase checkpoint during replication stress. **The EMBO journal,** 28 (8): 1142-1156.

Tsurimoto, T. and Stillman, B. (1991) Replication factors required for SV40 DNA replication in vitro. I. DNA structure-specific recognition of a primer-template junction by eukaryotic DNA polymerases and their accessory proteins. **Journal of Biological Chemistry,** 266 (3): 1950-1960.

Tsurimoto, T. and Stillman, B. (1991) Replication factors required for SV40 DNA replication in vitro. II. Switching of DNA polymerase alpha and delta during initiation of leading and lagging strand synthesis. **Journal of Biological Chemistry,** 266 (3): 1961-1968.

Tsurimoto, T. and Stillman, B. (1989) Purification of a cellular replication factor, RF-C, that is required for coordinated synthesis of leading and lagging strands during simian virus 40 DNA replication in vitro. **Molecular and cellular biology,** 9 (2): 609-619.

Tsurimoto, T., Melendy, T. and Stillman, B. (1990) Sequential initiation of lagging and leading strand synthesis by two different polymerase complexes at the SV40 DNA replication origin. **Nature,** 346 (6284): 534-539.

Tuduri, S., Tourrière, H. and Pasero, P. (2010) Defining replication origin efficiency using DNA fiber assays. **Chromosome Res**. 18(1):91-102.

Turchi, J.J. and Bambara, R.A. (1993) Completion of mammalian lagging strand DNA replication using purified proteins. **Journal of Biological Chemistry,** 268 (20): 15136-15141.

Turchi, J.J., Huang, L., Murante, R.S., et al. (1994) Enzymatic completion of mammalian lagging-strand DNA replication. **Proceedings of the National Academy of Sciences,** 91 (21): 9803-9807.

Ünsal-Kaçmaz, K., Chastain, P.D., Qu, P., et al. (April 15, 2007) The Human Tim/Tipin Complex Coordinates an Intra-S Checkpoint Response to UV That Slows Replication Fork Displacement. **Molecular and cellular biology,** 27 (8): 3131-3142.

Uziel, T., Lerenthal, Y., Moyal, L., et al. (2003) Requirement of the MRN complex for ATM activation by DNA damage. **The EMBO journal,** 22 (20): 5612-5621.

Van Hatten, R.A., Tutter, A.V., Holway, A.H., et al. (2002) The Xenopus Xmus101 protein is required for the recruitment of Cdc45 to origins of DNA replication. **The Journal of cell biology,** 159 (4): 541-547.

Vashee, S., Cvetic, C., Lu, W., et al. (2003) Sequence-independent DNA binding and replication initiation by the human origin recognition complex. **Genes & development,** 17 (15): 1894-1908.

Waga, S. and Stillman, B. (1998) The DNA replication fork in Eukaryotic cells. **Annual Review of Biochemistry,** 67 (1): 721-751.

Wall, M.E., Wani, M.C., Cook, C.E., et al. (1966) Plant Antitumor Agents. I. The Isolation and Structure of Camptothecin, a Novel Alkaloidal Leukemia and Tumor Inhibitor from Camptotheca acuminata1,2. **Journal of the American Chemical Society,** 88 (16): 3888-3890.

Wang, B. and Elledge, S.J. (2007) Ubc13/Rnf8 ubiquitin ligases control foci formation of the Rap80/Abraxas/Brca1/Brcc36 complex in response to DNA damage. **Proceedings of the National Academy of Sciences,** 104 (52): 20759-20763.

Wang, B., Matsuoka, S., Ballif, B.A., et al. (2007) Abraxas and RAP80 Form a BRCA1 Protein Complex Required for the DNA Damage Response. **Science,** 316 (5828): 1194-1198.

Wang, F., Fang, Q., Ge, Z. et al. (2012) Common *BRCA1* and *BRCA2* mutations in breast cancer families: a meta-analysis from systematic review. **Mol Biol Rep**. 39(3):2109-18.

Wang, X. and Haber, J.E. (2004) Role of *Saccharomyces* Single-Stranded DNA-Binding Protein RPA in the Strand Invasion Step of Double-Strand Break Repair. **PLoS Biol,** 2 (1): e21.

White, D., Rafalska-Metcalf, I.U., Ivanov, A.V., et al. (2012) The ATM Substrate KAP1 Controls DNA Repair in Heterochromatin: Regulation by HP1 Proteins and Serine 473/824 Phosphorylation. **Molecular Cancer Research,** 10 (3): 401-414.

Williams, G.H. and Stoeber, K. (2012) The cell cycle and cancer. **The Journal of pathology,** 226 (2): 352-364.

Williams, R.S., Dodson, G.E., Limbo, O., et al. (2009) Nbs1 Flexibly Tethers Ctp1 and Mre11-Rad50 to Coordinate DNA Double-Strand Break Processing and Repair. **Cell,** 139 (1): 87-99.

Wong, J.M.S., Ionescu, D. and Ingles, C.J. (2003) Interaction between BRCA2 and replication protein A is compromised by a cancer-predisposing mutation in BRCA2. **Oncogene,** 22 (1): 28-33.

Wu, R.S., Kumar, A. and Warner, J.R. (1971) Ribosome Formation is Blocked by Camptothecin, a Reversible Inhibitor of RNA Synthesis. **Proceedings of the National Academy of Sciences,** 68 (12): 3009-3014.

Wu, Y., Shin-ya, K. and Brosh, R.M. (2008) FANCJ Helicase Defective in Fanconia Anemia and Breast Cancer Unwinds G-Quadruplex DNA To Defend Genomic Stability. **Molecular and cellular biology,** 28 (12): 4116-4128.

Wu-Baer, F., Lagrazon, K., Yuan, W., et al. (2003) The BRCA1/BARD1 Heterodimer Assembles Polyubiquitin Chains through an Unconventional Linkage Involving Lysine Residue K6 of Ubiquitin. **Journal of Biological Chemistry,** 278 (37): 34743-34746.

Xia, Y., Pao, G.M., Chen, H., et al. (2003) Enhancement of BRCA1 E3 Ubiquitin Ligase Activity through Direct Interaction with the BARD1 Protein. **Journal of Biological Chemistry,** 278 (7): 5255-5263.

Yamaguchi-Iwai, Y., Sonoda, E., Sasaki, M.S., et al. (1999) Mre11 is essential for the maintenance of chromosomal DNA in vertebrate cells. **The EMBO journal,** 18 (23): 6619-6629.

Yan, Z., Delannoy, M., Ling, C., et al. (2010) A Histone-Fold Complex and FANCM Form a Conserved DNA-Remodeling Complex to Maintain Genome Stability. **Molecular cell,** 37 (6): 865-878.

Yarden, R.I., Pardo-Reoyo, S., Sgagias, M., et al. (2002) BRCA1 regulates the G2/M checkpoint by activating Chk1 kinase upon DNA damage. **Nature genetics,** 30 (3): 285-289.

Yoshizawa-Sugata, N. and Masai, H. (2007) Human Tim/Timeless-interacting Protein, Tipin, Is Required for Efficient Progression of S Phase and DNA Replication Checkpoint. **Journal of Biological Chemistry,** 282 (4): 2729-2740.

Yu, X. and Baer, R. (2000) Nuclear Localization and Cell Cycle-specific Expression of CtIP, a Protein That Associates with the BRCA1 Tumor Suppressor. **Journal of Biological Chemistry,** 275 (24): 18541-18549.

Yu, X., Jacobs, S.A., West, S.C., et al. (2001) Domain structure and dynamics in the helical filaments formed by RecA and Rad51 on DNA. **Proceedings of the National Academy of Sciences,** 98 (15): 8419-8424.

Zegerman, P. and Diffley, J.F.X. (2007) Phosphorylation of Sld2 and Sld3 by cyclin-dependent kinases promotes DNA replication in budding yeast. **Nature,** 445 (7125): 281-285.

Zhang, F., Fan, Q., Ren, K., et al. (2009) PALB2 Functionally Connects the Breast Cancer Susceptibility Proteins BRCA1 and BRCA2. **Molecular Cancer Research,** 7 (7): 1110-1118.

Zhang, J. and Powell, S.N. (2005) The Role of the BRCA1 Tumor Suppressor in DNA Double-Strand Break Repair. **Molecular Cancer Research,** 3 (10): 531-539.

Zou, L., Cortez, D. and Elledge, S.J. (2002) Regulation of ATR substrate selection by Rad17-dependent loading of Rad9 complexes onto chromatin. **Genes & development,** 16 (2): 198-208.

Zou, L. and Elledge, S.J. (2003) Sensing DNA Damage Through ATRIP Recognition of RPA-ssDNA Complexes. **Science,** 300 (5625): 1542-1548.

Zou, L., Liu, D. and Elledge, S.J. (2003) Replication protein A-mediated recruitment and activation of Rad17 complexes. **Proceedings of the National Academy of Sciences,** 100 (24): 13827-13832.